Predictive control for residential capacity controlled heat pumps in a smart grid scenario

N. Saraf

Master of Science Thesis

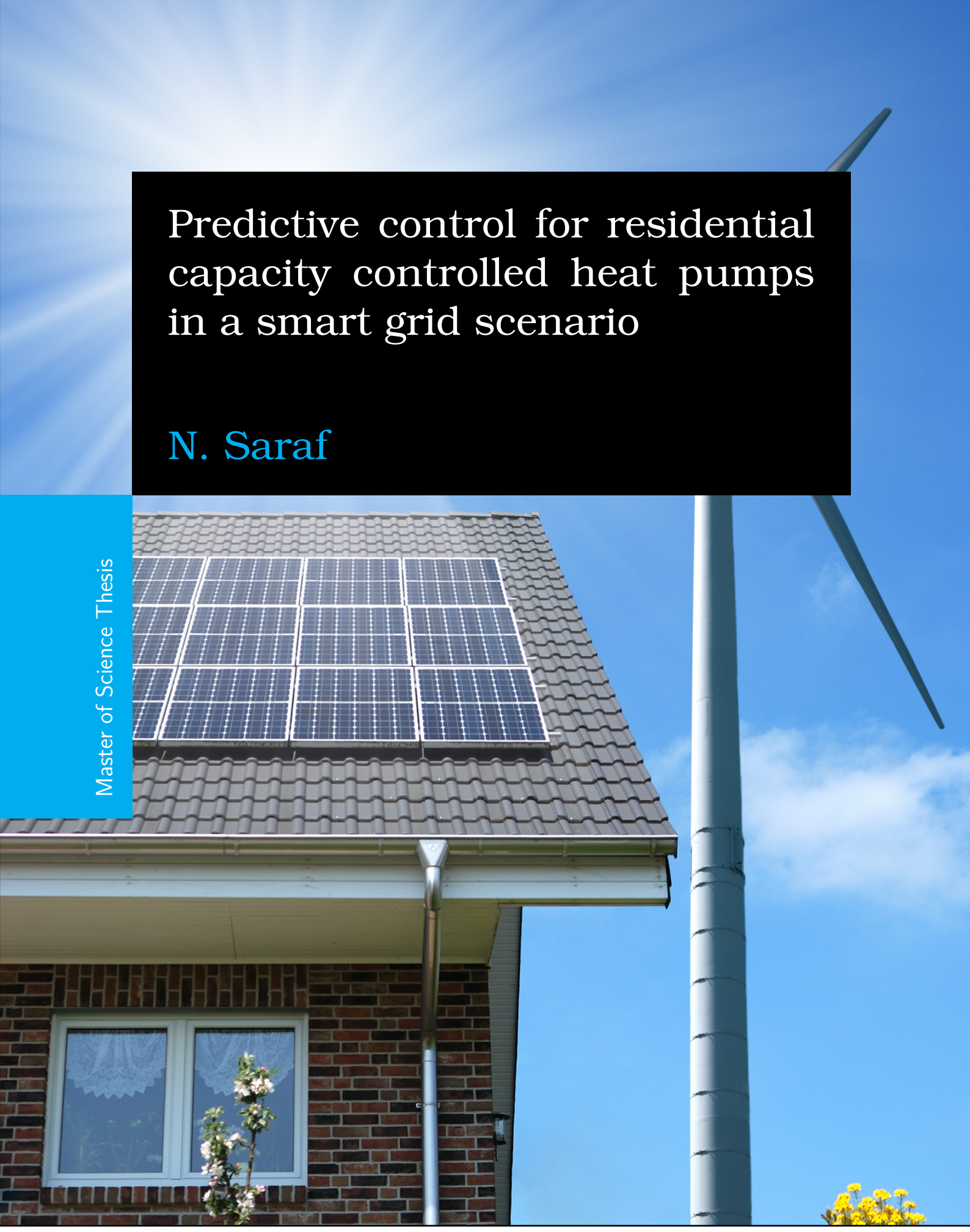

TU Delft Delft University of Technology

Delft Center for Systems and Control

Predictive control for residential capacity controlled heat pumps in a smart grid scenario

Master of Science Thesis

For the degree of Master of Science in Mechanical Engineering at Delft University of Technology

N. Saraf

July 27, 2015

Faculty of Mechanical, Maritime and Materials Engineering (3mE) · Delft University of Technology

The work in this thesis was carried out at the Fraunhofer Institute for Solar Energy Systems ISE. Their support and cooperation is hereby gratefully acknowledged.

Abstract

Residential heating systems are one of the major consumers of energy globally. Minimizing this energy consumption and costs calls for energy efficient operation of heating systems, and increasing use of renewable energy. The integration of renewable energy sources in the electricity network is challenging due to the fluctuation in their generation. The use of thermal storage to decouple heat demand and electricity supply provides the possibility to integrate power from renewable energy sources and demand side management. Capacity controlled heat pumps provide efficient heating and high flexibility in operation when coupled with thermal storage. This allows using innovative optimal control strategies to minimize energy consumption and electricity costs.

Model predictive control (MPC) for heat pumps has been identified as one of the possible solutions to this challenge. MPC offers properties such as constraint handling, multivariable control and optimal performance with conflicting objectives. It has been shown to outperform conventional control strategies and the benefits are quantified in this thesis. For the best performance, the optimization problem formulation must accurately represent the control objectives of the building energy management system and the problem should be computationally tractable.

The heating system has characteristics such as dead-zone in operation and nonlinear dependency of the efficiency of the capacity controlled heat pump on control inputs. Due to these nonlinear characteristics, the resulting optimization problem is nonlinear and non-convex. The solution of this problem demands higher computational power making it unsuitable for implementation in embedded controllers, for which simplified formulations are desirable. Although the nonlinear non-convex formulation represents the control objectives most accurately, its performance depends on a detailed heat pump model which limits its wide-spread use. Moreover, a nonlinear programming algorithm that is used to solve this problem typically obtains a suboptimal solution (local optimum) instead of the global one. In this thesis, simplifying approximations are proposed that lead to convex optimization problem formulations, which guarantee faster convergence to a solution and do not need a detailed heat pump model. Different problem formulations are studied through simulations in order to investigate

the influence of simplifications on quality of the controller performance, load shifting, energy efficiency and costs, against a baseline non-predictive control strategy in multiple tariff scenarios.

The heat pump coefficient of performance being a significant entity in the problem formulation, a detailed analysis of its characteristics is presented. Based on the analysis, a new approach to model heat pump performance is suggested and used. The controlled system simulation results indicate that using the proposed convex optimization problem formulation based MPC potentially saves around 10% costs as compared to the baseline control strategy and the performance is comparable to the nonlinear non-convex optimal control method. This cost saving potential is significant considering large-scale use. The suggested control methodology is a step forward towards electricity grid balancing by virtue of demand side management in smart grids, where heat pumps contribute to maintain load balance through thermal storage and dynamic electricity tariffing while reducing costs incurred by the end user making it a win-win proposition.

Keywords: Economic model predictive control, building energy management, heat pump coefficient of performance

Table of Contents

List of Figures

List of Tables

Acknowledgements

Hereby, I would like to thank everybody who supported me during the course of this thesis work. Firstly, I would like to thank my supervisors Dr. Tamás Keviczky (DCSC) and Mr. David Fischer (Fraunhofer ISE) who guided me throughout the course of this thesis work. It was due to the efficient meetings with Dr. Keviczky and his expertise in predictive control systems that I could produce meaningful results in this thesis. Besides *MPC* and *heat pumps*, I could learn a lot more through the discussions with them which will always help me in the future.

Thanks to Mr. Fischer, I had the opportunity to work on this challenging thesis project at the Fraunhofer institute for solar energy systems located in the beautiful city of Freiburg in Germany. I could clarify my misconceptions regarding the *heating system* through insightful discussions with Thomas Wirtz, who also wrote his thesis at ISE. He also helped me with issues regarding Linux and some complicated installations. His time, effort and patience for the same is hereby appreciated. I also acknowledge the previous efforts of Tonatiuh Toral and Mr. Fischer on the *Green heat pump* project which gave me the platform to take it a step further. I thank all my colleagues in the intelligent energy systems group for their cooperation and maintaining a pleasant and motivating work environment at the institute.

Special thanks to Dr. Simone Baldi, Mr. Vahab Rostampour and Prof. Hans Hellendoorn for being a part of the final exam committee. Last but not the least, I would like to thank my family and friends for always supporting me during the difficult times.

Delft, University of Technology — N. Saraf
July 27, 2015

"It is far better to foresee even without certainty than not to foresee at all."

–*Henri Poincare* in The Foundations of Science

"Programming today is a race between software engineers striving to build bigger and better idiot-proof programs, and the Universe trying to produce bigger and better idiots. So far, the Universe is winning."

–*Unknown*

Chapter 1

Introduction

Residential heating systems roughly cover a third of the domestic energy use in countries such as Germany. In developed countries, the main building stock already exists in place and renovation of buildings is expensive but the supervisory control systems can be improved at comparatively lower costs [1]. The use of air source heat pumps is an efficient method to provide heat for temperature control and domestic hot water in residential buildings. Capacity control of heat pump allows a flexible operation. The use of thermal storage makes it possible to decouple thermal production and electrical load from the heat pump. This allows the use of innovative energy efficient operation control strategies with possibility to include renewable energy which do not have uniform production [2], [3].

Use of model predictive control has been shown to outperform rule based control strategies [1] such as conventional heating curve based control [4]. It can be used to exploit the energy saving potential of demand side management by thermal storage. Moreover, the predictive control strategy enables to make use of weather forecasts, occupancy predictions [5] for optimal operation and optimization of costs in a dynamic electricity tariff scenario [4].

1-1 Motivation

In order to achieve European Union's energy goal of reducing domestic emmissions by 80%, increase in energy efficiency and integration of renewable energy sources is vital [6]. The residential sector, especially heating, being one of the primary consumers; it is important to replace inefficient heating systems. The new technology replacing such systems must address future challenges such as cost and energy efficient operation in a smart grid. Current practice for electricity distribution management is to adjust the production based on demand which leads to wastage of energy unless the surplus is stored and later used efficiently. In a future scenario such as smart grid, for efficient use of energy, the strategy is to manage the demand according to the production i.e. demand side management.

1-1-1 Smart grid scenario

Smart electricity grid uses communication technology to gather information on the behaviour of electrical demand and supply sides to enable automatic adaptation in order to improve efficiency and reliability of the electricity distribution and production. This technology offers the possibility of efficiently incorporating input from renewable energy sources such as wind and solar power which have fluctuating production. The communication between suppliers, consumers and storage facilities allows use of intelligent controls to achieve peak shaving, load shifting and demand side management through variable electricity prices. In this thesis, the residential heating system is considered to be in a futuristic smart grid scenario with the focus being on its supervisory control strategy and overcoming the associated challenges for optimal performance.

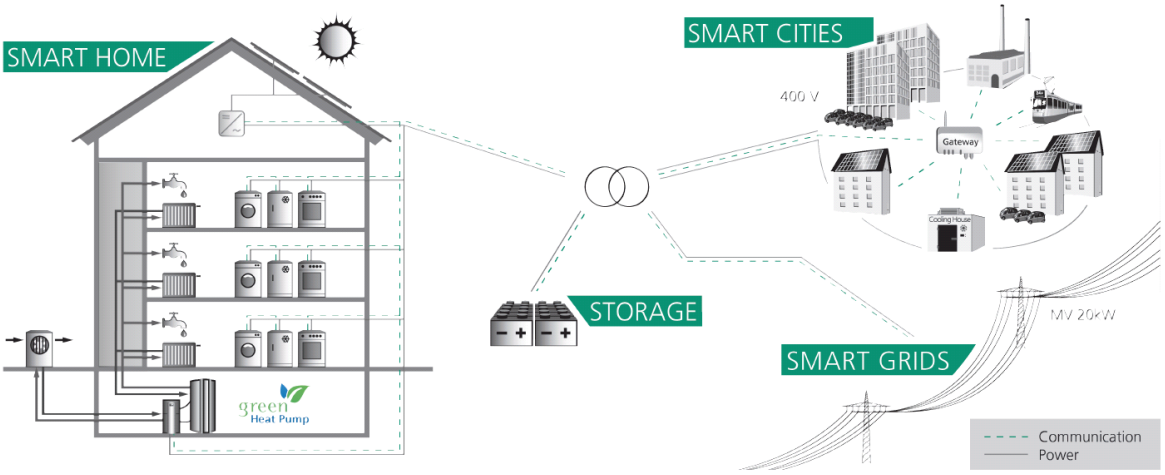

Figure 1-1: Residential heating system in smart grid

Figure 1-1 shows the broader scope of the control strategy application. By implementing smart controls similarly to majority of the buildings in a city, maximum energy and cost saving potential through smart grids can be realized.

1-1-2 Role of heat pumps and thermal storage in a smart grid

For balancing grid load, some form of storage is required. Electricity can be directly stored in batteries of hybrid electric vehicles, for instance, which can be charged from the grid. It can also be stored indirectly in the form of heat in thermal storage e.g. hot water tanks. Heat pump is a device which transfers (pumps) heat from a lower temperature reservoir (heat source) to a higher temperature reservoir (heat sink) using electrical energy. Heat pumps can thus act as an interface between electrical and thermal energy. Given that heat is relatively simple and cheap to store in thermal storage, heat pumps have the potential to be a significant component in grid balancing. The storage acts as a heat buffer which is essential for management of heat pump in smart grid. This property also helps in saving the surplus production from renewable sources which is often wasted.

Replacing conventional heating systems such as gas boilers which run on energy provided by fossil fuels, by heat pumps, reduces local direct emissions. This also leads to a twofold increase in the electricity demand [7] which can be partially or completely compensated by increasing supply from renewable energy sources in the smart grid through local or remote production. It is important to note that if direct electrical heating is used to meet the same heat demand, the increase in electricity demand would be upto 8 to 10 times in comparison. This supports the use of heat pumps as they are highly energy efficient when compared to electrical heating. Moreover, the use of heat pump with thermal storage promotes the replacement of electricity generated from fossil fuels by renewable sources because with smart controls, this flexible heating system can operate with fluctuating power input.

In order to exploit these properties of heat pumps and thermal storage in a smart grid, research is needed on control algorithms which can optimize the system performance for cost and energy efficiency while achieving load shifting and demand side management.

1-2 Research goals

The literature review [8] preceding this thesis work investigated the open problems linked with the control design for residential heating systems. It could be concluded that predictive control was identified as the most suitable method with the benchmark strategy being rule based method. However, it was uncertain as to how good is the performance of predictive control method as compared to rule based methods because the systems and objectives considered in past works were not the same. Moreover, the same strategy was not tested with active thermal storages providing both domestic hot water supply and space heating. The benefits of using predictive control over rule based control concerning the use of renewable energy also need to be quantified. To implement a predictive control strategy, a suitable cost function for optimization needs to be determined which accurately represents the control objectives. For faster convergence to an optimal solution, convex optimization problem formulations are desirable. Due to the heating system nonlinearities, the resulting optimization problem formulation not only undesirably relies on an accurate heat pump model but it is also nonlinear non-convex; which implies that there is a need to investigate different simplified formulations in order to determine the most suitable one. Based on the above mentioned facts, the research goals of this thesis are stated as follows:

- Quantify the potential benefits of using model predictive control against conventional methods and the cost saving potential in different tariff scenarios.
- Determine the most suitable optimization problem formulation to achieve the control objectives.
- Investigate the influence of simplifications on the overall performance of the controller.

1-3 Thesis contributions

Through this thesis work, the problem of formulating the cost function for predictive control of residential heat pumps and active thermal storage in a smart grid was addressed following

a detailed analysis of the heat pump coefficient of performance. In order to achieve the thesis goals, a simulation framework for testing different control algorithms was further developed. The framework was also adapted later such that it can be interfaced with an advanced thermal system simulation software (*ColSim*) for software-in-the-loop (SiL) simulations.

I proposed a new approach to model the heat pump performance for the purpose of estimating the electricity consumption. The thesis work focussed on investigating whether the performance of control strategy depends on an accurate model of the heat pump and the consequences of not using it have been quantified along with detailed explanation. The simulation results in multiple tariff scenarios for the same investigation also provided reflections on sizing of the system components considered. The approach for convex optimal control problem formulation that is derived in this thesis, is an original contribution to the existing literature on the topic of optimal control problem formulations for capacity controlled heat pumps.

The source code development of simulation framework relied completely on open-source tools such as Python [9] and associated libraries. The optimization problems were solved using open-source solvers and the 'OpenOpt' framework [10].

1-4 Structure of this report

The contents of this thesis have been organized into the following four chapters. This section gives an overview of the contents discussed in each chapter.

Chapter 2 describes the residential heating system. The working of its compoenents is briefly described with relevance to the control problem definition. This is followed by the description of storage and building system model. Since a heat pump model is required to estimate electricity consumption, which is used for control problem formulations, the last section includes its modeling approaches. It presents a detailed analysis of the heat pump coefficient of performance followed by the description of models and validation results.

Chapter 3 includes a detailed description of control methods. First, the control objectives and performance indicators are stated. Based on this, and the constraints of the system, model predictive control algorithms which differ in the optimization problem formulation are mathematically described in detail. This also includes the derivation of different formulations while explaining why they were considered. The chapter is concluded by a short description of the baseline control strategy which represents the benchmark for evaluation of predictive control methods.

Chapter 4 focusses on the comparison of control strategies described in Chapter 3. The performance is tested through simulations in three different scenarios. A detailed explanation for results obtained in each scenario is included. This chapter also includes the quantification of benefits of using predicitve control based on a one year simulation with each control strategy followed by a summary of the findings.

Chapter 5 concludes this report with a summary of results and answers to the research questions. It also includes suggestions for future work on this thesis topic.

Chapter 2

System description and modeling

This chapter describes the physical system and its modeling considered for control in this thesis along with basic terminology related to it. Section 2-1 includes a brief description of each component of the system with relevance to the control problem definition. This is followed by the derivation and description of the model (Section 2-2) used for controller design. Important non-linear characteristics of the heat pump which were considered while designing the controller are described in detail in Section 2-3.

2-1 Components of the residential heating system

The residential heating system as shown in Figure 2-1 mainly comprises of a heat pump (HP), a stratified thermal energy storage (TES), solar devices (PV and STC) and ideal heat exchangers (HX). It also includes auxiliary heaters (not shown) and subsystem components such as valves and pumps which are associated with the main components.

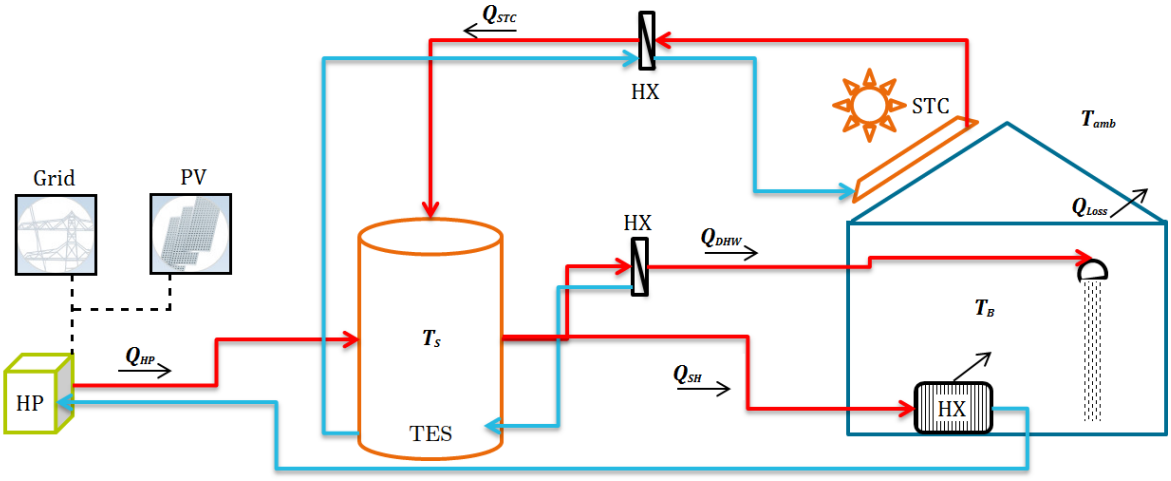

Figure 2-1: Schematic diagram of the system

The subsystem components are not directly considered for the supervisory control strategy but are a part of the controlled system as they are involved in executing the desired control actions (heat flows) through lower level controllers. Figure 2-1 shows the heat flows between each component indicated by red solid lines (hot water flow) and the blue lines indicating return water in the closed water loops. The power flow (dotted lines) indicates that the heat pump operates on electrical supply from the electricity grid and power from the solar panels. The following paragraphs briefly explain the functions of each component and their interconnections referring Figure 2-1:

Heat pump (HP) Heat pumps can be classified on the basis of heat source. Ground source and air source heat pumps are commonly used in residential heating systems [11]. In this thesis only[1] air source heat pumps have been considered and the term 'heat pump' henceforth refers to this class of heat pumps. A detailed description of the working of heat pumps and related terminology is included in the appendix of this report (Section A-1). Capacity control allows modulating the heat supplied by the heat pump (Q_{HP}) by altering the compressor frequency.

The function of the heat pump is to supply heat to the stratified thermal storage where the quantity of heat to be supplied per unit time and the temperature at which it is supplied are controlled by the supervisory controller. The lower level controllers accordingly adjust the compressor frequency and the mass flow rate of the pump in water loop, to track the desired heat transfer rate and temperature of water supply respectively. This is because the heat pump operates in two modes:

1. Domestic hot water (DHW) mode: In this operating mode, the heat pump delivers heat to the upper part of the stratified storage at a temperature above the mean storage temperature (T_S). The reason is that the upper part of the storage stores water at a higher temperature for DHW supply as compared to lower part which stores water for the space heating loop.

2. Space heating mode: In this operating mode heat is supplied through a layer in the lower part of the storage at a temperature lower than DHW supply temperature. This supply temperature can be above or below T_S.

The storage thus has a pair of inlets and feedback water pipes connected to the heat pump corresponding to each operating mode (Figure 2-2). The switching between these two operating modes is done by a subsystem with a lower level controller as guided by the supervisory controller. The heat pump considered in this system has a compressor speed modulation range of 1020 to 7020 revolutions per minute (rpm). This range roughly corresponds to heat transfer of 5 to 35 kW and varies depending on the ambient temperature. Due to high amount of mechanical losses, the heat pump does not operate in the compressor speed range of 0 to 1020 rpm. This means that there is a dead-band in the heat pump operation and it will thus remain turned off for input signals corresponding to this rpm range.

Thermal energy storage (TES) The TES decouples the heat supply from the heat pump and the heat extraction from the demand side (building[2]). It takes inputs from heat pump

[1] The inferences of this thesis are also applicable to ground source heat pumps.
[2] Standard German multi-family house with six dwellings.

and solar thermal collector (STC) in the form of hot water and stores the surplus heat for future use. It provides the thermal inertia essential for demand side management. The benefit of having an external storage tank is that it can be controlled independently without any influence on the building thermal comfort. Through stratification, water at different temperatures can be stored in the same tank which has a temperature gradient profile (high to low) throughout its length (top to bottom). It also has a layer with a steep gradient (thermocline) which separates the hot (upper) and warm (lower) part of the storage. Depending on the demand, heat in the form of hot water is extracted from the corresponding outlet of the storage for heating DHW (Q_{DHW}) and heat (Q_{SH}) for maintaining zone temperature (T_B). The storage considered in this system has a water storage capacity of 3000 litres.

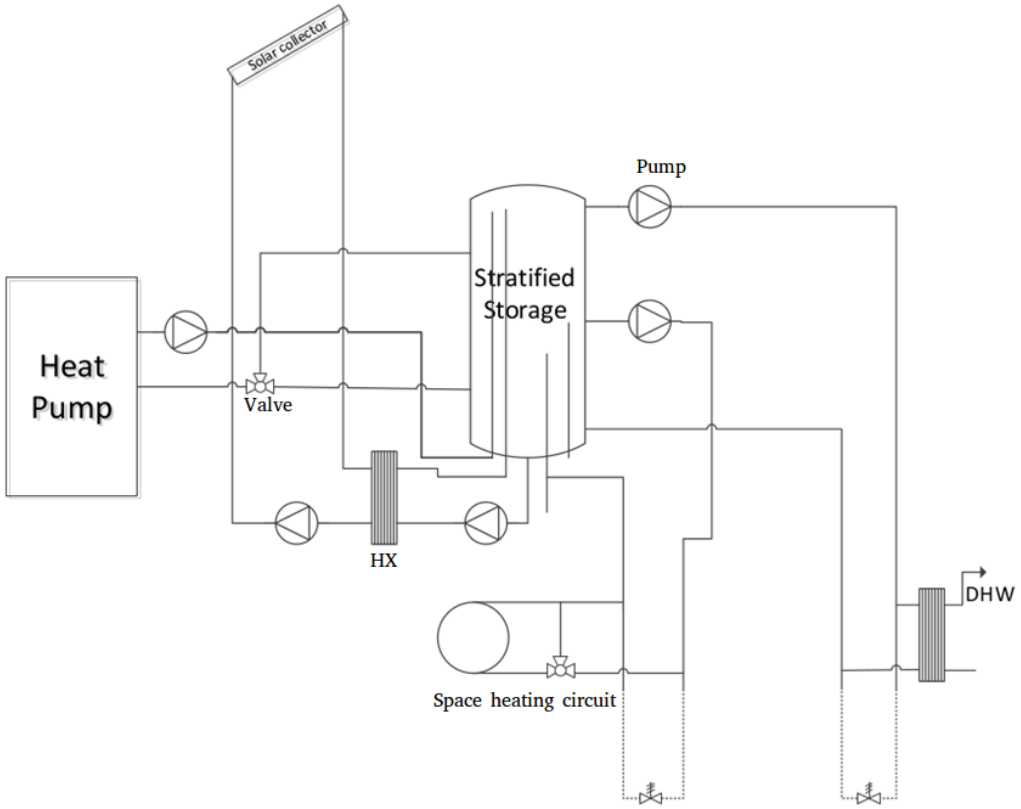

Figure 2-2: Heating circuit

Backup (auxiliary) heaters Two backup heaters, one each for DHW and space heating, of 5 kW capacity are considered in this system for heating when the heat pump capacity is not sufficient to provide required quantity of heat. They are mainly needed during extreme weather conditions.

Solar devices A solar thermal collector of 15 m^2 area and a solar panel (PV) with 10 kWp capacity are assumed to be installed in the system. The STC supplies heat (Q_{STC}) only to the top part of the storage for DHW considering its higher supply temperature. The electrical power from PV is consumed by the house and the residual can either be converted to heat by

the HP or be fed to the grid, which returns money to the user based on feed-in tariff[3].

2-2 Modeling system dynamics

This section presents the mathematical model of the system derived for model based control considering system characteristics explained in Section 2-1. A first principles modeling approach has been used based on thermal energy balance to derive a linear time invariant (LTI) model [12]. It was verified from the literature review [8] that this approach is the most suitable one in order to model building thermal systems for model based controller design.

2-2-1 Modeling considerations

The heat pump, solar thermal collector and backup heaters are the main actuators in this system as they supply heat ($\dot{Q}_{HP_1}, \dot{Q}_{HP_2}, \dot{Q}_{STC}, \dot{Q}_{BH_1}, \dot{Q}_{BH_2}$) to the stratified TES (Figure 2-3). The space heating supply ($\dot{Q}_{Htg}$) to the building is also controlled by the supervisory controller which means that the TES is also an actuator (in reality, the actuator is the pump, a subsystem component of TES which controls warm water supply from lower part of storage to building by varying mass flow rate). The heat supplied from these actuators represents the control actions. The state variables of this system are the measured temperatures representing the storage and the building state. Since the temperatures of the storage and building are to be maintained as desired, the system state variables (T_{S_1}, T_{S_2}, T_B) also represent the outputs of the system. The DHW consumption, heat losses from the storage and building represent the disturbances acting on the system. The following assumptions and simplifications are made while modeling the system:

- The stratified storage is assumed to have negligible mixing. It is modeled as two ordinary thermal storage units with 3:7 volume ratio containing water at a single temperature in each volume as shown in Figure 2-3. The two parts are separated by a thermocline. This simplifies the analysis of heat flow for the two operating modes of the heat pump and also the effect of heat extracted from the TES for DHW and space heating.
- The building is assumed to be a single zone, the state of which is represented by one temperature.
- The heat pump is considered to operate on electricity obtained from both sources (grid and PV) at any time instant.
- The DHW heat ($\dot{Q}_{DHW}$) is extracted from the upper part of the storage and the return water is given back to the storage in the lower part. By equating mass flow rates at the two parts of storage for DHW, two components of $\dot{Q}_{DHW}$ are obtained ($\dot{Q}_{DHW_1}, \dot{Q}_{DHW_2}$) which represent the DHW heat extracted from each part of the storage (Section A-2).

Based on these considerations, the energy balance equations are derived as explained in the following subsection.

[3]Also known as renewable energy payment. German feed-in tariff structure (year 2012) for roof-top solar panels with 10 kWp has been considered - 13.68 € cents per kWh.

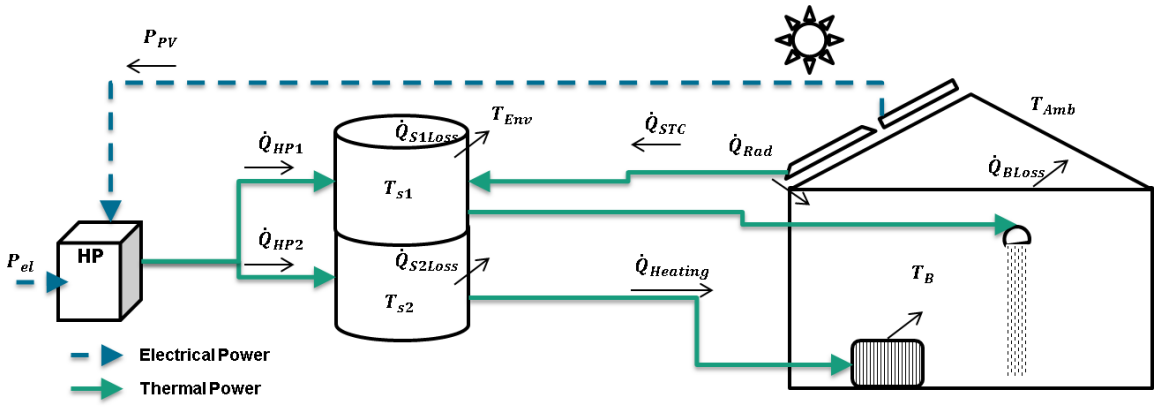

Figure 2-3: Modeled system [12]

2-2-2 Thermal energy balance equations

Equating the heat flows to and from the TES gives the following continuous-time equations:

$$C_{S_1}\dot{T}_{S_1} = \underbrace{\kappa_S \cdot A_{S_1} \cdot (T_{\text{env}} - T_{S_1})}_{\dot{Q}_{S1_{\text{Loss}}}} + \dot{Q}_{HP_1} + \dot{Q}_{HP_{1_{PV}}} + \dot{Q}_{STC} + \dot{Q}_{BH_1} - \dot{Q}_{DHW_1} \tag{2-1a}$$

$$C_{S_2}\dot{T}_{S_2} = \underbrace{\kappa_S \cdot A_{S_2} \cdot (T_{\text{env}} - T_{S_2})}_{\dot{Q}_{S2_{\text{Loss}}}} + \dot{Q}_{HP_2} + \dot{Q}_{HP_{2_{PV}}} - \dot{Q}_{Htg} + \dot{Q}_{BH_2} - \dot{Q}_{DHW_2} \tag{2-1b}$$

$$C_B\dot{T}_B = \dot{Q}_{Htg} - \dot{Q}_{B_{\text{Loss}}} \tag{2-1c}$$

Table 2-1 describes the terms and their values. Note: $\dot{Q}$ represents the rate of heat transfer and not the absolute quantity of heat supplied/extracted. Equations (2-1) can be written in state space representation as follows:

$$\underbrace{\begin{bmatrix}\dot{T}_{S_1}(t)\\ \dot{T}_{S_2}(t)\\ \dot{T}_B(t)\end{bmatrix}}_{\dot{x}} = \underbrace{\begin{bmatrix}-\frac{\kappa_S \cdot A_{S_1}}{C_{S_1}} & 0 & 0\\ 0 & -\frac{\kappa_S \cdot A_{S_2}}{C_{S_2}} & 0\\ 0 & 0 & 0\end{bmatrix}}_{A} \underbrace{\begin{bmatrix}T_{S_1}(t)\\ T_{S_2}(t)\\ T_B(t)\end{bmatrix}}_{x} + \underbrace{\begin{bmatrix}\frac{1}{C_{S_1}} & 0 & 0 & \frac{1}{C_{S_1}} & 0 & \frac{1}{C_{S_1}} & 0 & \frac{1}{C_{S_1}}\\ 0 & \frac{1}{C_{S_2}} & -\frac{1}{C_{S_2}} & 0 & \frac{1}{C_{S_2}} & 0 & \frac{1}{C_{S_2}} & 0\\ 0 & 0 & \frac{1}{C_B} & 0 & 0 & 0 & 0 & 0\end{bmatrix}}_{B} \underbrace{\begin{bmatrix}\dot{Q}_{HP_1}(t)\\ \dot{Q}_{HP_2}(t)\\ \dot{Q}_{Htg}(t)\\ \dot{Q}_{BH_1}(t)\\ \dot{Q}_{BH_2}(t)\\ \dot{Q}_{HP_{1_{PV}}}(t)\\ \dot{Q}_{HP_{2_{PV}}}(t)\\ \dot{Q}_{STC}(t)\end{bmatrix}}_{u} + \underbrace{\begin{bmatrix}-\frac{1}{C_{S_1}} & \frac{\kappa_S \cdot A_{S_1}}{C_{S_1}} & 0 & 0\\ 0 & \frac{\kappa_S \cdot A_{S_2}}{C_{S_2}} & 0 & -\frac{1}{C_{S_2}}\\ 0 & 0 & -\frac{1}{C_B} & 0\end{bmatrix}}_{E} \underbrace{\begin{bmatrix}\dot{Q}_{DHW_1}(t)\\ T_{\text{env}}\\ \dot{Q}_{B_{\text{Loss}}}(t)\\ \dot{Q}_{DHW_2}(t)\end{bmatrix}}_{z} \tag{2-2}$$

The state variables (x) and outputs (y) are the same. Thus,

$$\dot{x}(t) = Ax(t) + Bu(t) + Ez(t) \tag{2-3}$$

$$y = Cx(t) + Du(t) \tag{2-4}$$

where, C is an identity matrix of size 3 and D is a null matrix of size 3×8 and z represents the vector of known disturbances.

Table 2-1: Terminology

Term	Description	Value	Units
Control Inputs			
$\dot{Q}_{HP_1}$	Heat supplied from HP to upper part of TES (DHW mode)	-	kW
$\dot{Q}_{HP_2}$	Heat supplied from HP to lower part of TES (space heating mode)	-	kW
$\dot{Q}_{HP_{1_{PV}}}$	Heat supplied from HP to upper part of TES using PV electricity	-	kW
$\dot{Q}_{HP_{2_{PV}}}$	Heat supplied from HP to lower part of TES using PV electricity	-	kW
$\dot{Q}_{BH_1}$	Heat supplied from backup heater (BH) to upper part of TES	-	kW
$\dot{Q}_{BH_2}$	Heat supplied from BH to lower part of TES	-	kW
$\dot{Q}_{STC}$	Heat supplied from solar thermal collector to TES (upper part)	-	kW
$\dot{Q}_{Htg}$	Heat input from lower part of TES to building for space heating	-	kW
States/Outputs			
T_{S_1}	Temperature of upper TES	-	K
T_{S_2}	Temperature of lower TES	-	K
T_B	Zone temperature	-	K
Disturbances			
$\dot{Q}_{DHW_1}$	Heat taken from upper TES layer for DHW heating	From DHW load profile	kW
T_{env}	Temperature of storage environment (Assumed to be constant)	293	K
$\dot{Q}_{DHW_2}$	Heat taken from lower TES layer for DHW heating	From DHW load profile	kW
$\dot{Q}_{B_{\text{Loss}}}$	Heat loss from the building (non-negative Space heating load)	From heat load profile	kW
Coefficients			
C_{S_1}	Thermal capacity of upper TES	3698.7984	kJ/K
C_{S_2}	Thermal capacity of lower TES	8630.5296	kJ/K
C_B	Overall thermal capacity of building	264600	kJ/K
κ_S	Overall coefficient of heat transfer between TES and its environment	0.00126	kW/m^{2}K
A_{S_1}	Area of upper storage in contact with surrounding air	2.4	m^2
A_{S_2}	Area of lower storage in contact with surrounding air	5.6	m^2

The control inputs (u) in (2-2) are heat flows which will be delivered by the subsystems and lower level controllers. These heat flows could be substituted by product of appropriate

mass flow rates and temperature differences to directly control the subsystems (eg. pumps). However, this would lead to nonlinear dynamical equations. The use of heat flows as control inputs makes it possible to have an LTI model of the system at the cost of dependence on lower level controllers to precisely deliver the actions indicated by the supervisory control strategy. It is also important to note that the model obtained is assumed to be perfect and the investigation of modeling errors and system model validation are out of the scope of this thesis. This means that the control strategy results based on this ideal model represent a theoretical benchmark or a performance bound.

2-2-3 Discretization

A discrete-time model is required considering practical implementation and also the controller implementation on software framework. The continuous-time model matrices obtained by substituting coefficient values from Table 2-1 in (2-2) are:

$$A = 10^{-7} \times \begin{bmatrix} -8.176 & 0 & 0 \\ 0 & -8.176 & 0 \\ 0 & 0 & 0 \end{bmatrix}$$

$$B = 10^{-5} \times \begin{bmatrix} 27 & 0 & 0 & 27 & 0 & 27 & 0 & 27 \\ 0 & 11.587 & -11.587 & 0 & 11.587 & 0 & 11.587 & 0 \\ 0 & 0 & 0.378 & 0 & 0 & 0 & 0 & 0 \end{bmatrix}$$

$$E = 10^{-5} \times \begin{bmatrix} -27 & 0.08176 & 0 & 0 \\ 0 & 0.08176 & 0 & -11.587 \\ 0 & 0 & -0.378 & 0 \end{bmatrix}$$

Observing the above matrices it is clear that the system has very slow dynamics as the eigen values are close to zero. However, the values of coefficients used are appropriate considering the system properties such as a large capacity storage and TES material with high insulating capability. The model was discretized using zero order hold sampling [13] method with a sampling rate of 1 hour i.e. 3600 seconds. In [4] and [14], it is mentioned that a sampling period of 30 minutes is sufficient to capture the system dynamics. However, since a storage of larger capacity is used, a sampling period of 1 hour is suitable in our case as the dynamics of a larger TES are slower. The control actions are also scheduled every 1 hour as more frequent control action causes the heat pump to modulate aggressively and also frequently switch on/off. Hence, having less frequent control action improves overall equipment performance [14]. If the control inputs are applied with lower frequency, the controller has more restrictions which would limit the performance. This justifies that a 1 hour sampling rate is suitable considering the system properties. The results of the discretization and details are included in Section A-3. Equations (2-2) can be written in discrete-time state space representation as:

$$x_{k+1} = A_d x_k + B_d u_k + E_d z_k \tag{2-5}$$

$$y_k = C_d x_k + D_d u_k = x_k \tag{2-6}$$

In the above equations the symbols have their usual meaning as explained earlier with the subscripts k and d representing the (discrete) time instant and discretized version respectively.

2-3 Heat pump performance model

Achieving minimum energy consumption requires optimal performance of the heat pump. A predictive controller requires predictions of the heat pump performance to maximize its efficiency and calculate optimal control actions. Many approaches have been considered in literature [8] to model heat pump performance. This section presents the modeling approaches relevant to this thesis and heat pump performance characteristics which need to be considered before deriving an optimal control problem formulation.

2-3-1 Coefficient of Performance (COP)

Definition

The efficiency or performance of the heat pump is measured by COP which is defined as the ratio of heat transferred by the heat pump (Q_{HP}) to the work done (W). Alternatively, it can be defined as the ratio of heat transfer rate ($\dot{Q}_{HP}$) from the heat pump to the electrical power consumed (P_{el}). Mathematically,

$$\text{COP} = \frac{Q_{HP}}{W} = \frac{\dot{Q}_{HP}}{P_{el}}$$
$$W = Q_{sink} - Q_{source}$$

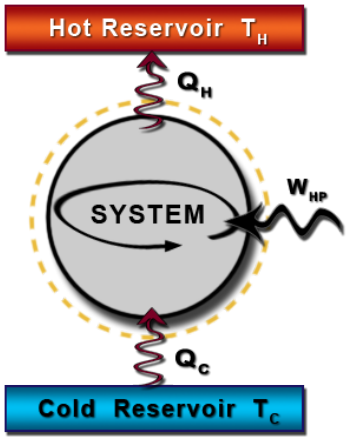

Figure 2-4: Heat pump cycle[4]

Q_{sink} = heat supplied to the hot side = Q_{HP} and,
Q_{source} = heat extracted from the ambient

$$P_{el} = \dot{Q}_{HP} - \dot{Q}_{source}$$

Using the second law of thermodynamics and the equations stated above,

$$\text{COP} = \frac{\dot{Q}_{HP}}{P_{el}} = \frac{T_{\text{sup}}}{T_{\text{sup}} - T_{\text{amb}}} \tag{2-7}$$

[4] Image retrieved from http://www.learnthermo.com/T1-tutorial/ch04/lesson-F/pg11.php

Since air to water heat pumps are considered, in the above equation T_{sup} represents (approximately the condenser temperature) the temperature of the water supplied to the thermal storage (hot side/sink). The last expression (2-7) indicates that the ideal COP of heat pump at a particular operating load is dependent on ambient air (approximately the evaporator temperature) and supply water temperatures. This relation is not valid to estimate the COP at part load operation and, data based modeling techniques are used for its estimation [8]. As observed in (2-7), the electricity consumption of the heat pump is determined by the COP and the heat transfer rate, which is a control variable. The electricity bill which depends on electricity consumed for heating, is the target function to be minimized (Section 3-1) and therefore, it is important to estimate the COP in order to formulate the cost function. How the heat pump models were used for the formulations will be explained in detail in Chapter 3.

High fidelity model

To study the COP characteristics and derive simplified heat pump models for control, a high fidelity TRNSYS[5] model of heat pump was used. This detailed model was not suitable for control as it was a ratio of high order polynomial fits ($\dot{Q}_{HP}$ and P_{el}). Moreover, the inputs and outputs of this model were not the same as required for the optimal control problem formulations described later (Section 3-3). The polynomials are not essential for this discussion and are not presented on that account. The inputs and outputs of the detailed model are:

- Inputs: Ambient temperature (T_{amb}), supply water temperature from HP (T_{sup}), return water temperature (T_{ret}) to the HP and compressor frequency in rpm.
- Outputs: COP, power consumed (P_{el}) by the HP and heat transfer rate ($\dot{Q}_{HP}$).

For our system, the variables of interest being T_{sup}, T_{amb}, and the rate of heat transfer $\dot{Q}_{HP}$, which also determines part load operation, the simplified model has these variables as inputs at a constant return water temperature of 293 K. The characteristics of COP with respect to these variables were analyzed through the plots obtained using detailed model as shown below.

Characteristic curves

The following statements can be inferred from Figures 2-5, 2-6 and 2-7:

- The variation of COP against compressor frequency (rpm) is nonlinear and also depends upon the ambient and supply water temperatures. The dependency on these temperatures is also nonlinear as the curves are not parallel in Figures 2-5 and 2-6).
- The heat pump COP varies in a contradictory manner w.r.t. the operating frequency on either side of the optimal one of $\approx$ 2200 rpm (Figure 2-5, 2-6).

[5] A detailed simulation software for thermal systems [15]

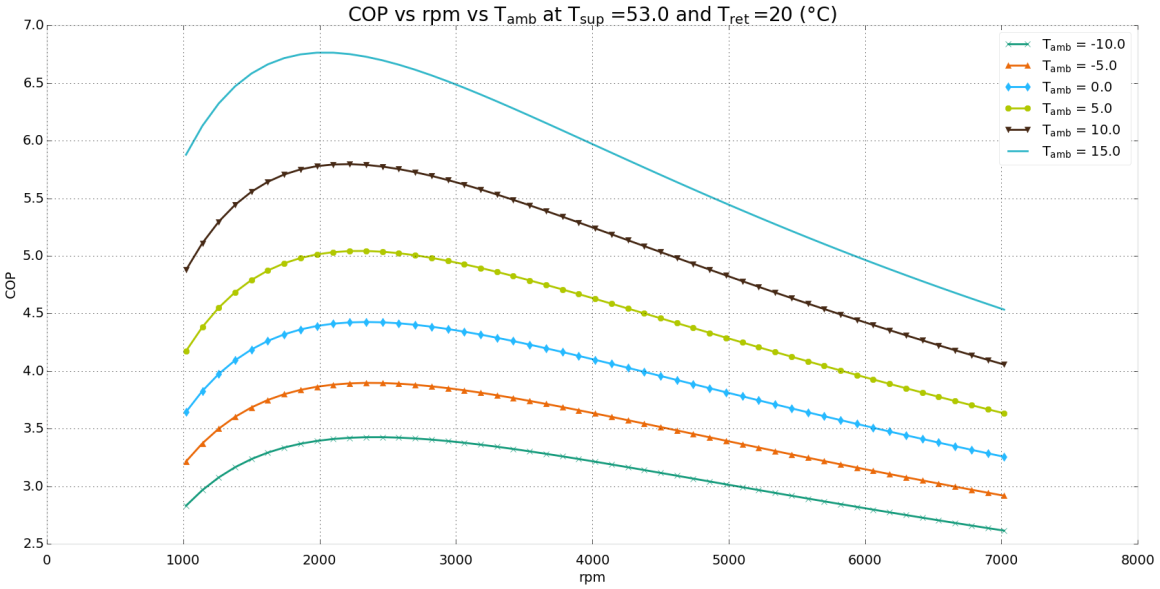

Figure 2-5: COP variation with compressor rpm and ambient temperature at a given supply water temperature

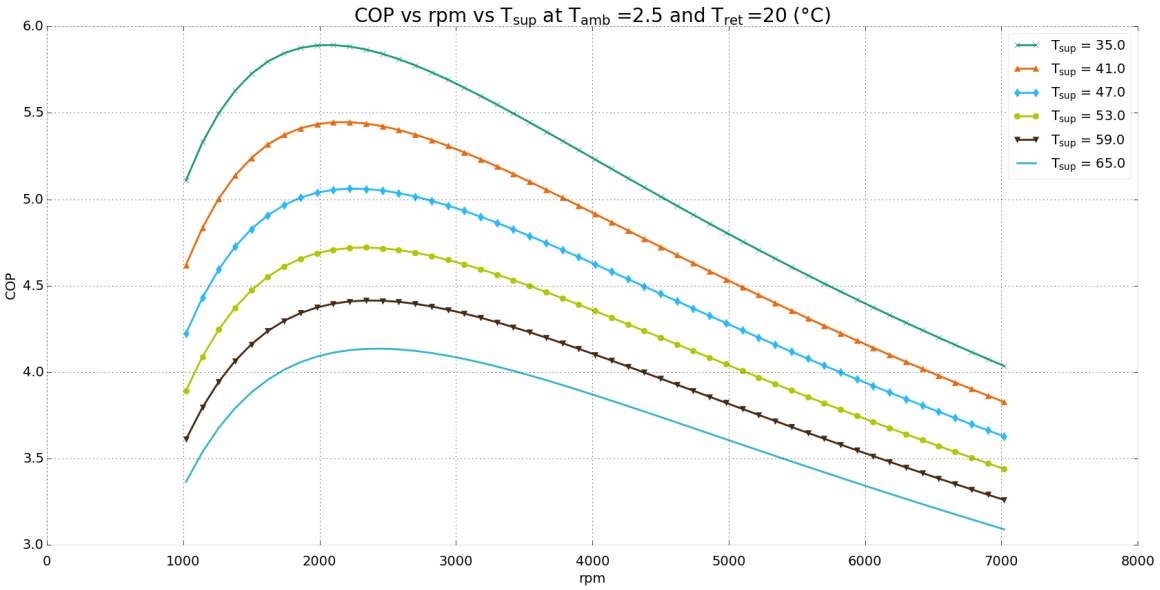

Figure 2-6: COP variation with compressor rpm and supply water temperature at a given ambient air temperature

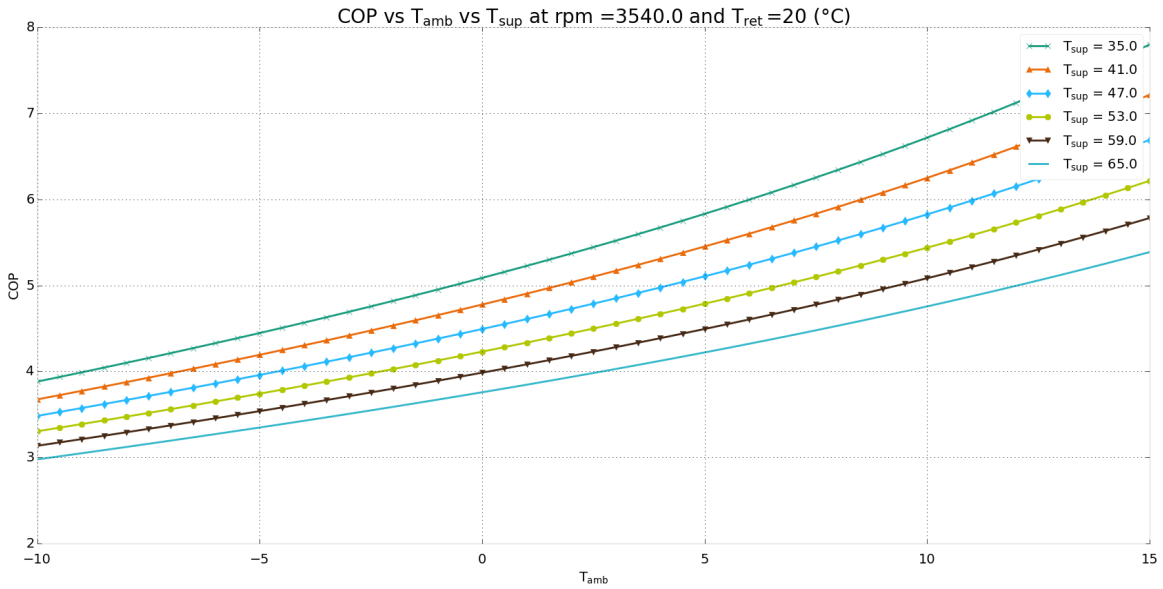

Figure 2-7: COP variation with ambient and supply water temperature at a given compressor frequency

- The COP increases with increase in ambient temperature but the rate of increase is not uniform and also depends on the supply water temperature (Figure 2-7).

The aforementioned characteristics are hard to capture with a low order model.

Simplified model

Using the data from the detailed model and based on the characteristics observed, a simplified low order model for COP was obtained in past works at Fraunhofer ISE. The following model structure was used:

$$\mathrm{COP} = (a_0 + a_1 T_{\mathrm{sup}} + a_2 T_{\mathrm{amb}}) \left(1 + a_3 \underbrace{\frac{\dot{Q}_{HP}}{\bar{\dot{Q}}_{HP}}}_{PLR} \right) \tag{2-8}$$

The coefficients (Table 2-2) were fitted from detailed model data. In (2-8), a new term $\bar{\dot{Q}}_{HP}$ is introduced which is derived from the ambient temperature to define the upper bound on $\dot{Q}_{HP}$ at maximum operating frequency or full load condition. The ratio of $\dot{Q}_{HP}$ and $\bar{\dot{Q}}_{HP}$ is defined as the part load ratio (PLR). The part load ratio indicates the capacity at which the heat pump is operating on a scale of 0 to 1. This model has some limitations in capturing the nonlinearities described earlier. The structure cannot fit the conflicting behaviour of COP with compressor frequency below optimal rpm. Hence, the data used to fit and validate this model was only in the range of compressor frequency above 2200 rpm. Even though this model partially neglects nonlinearities (part load behaviour below optimal compressor rpm),

Table 2-2: COP model coefficients

Coefficient	Value	Unit
a_0	-2.47881	-
a_1	-0.06575	K^{-1}
a_2	0.10109	K^{-1}
a_3	-0.3912	-

the simplicity of this model is desirable for control. It satisfactorily captures the remaining nonlinear characteristics. Since identification and validation of this model were not a part of this thesis work, the results are not provided and can be referred in [12].

2-3-2 Inverse of COP

In past works (cf. [4]), the approach to estimate the electricity consumption for control problem formulations was to model the heat pump performance through COP. As described earlier the COP has multiple nonlinear characteristics and modeling it with a low order model has limitations with respect to accuracy. Considering this, a novel approach to model the heat pump performance was investigated in this thesis and the advantages of using this approach are highlighted in this section.

As mentioned earlier (2-8), the electricity consumption of the heat pump has a direct variation with the inverse of COP. Hence, the characteristics of inverse of COP (COP_{inv}) were analysed and modeled for representing the heat pump performance.

Characteristic curves

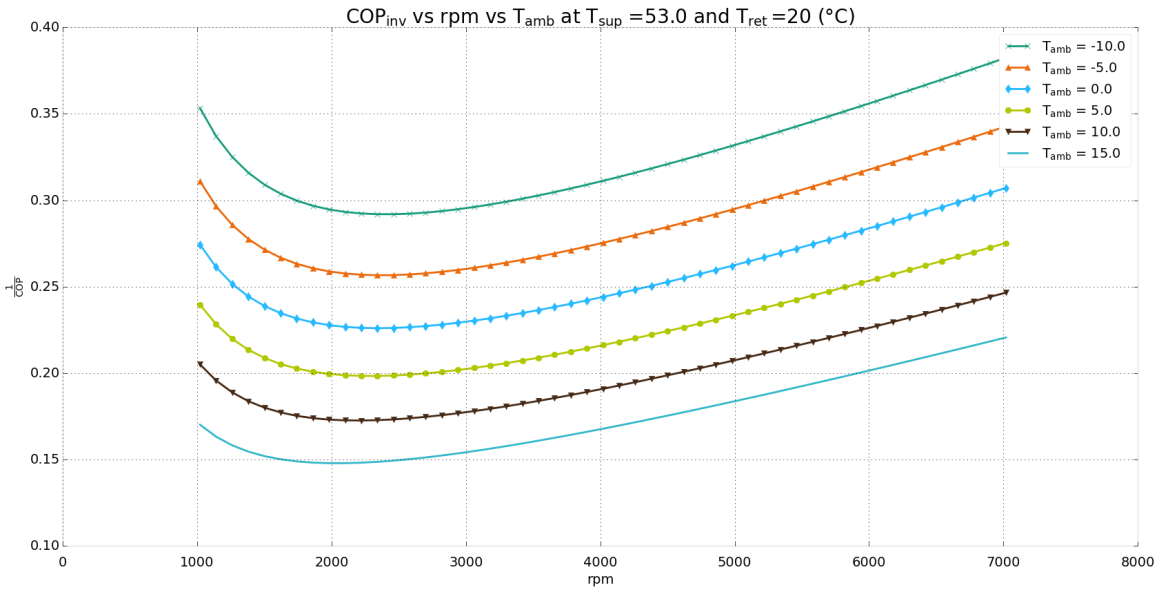

Figure 2-8: COP inverse variation with compressor rpm and ambient temperature at a given supply water temperature

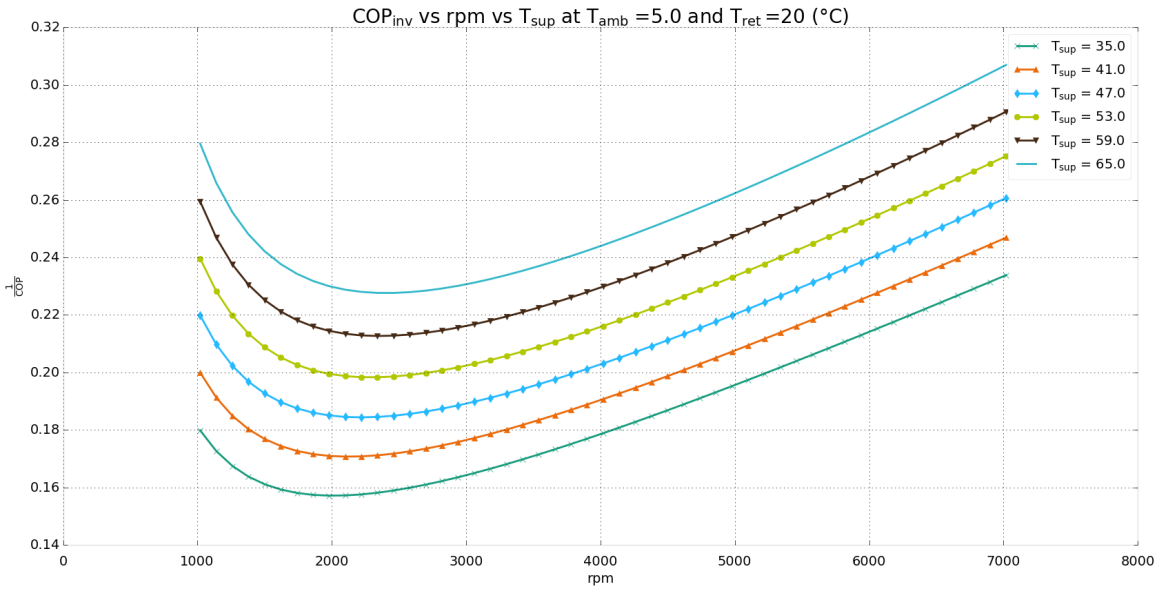

Figure 2-9: COP inverse variation with compressor rpm and supply water temperature at a given ambient temperature

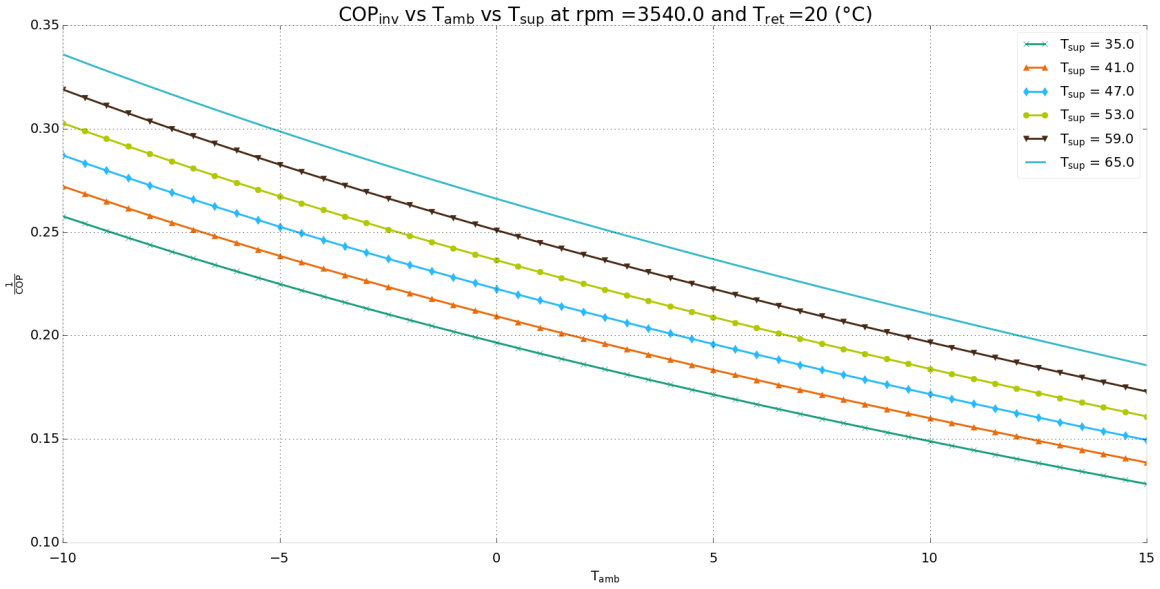

Figure 2-10: COP inverse variation with ambient and supply water temperature at a given compressor frequency

The main conclusions from the plots (Figures 2-8, 2-9 and 2-10) in comparison with the COP characteristics are as follows:

- The nonlinear variation of COP_{inv} against T_{amb} and T_{sup} is negligible as the curves in respective figures (2-8 and 2-9) are parallel to each other and mostly equidistant.

- Analogously, Figure 2-10 suggests that COP_{inv} variation with ambient temperature is independent of the supply temperature.
- These observations suggest that modeling the heat pump performance with inverse of COP has the advantage of obtaining more accurate relation with T_{amb} and T_{sup} while using a simple model structure.

Simplified model for inverse of COP

It is important to note that for non-tracking control problem formulations, ideally a perfect model for heat pump performance is essential such that it accurately describes all the characteristics and nonlinearities of COP while having a simple model structure. Taking this into account, a simpler nonlinear model which describes all the nonlinear characteristics, was derived from the detailed model. To overcome limitations of previous HP performance modeling approach, the data[6] used for fitting the model covered whole range of HP operation i.e. 1020 to 7020 rpm. The model structure and coefficients are given below:

$$\text{COP}_{\text{inv}} = \frac{1}{\text{COP}} = a_0 + a_1 \cdot T_{\text{sup}} + a_2 \cdot T_{\text{amb}} + a_3 \cdot \dot{Q}_{HP} + a_4 \cdot (\dot{Q}_{HP} - a_5)^{a_6} \tag{2-9}$$

Table 2-3: COP inverse model coefficients

Coefficient	Value	Unit
a_0	38.70223	-
a_1	0.00252	K^{-1}
a_2	-0.00749	K^{-1}
a_3	-8.33031	s/kJ
a_4	8.31627	s/kJ
a_5	4.46513	kW
a_6	1.00032	-

The data was fitted using nonlinear least squares algorithm. Optimization results with different initial guesses were observed and the best fit from the trials correspond to the values in Table 2-3 for (2-9).

Validation The degree of accuracy of the fit is measured through the statistical analysis presented as follows:

- Coefficient of determination (R^2) = 0.9349
  This (R^2 close to 1) indicates that the data from detailed model and (2-9) are strongly correlated. The correlation is graphically represented in Figure 2-11.
- The root mean square error RMSE = 0.01769 with coefficient of variation = 0.06888
- The normalized RMSE = 0.05487 i.e. 5.487%. With this it can be inferred that the model represents the true system with decent accuracy which also means that the characteristics of COP inverse are sufficiently captured.

[6]Number of data points = 51^3 (51 values each over whole range of T_{amb}, T_{sup} and rpm)

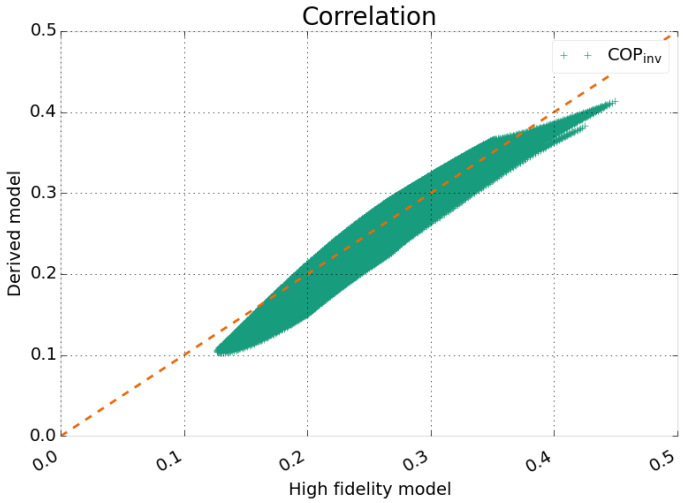

Figure 2-11: Validation of the fit for COP inverse model. The figure shows that the outputs from the detailed model and derived model are very close as the points are tightly clustered around the dashed line that represents perfect fit.

- The spread of the data from the detailed model (measured data) and simplified model (2-9) output is shown in Figure 2-12. It shows that only a small part of the original data was not fitted (the region with values between 0.4 and 0.45) which corresponds to low values of COP. The model sometimes also has values in the range 0.1 and 0.125 which were not present in the original data. These range of values also correspond to the higher offsets observed between data from detailed model and the derived model in Figure 2-11. In summary, the spread of data indicates that the model covers almost whole range of data with marginal offsets.

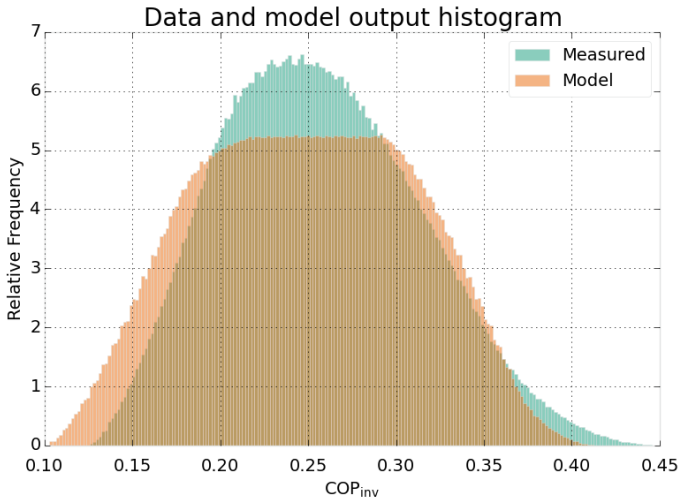

Figure 2-12: Histogram showing spread of data values

The validation results indicate sufficient accuracy to represent the true model for predicting the COP (inverse) behaviour. This model was used as the true system performance indicator to test the mismatch as no other model was available with the same set of inputs and outputs as required.

Summary In this chapter the residential heating system was described along with its mathematical model based on thermal energy balance. The characteristics of coefficient of performance of a capacity controlled heat pump were analysed in detail in order to model the heat pump. The simplified heat pump models which will be used in the next chapter were derived from a detailed TRNSYS model for application in optimal control problem formulations and calculation of the electricity bill. The next chapter describes the control algorithms in detail.

Chapter 3

Control strategy

The previous chapter described in detail the characteristics of the system which need to be taken into account while designing a controller. The focus of this chapter is the design of model predictive controller (Section 3-2). The performance benchmark for it is a rule based method described in Section 3-4. The specific objectives (Section 3-1) to be achieved by the control strategy while satisfying the constraints (Section 3-3-3) imposed by the system are explained in detail. Different optimization problem formulations (Section 3-3) are derived based on simplifications considered for achieving the same targets with a simpler and faster controller.

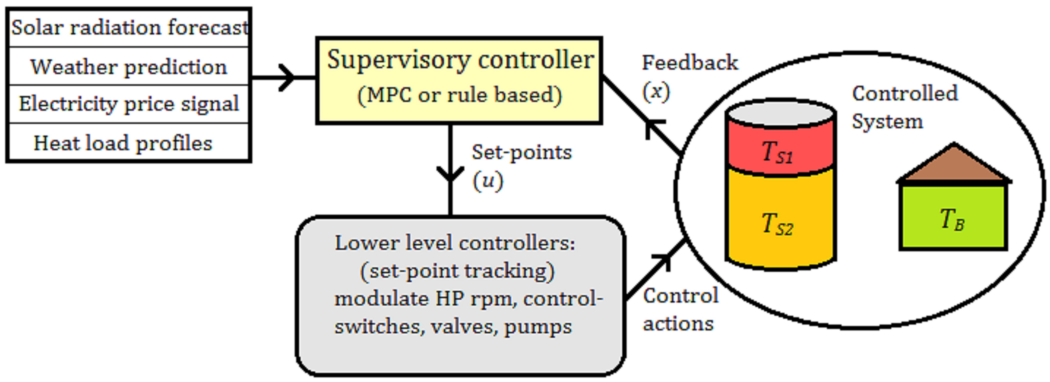

Figure 3-1: Building energy management system

3-1 Objectives of the control strategy

As discussed in Chapter 2, the focus is on design of supervisory control strategy for main system components (slow dynamics) and the control inputs are provided by subsystem components (fast dynamics) with lower level controllers. This hierarchy is described in Figure 3-1. In other words, the supervisory controller provides set-points which are perfectly tracked by

the second control layer for desired system performance. The information exchange and control action is provided by the subsystem components.

The set-points must be such that the following objectives are achieved:

- The electricity bill should be minimized. This means that the product of electricity consumption and cost of electricity should be minimized.
- Maximize the use of solar power, considering it to be cheaper than the conventional power source.
- The heat losses from the storage should be minimum.
- All constraints (Section 3-3-3) of the system must be satisfied in the cheapest possible way.

The supervisory controller also has the following tasks which can be achieved by setting the control inputs (Table 2-1):

- When considering use of solar power: decide whether to consume it for heating or sell it to the electricity grid. This is done by setting the decision variables $\dot{Q}_{HP_{1_{PV}}}$ and $\dot{Q}_{HP_{2_{PV}}}$.
- Determine the maximum quantity out of the available heat to be used from the STC. The corresponding decision variable is $\dot{Q}_{STC}$ and the available heat input is $\dot{Q}_{STC_{max}}$.
- Heat the building space over the lower limit on temperature when it is more cost efficient, while respecting the upper limit. This is to exploit the thermal inertia of the building without violating the thermal comfort requirements.
- Use the backup heaters only when the heat pump is not capable of delivering sufficient heat. This is because the backup heaters are not efficient but might be needed when the ambient air temperature is very low.
- At every time step (1 hour), the heat pump operates in two modes i.e. DHW and space heating. The supervisory controller sets the duration of operation in each mode. The relevant variables are $\dot{Q}_{HP_1}$, $\dot{Q}_{HP_2}$, $\dot{Q}_{HP_{1_{PV}}}$ and $\dot{Q}_{HP_{2_{PV}}}$.
  The fraction $(\dot{Q}_{HP_1} + \dot{Q}_{HP_{1_{PV}}})/(\dot{Q}_{HP_2} + \dot{Q}_{HP_{2_{PV}}})$ is the ratio of duration for which the heat pump operates in DHW mode and space heating mode (Section 3-3-2).

To judge the performance of different control strategies and compare them, a set of parameters need to be calculated. In this thesis, the following parameters were used to determine and compare the quality of the controller performance (Chapter 4). These parameters also summarize the control objectives and were also considered while formulating optimal control problems (Section 3-3) discussed later in this chapter.

Key performance indicators (KPIs)

- Money spent on heating: Minimizing the money spent by the end user is the primary goal of the controller. However, the controller which minimizes the money spent is not necessarily the most suitable one and other performance indicators are also considered.
- Money saved by local consumption of PV electricity: This indicates how much money the end user can save by using renewable energy devices for heating instead of selling to the grid for lower incentives. The controller should maximize this KPI.
- Money earned by feed-in of surplus PV electricity: When this locally produced electricity cannot be self-consumed, it will be contributed to the grid. Based on the feed-in tariff rates, the money earned is calculated. The feed-in tariffs are expected to sharply decline for PV generated electricity in near future. So if the money earned by feed-in is too high or considerably higher than the money saved by self consumption, the sizing of the solar panels needs to be reconsidered to have better returns over investment ratio.
- Electricity consumed for heating: This indicates how effective the control strategy is when minimizing indirect CO_2 emissions. This is usually not the concern of end user but important considering environmental factors and to quantify how much advanced control methods can contribute in emission reduction.
- Seasonal performance factor (SPF): SPF is defined as the ratio of the total heat supplied to the total work done by the heating system. It indicates how efficiently the heat pump is operated. Higher SPF indicates more efficient performance.
- Thermal losses of storage: The heat lost by the thermal storage must be minimum as this represents the heat wasted or indirectly the electricity wasted by storing in the form of heat. Higher storage losses indicate that the controller causes excessive heating of the TES. If the storage losses are very high for all control strategies, the inference that can be drawn is that the storage is over-sized or lacks desired insulation capacity.
- STC heat utilized: The controller should maximize the use of this free heat source which also means minimizing the heat wasted from this solar device. Again, if all controllers considered fail to utilize this effectively, the indication is that the STC is over-sized. Conversely, if always and almost all of the available heat is used, the indication is that the STC is under-sized.
- No. of HP on/off switchings: It is important to have minimum damage on the utility because of the control actions. This does not directly influence the electricity bill. However, this KPI is considered as a smooth operation of the heat pump is better for the overall performance of the equipment (minimum wear). This means that the controller should implicitly switch off the heat pump operation only when there is no demand for heat or heating the storage is not cost efficient. This seems to be obvious or trivial. However, due to limitation in the heat pump modulation (dead-band), whenever the desired control action corresponds to an input in the dead-band region, the controller keeps the heat pump turned on for a short duration - switches off and then again switches on at the next time step if needed in order to strictly respect the constraints

[0]The KPI calculations are briefly explained in Section A-4.

(Section 3-3-5). If the dead-band is neglected completely, it is impossible to strictly satisfy constraints of the system. Another alternative to completely avoid this switching behaviour in a post-processing step is to have the characteristic exactly defined in the objective function or control problem formulation which is out of the scope of this thesis work. This KPI shows the count for average number of times per unit time step when the input from the controller lies in the 'dead-zone'.

- Average computation time per step: This KPI indicates[1] the speed of computations for different controllers.

3-2 Model predictive control

Model predictive control (MPC) is a control algorithm which makes use of a model of the dynamical system to predict its future evolution in order to optimize the control signal. This section briefly explains why this control method is suitable for achieving the objectives described in previous section and some key properties.

3-2-1 Motivation

Model Predictive Control (MPC) [16] is the only control technique which can make use of future predictions during controller design while accounting for system operation constraints [17]. Predictive control offers the following properties which are essential for achieving the specified control objectives:

- Multivariable control
- Constraint handling
- It can incorporate prediction data
- Use of feedback by receding horizon principle
- Approximately optimal closed-loop performance

In predictive control, an open-loop finite horizon optimal control problem is solved at each time step to compute a sequence of control inputs over the horizon, using the current state information for predictions. The control signal which is applied to the system is only the first input from the sequence. At the next time step, the horizon is shifted and a new optimal control problem is solved based on the state update. This process of shifting the horizon at each step to incorporate feedback is usually referred to as *receding horizon principle* and hence MPC is also known as receding horizon control. The closed-loop performance of MPC depends on the cost function (performance index) and tuning parameters which include length of the finite horizon (prediction horizon) and length of the control horizon (degrees of freedom).

[1] Based on simulations on computer with processor specification: Intel Core i5-3337U CPU @ 1.80GHz × 4

3-2-2 Tuning parameters

Prediction horizon (N): It is defined as the number of time steps which represents the length of the finite horizon over which the open-loop optimal control problem is solved at each time step. A higher value of N allows use of more predictions at the cost of larger sized optimization problem, which generally gives a better performance on account of higher flexibility but that might not be the case if there is a mismatch in predictions. Hence, it has to be tuned to solve this trade-off. We use a prediction horizon of 12 time steps which is equivalent to 12 hours of time and hence, at each step prediction data of next 12 hours is also incorporated in the optimization problem i.e. $N = 12$.

Control horizon: It is defined as the number of time steps over which the control sequence is optimized at each time step. Tuning it to a value lesser than N leads to lesser degrees of freedom and more aggressive control actions. In order to have controller with maximum flexibility, this value was kept at its maximum value equal to the length of prediction horizon N.

3-2-3 Economic MPC

In conventional reference tracking problems, MPC is typically formulated with a quadratic cost function which penalizes the deviations of state and inputs from their optimal steady-state values over the prediction horizon. Since the control objectives defined in Section 3-1 do not include reference tracking of any state or output variable, the conventional quadratic cost function is not suitable for achieving the optimal control action. For example, if the reference for the state is assumed to be its lower bound, a conventional quadratic cost function described previously would mean that the objective is to minimize the storage and building temperatures with minimum control action. However, a positive deviation from the target could lead to a more *profitable* control action that minimizes the electricity bill, which is the main *economic* objective. In order to avoid this drawback of the conventional quadratic cost function, we use an economic objective function, which directly or indirectly reflects the process economics i.e. represents the control objectives. In recent literature, this predictive control approach is usually referred as *economic model predictive control* [18], [19], [20]. The predictive control strategies discussed in this thesis follow this approach and differ in formulation of the cost function.

3-3 MPC problem formulations

This section presents the optimal control problem formulations considered for achieving the objectives of the control strategy. To represent the electricity bill characteristics in the objective function, the nonlinear heat pump performance models were used. To derive convex problem formulations, simplifications were made as explained in the following subsections (Sections 3-3-6 and 3-3-7). The influence of these simplifications were analysed through simulation results and further modifications were made accordingly to overcome the limitations while preserving the convexity of the problem formulation. The performance achieved with the best convex formulation must be compared with a nonlinear non-convex optimization based control method to check the performance loss due to the simplifications considered.

This was done by formulating the nonlinear non-convex optimal control problem (Section 3-3-8) using the heat pump model (2-9) as it is in the cost function (Note: The heat pump performance model used to derive the formulations in Sections 3-3-6 and 3-3-7 was the COP model (2-8) as the model (2-9) was obtained during a later stage of the work. However, it does not change the formulation method and conclusions which will be obvious from the relevant sections).

3-3-1 Objective function definition

The main objective of the controller is to minimize the electricity bill of the residential heating system and the remaining objectives directly or indirectly comply with the same target. For example, minimizing the heat lost by storage is explicitly defined as a control objective but optimizing the electricity bill needs minimum power consumption, which would indirectly minimize losses. Hence, the economics of the system defined solely through the electricity bill subject to constraints (Section 3-3-3) incorporates all the control objectives (Section 3-1). The control input sequence over the prediction horizon at any time step t can be defined as the solution of the following optimal control problem:

$$\min_{U_t'} \underbrace{\sum_{k=0}^{N-1} \text{Bill}_{t+k|t}(x_{t+k|t}, u_{t+k|t}, z_{t+k}, d_{t+k})}_{J} \tag{3-1a}$$

$$\text{s.t. } x_{t+k+1|t} = A_d x_{t+k|t} + B_d u_{t+k|t} + E_d z_{t+k}, \forall k = 0, 1, ..., N-1 \tag{3-1b}$$

$$u_{t+k|t} \in \mathcal{U}(t+k), \forall k = 0, 1, ..., N-1 \tag{3-1c}$$

$$x_{t+k|t} \in \mathcal{X}(t+k), \forall k = 1, 2, ..., N \tag{3-1d}$$

$$x_{t|t} = x(t) \tag{3-1e}$$

Equation (3-1a) represents the time-varying cost which is a function of the state variables (x), inputs (u), known disturbances (z), and vector of external signals (d) which contains the following information: ambient temperature forecast and electricity price predictions (grid and feed-in). The subscript '$t+k|t$' assigned to these variables represents value of the variable at time step $t+k$ as predicted at time step t. The symbol $U_t' = \left[u_{t|t}^T \; u_{t+1|t}^T \; \cdots \; u_{t+N-1|t}^T \right]^T$ represents the vector of decision variables. The prediction of the system state at any time step $t+k$ is defined as a function of the decision variables by applying the initial condition $x(t)$ i.e. $x_{t|t}$ to the LTI discrete-time state space model (3-1b). Equations (3-1c) and (3-1d) represent the time-varying constraints on input and state variables respectively where $\mathcal{U}(t+k) \subseteq \mathbb{R}^8$ denotes the feasible set of inputs and $\mathcal{X}(t+k) \subseteq \mathbb{R}^3$ denotes the permissible set of state variables at time step $t+k$. These time-varying bounds are defined by ambient temperature (T_{amb}), predicted data for solar radiation and availability of the PV electricity for heating as explained in Section 3-3-3. The formulations described in the following sections differ in the description of the bill (3-1a) as a function of the state and exogenous input variables. A general description of the 'bill' which will be used later in this section for describing each formulation is given below (Section 3-3-2).

3-3-2 Electricity bill for heating

The electricity bill *per unit sampling time* can be expressed as follows:

$$\text{Bill} = \text{ecost} \times (P_{el_{HP}} + P_{el_{BH}}) + \text{PVcost} \times P_{el_{PV}} \tag{3-2}$$

In the above expression, $P_{el_{HP}}$ represents the electrical power consumed by the heat pump using power from the grid which does not include the power input from solar energy produced on-site. $P_{el_{BH}}$ is the power consumed by the auxiliary (backup) heaters and $P_{el_{PV}}$ represents the electrical power utilised from the solar PV panels for the purpose of heating. The price signals 'ecost' and 'PVcost' represent the cost of electricity obtained from the grid, and feed-in tariff for solar power respectively. To complete the definition of the bill, the expressions for $P_{el_{HP}}$, $P_{el_{PV}}$ and $P_{el_{BH}}$ are derived as follows considering the operation of heat pump in two modes.

Heat pump operation The heat pump supplies heat to the stratified thermal storage which is considered to be having two layers at temperatures T_{S_1} and T_{S_2} for domestic hot water (DHW) supply and space heating (Htg). The heat pump system supplies water at a higher temperature to the top part of the storage (T_{sup_1}) and at a lower temperature to the bottom part (T_{sup_2}) as required ($T_{S_1} \geq T_{S_2}$) such that $T_{\text{sup}_i} = T_{S_i} + \Delta T, i \in \{1, 2\}$ where T_{sup_i} is assumed to be greater than the storage temperature by a constant difference $\Delta T = 2°\text{C}$. For this reason the heat pump operation is considered to be analogous to parallel operation (sum) of two virtual heat pumps (HP_1 and HP_2) working at different operating points. In reality there is a single heat pump (actuator) which cannot supply water at two different temperatures at the same time. However, it can be operated for a fraction of the sampling period with supply temperature of T_{S_1} and for the remaining time with supply temperature of T_{S_2} at a constant rate of heat delivered $\dot{Q}_{HP}$. The difference in supply temperatures at same operating heat transfer rate is brought about by the pump (sub-system) in the water loop (load side) which controls the mass flow rate in that loop. The change in the supply temperatures of the heat pump changes COP during the two parts of the operation in one sample time h. Per unit sample time, the rate of heat transfer of the HP should be equal to the sum of rate of heat delivered by the two virtual heat pumps in order to deliver the same quantity of heat during that time step of h units. We know that:

$$Q_{HP_1} = \dot{Q}_{HP_1} \cdot h \quad \text{(heat supplied by HP}_1 \text{ at } T_{\text{sup}_1} \text{ during sampling time } h) \tag{3-3a}$$

$$Q_{HP_2} = \dot{Q}_{HP_2} \cdot h \quad \text{(heat supplied by HP}_2 \text{ at } T_{\text{sup}_2} \text{ during sampling time } h) \tag{3-3b}$$

From the optimization solution the values of $\dot{Q}_{HP_1}$ and $\dot{Q}_{HP_2}$ are known which means Q_{HP_1} and Q_{HP_2} can be calculated from the above equations. The heat produced by heat pump during one sample is Q_{HP} which is the sum of the heat produced by the two virtual heat pumps:

$$\dot{Q}_{HP} \cdot h = Q_{HP} = Q_{HP_1} + Q_{HP_2} \tag{3-4}$$

From (3-3) and (3-4),

$$\dot{Q}_{HP} = \dot{Q}_{HP_1} + \dot{Q}_{HP_2} \tag{3-5}$$

From the above equation, the rate of heat to be supplied by the heat pump during each sampling period is calculated. We get $h_1 + h_2 = h$ where h_1 and h_2 are defined as:

$$h_1 = \frac{Q_{HP_1}}{\dot{Q}_{HP}} \tag{3-6}$$

$$h_2 = \frac{Q_{HP_2}}{\dot{Q}_{HP}} \tag{3-7}$$

Using first part of (3-4),

$$\frac{h_1}{h} = \frac{Q_{HP_1}}{Q_{HP}} \tag{3-8a}$$

$$\frac{h_2}{h} = \frac{Q_{HP_2}}{Q_{HP}} \tag{3-8b}$$

From the above equations it is known that for how much time the heat pump should operate in DHW mode ($T_{\sup_1}$) and space heating mode ($T_{\sup_2}$).

Calculation of power consumed Without loss of generality, it can be assumed that the heat pump operates in the first part of the sampling period (h_1 units) in DHW mode and the second (h_2 units) in space heating mode. This means the heat pump first supplies absolute heat of Q_{HP_1} and then Q_{HP_2} which makes the total heat supplied during the sample as required i.e. Q_{HP}. The power consumed ($P_{el_{HP}}$) is different during the two parts ($P_{el_{HP1}}$ and $P_{el_{HP2}}$) of the sampling period depending on the COP as the rate of heat transfer $\dot{Q}_{HP}$ remains same during that period. Hence, the electrical power consumed during h time units ($P_{el_{HP}}$) is the weighted mean of $P_{el_{HP1}}$ and $P_{el_{HP2}}$. This can be explained mathematically as follows:

Let W_1 represent the work done while operating in DHW mode to produce Q_{HP_1} units of heat and W_2 represent the work done while operating in space heating mode. The total work done is the sum of work done in each operating mode:

$$W = W_1 + W_2 \tag{3-9}$$

The power consumed during each part of h is the ratio of the work done and the time for the corresponding mode of operation.

$$W_1 = P_{el_{HP1}} \cdot h_1 \tag{3-10a}$$

$$W_2 = P_{el_{HP2}} \cdot h_2 \tag{3-10b}$$

Substituting these equations in (3-9),

$$W = P_{el_{HP1}} \cdot h_1 + P_{el_{HP2}} \cdot h_2 \tag{3-11}$$

$$W = P_{el_{HP}} \cdot h \tag{3-12}$$

$$\implies P_{el_{HP}} \cdot h = P_{el_{HP1}} \cdot h_1 + P_{el_{HP2}} \cdot h_2$$

$$\implies P_{el_{HP}} = P_{el_{HP1}} \cdot \frac{h_1}{h} + P_{el_{HP2}} \cdot \frac{h_2}{h} \tag{3-13}$$

It is known that the heat transfer rate is the same during the sample but with different COPs for the two parts depending on the supply temperature. Using the definition of COP (Section 2-3-1):

$$P_{el_{HP1}} = \frac{\dot{Q}_{HP}}{\text{COP}_1} \tag{3-14}$$

$$P_{el_{HP2}} = \frac{\dot{Q}_{HP}}{\text{COP}_2} \tag{3-15}$$

Substituting (3-14), (3-15) and (3-8) in (3-13),

$$P_{el_{HP}} = \frac{\dot{Q}_{HP}}{\text{COP}_1} \cdot \frac{Q_{HP_1}}{Q_{HP}} + \frac{\dot{Q}_{HP}}{\text{COP}_2} \cdot \frac{Q_{HP_2}}{Q_{HP}}$$

From (3-4) and (3-3),

$$P_{el_{HP}} = \frac{\dot{Q}_{HP_1}}{\text{COP}_1} + \frac{\dot{Q}_{HP_2}}{\text{COP}_2} \tag{3-16}$$

Using the same analogy, an expression for $P_{el_{PV}}$ can be written as:

$$P_{el_{PV}} = \frac{\dot{Q}_{HP_{1_{PV}}}}{\text{COP}_1} + \frac{\dot{Q}_{HP_{2_{PV}}}}{\text{COP}_2} \tag{3-17}$$

Assuming ideal backup electrical heaters for which the COP is 1, the expression for $P_{el_{BH}}$ can be written as follows:

$$P_{el_{BH}} = \dot{Q}_{BH_1} + \dot{Q}_{BH_2} \tag{3-18}$$

Substituting (3-16), (3-17) and (3-18) in (3-2) completes the general description of the bill in terms of the input variables and coefficient of performance:

$$\text{Bill} = \text{ecost} \times \left(\frac{\dot{Q}_{HP_1}}{\text{COP}_1} + \frac{\dot{Q}_{HP_2}}{\text{COP}_2} + \dot{Q}_{BH_1} + \dot{Q}_{BH_2} \right) + \text{PVcost} \times \left(\frac{\dot{Q}_{HP_{1_{PV}}}}{\text{COP}_1} + \frac{\dot{Q}_{HP_{2_{PV}}}}{\text{COP}_2} \right) \tag{3-19}$$

3-3-3 Constraints

The physical limits of the system components define the *hard constraints* which must be satisfied, whereas the performance requirements limit the range of system's state variables i.e. storage and zone temperatures. These limits are explained in this section and the compact notation in matrix form which define the sets $\mathcal{U}$ and $\mathcal{X}$ introduced earlier is derived in Section 3-3-6.

Storage temperature limits

In order to satisfy performance specifications, the hot water from storage layers must be supplied at a temperature within a certain range. For this purpose the storage layers must be maintained within that desired temperature range. Moreover, considering stratification,

the temperature of the upper storage layer (T_{S_1}) must be greater than the temperature of the lower storage layer (T_{S_2}). Mathematically,

$$\underline{T}_{S_1} \leq T_{S_1} \leq \bar{T}_{S_1} \tag{3-20}$$
$$\underline{T}_{S_2} \leq T_{S_2} \leq \bar{T}_{S_2} \tag{3-21}$$
$$T_{S_2} \leq T_{S_1} \tag{3-22}$$

In the above equations $\underline{T}_{S_1}$ and $\underline{T}_{S_2}$ represent the lower bounds on the upper and lower storage layers respectively whereas $\bar{T}_{S_1}$ and $\bar{T}_{S_2}$ represent the corresponding upper bounds. These bounds are time-varying and are calculated as follows using the ambient temperature (T_{amb}) data:

$$\underline{T}_{S_2} = \max(T_{HC},\, 30)\,^{\circ}\text{C} \tag{3-23}$$
$$T_{HC} = -0.0106 \cdot T_{\text{amb}}^2 - 1.12 \cdot T_{\text{amb}} + 46.316\,^{\circ}\text{C} \tag{3-24}$$
$$\underline{T}_{S_1} = \max(\underline{T}_{S_2},\, 50)\,^{\circ}\text{C} \tag{3-25}$$
$$\bar{T}_{S_2} = \max(T_{HC},\, 60)\,^{\circ}\text{C} \tag{3-26}$$
$$\bar{T}_{S_1} = 62^{\circ}\text{C} = 335\,\text{K} \tag{3-27}$$

Note: When the heat available from STC is greater than the DHW demand, $\bar{T}_{S_1}$ is lifted[2] by 10°C to 72°C. Equation (3-24) represents the heating curve where T_{HC} is the minimum supply water temperature for space heating depending on the ambient temperature.

Thermal comfort

The building (zone) temperature (T_B) has to be maintained in a range which depends on the allowed range of human thermal comfort levels. This can also be fixed to a single temperature value. However, in order to benefit from the thermal inertia of the building, the following range was considered:

$$\underline{T}_B \leq T_B \leq \bar{T}_B \quad \text{where,} \quad \underline{T}_B = 20^{\circ}\text{C} = 293\,\text{K} \quad \text{and} \quad \bar{T}_B = 21^{\circ}\text{C} = 294\,\text{K} \tag{3-28}$$

Heating capacity

Since the heat pump extracts heat from the environment, the maximum heating capacity limit $\bar{\dot{Q}}_{HP}$ also depends on the ambient temperature. Besides that, it also depends on the supply water temperature and is calculated from the high fidelity heat pump model f_H (Section 2-3-1) at maximum rpm (compressor frequency) and the constant return water temperature considered.

$$\bar{\dot{Q}}_{HP} = f_H(T_{\text{amb}},\, T_{\text{sup}},\, \text{rpm} = 7020,\, T_{\text{ret}} = 20^{\circ}\text{C}) \tag{3-29}$$

The value of T_{sup} assumed[3] was 2 units plus the mean of $\underline{T}_{S_1}$ and $\underline{T}_{S_2}$. Similarly, the minimum ($\underline{\dot{Q}}_{HP}$) and optimal ($\dot{Q}_{\text{opt}}$) heat transfer rates were calculated at respective rpm values (1020

[2]Performance specification to store STC heat

[3]Note: The value of supply water temperature is 2 units plus the corresponding storage layer temperature

and 2300). Using the definition (3-29), the time-varying bound on heat pump inputs can be expressed as:

$$0 \leq \dot{Q}_{HP} \leq \bar{\dot{Q}}_{HP}, \text{ where,} \tag{3-30}$$

$$\dot{Q}_{HP} = \dot{Q}_{HP_1} + \dot{Q}_{HP_2} + \underbrace{\dot{Q}_{HP_{1_{PV}}} + \dot{Q}_{HP_{2_{PV}}}}_{=\dot{Q}_{HP_{PV}}} \tag{3-31}$$

The backup heaters operate on electricity and have time-invariant bounds:

$$0 \leq \dot{Q}_{BH_i} \leq 5\,\text{kW},\ i \in \{1, 2\} \tag{3-32}$$

The maximum rate of heat transfer from the storage to the building for space heating is 40 kW:

$$0 \leq \dot{Q}_{Htg} \leq 40\,\text{kW}, \tag{3-33}$$

Solar power

The prediction data includes information regarding the PV electricity available, electrical load profile of the house and solar radiation forecast[4]. Using this data, the maximum heat production using solar power ($\bar{\dot{Q}}_{HP_{PV}}$ and $\bar{\dot{Q}}_{STC}$) is estimated from prediction models. This gives the estimated time-varying bounds on the solar input variables:

$$0 \leq \dot{Q}_{HP_{PV}} \leq \bar{\dot{Q}}_{HP_{PV}} \tag{3-34}$$

$$0 \leq \dot{Q}_{STC} \leq \bar{\dot{Q}}_{STC} \tag{3-35}$$

Prediction data

The known disturbances i.e. heat load for DHW ($\dot{Q}_{DHW}$) and space heating ($\dot{Q}_{B_{\text{loss}}}$) are obtained from statistical data developed by Fraunhofer ISE. The storage environment temperature (included in known disturbances) was considered to be constant = 20°C. For the 12 day simulations[5], the required data was converted from a whole year data (2012) using statistical methods in a parallel project at ISE [21]. This 12 *test days* data mainly includes characteristics of all seasons through typical days represented as January 1 to January 12, 2012 timeseries' in the results. It is important to note that all the prediction models, data and load profiles are considered to be perfect.

3-3-4 Feasibility

The constrained optimal control problem (3-1) might not always be feasible which means that the existence of an optimal solution is not guaranteed. This is mainly because:

- The control horizon (also the prediction horizon) is limited to 12 hours (finite).

[4] Using 2012 field test data from Fraunhofer ISE

[5] Results presented later in this chapter and the next one

- The heat pump has a limited heating capacity due to which under extreme conditions there is a chance that the storage and/or building temperature cannot be brought back in the desired range (state constraints) in this given time limit.
- The heat pump considered in the system cannot cool which means if any of the temperatures need to be reduced to a lower value in a certain duration of time, there is a possibility that no control action can achieve it.
- The initial condition (3-1e) may belong to the set of states discussed in the previous two statements.

In order to guarantee feasibility of the optimal control problem at any time step, a soft constraints approach was used. The input constraints (hard constraints) cannot be relaxed due to physical limitations. The state constraints which are limited by performance specifications (soft constraints) can however be relaxed by compromising the performance in case of infeasibility, by introducing non-negative scalar slack variables (ε_1, ε_2) in the formulation which collect the constraint violations. Problem (3-1) can then be re-stated as follows:

$$\min_{U_t} J + \underbrace{\sum_{k=1}^{N}\sum_{i=1}^{2}(\rho_1 \varepsilon_{i_{t+k|t}} + \rho_2 \varepsilon^2_{i_{t+k|t}})}_{J_{soft}} \tag{3-36a}$$

$$\begin{aligned}
\text{s.t. } & x_{t+k+1|t} = A_d x_{t+k|t} + B_d u_{t+k|t} + E_d z_{t+k}, \forall k = 0, 1, ..., N-1 \\
& u_{t+k|t} \in \mathcal{U}(t+k), \forall k = 0, 1, ..., N-1 \\
& \underline{x}_{t+k|t} - \begin{bmatrix} 1 \\ 1 \\ 1 \end{bmatrix} \varepsilon_{2_{t+k|t}} \leq x_{t+k|t} \leq \bar{x}_{t+k|t} + \begin{bmatrix} 1 \\ 1 \\ 1 \end{bmatrix} \varepsilon_{1_{t+k|t}}, \forall k = 1, 2, ..., N \qquad \text{(3-36b)} \\
& T_{S_{2_{t+k|t}}} \leq T_{S_{1_{t+k|t}}}, \forall k = 0, 1, ..., N \qquad \text{(3-36c)} \\
& x_{t|t} = x(t) \\
& \varepsilon_{1_{t+k|t}}, \varepsilon_{2_{t+k|t}} \geq 0 \qquad \text{(3-36d)}
\end{aligned}$$

Equation (3-36) represents the soft-constrained problem where the vector of decision variables is $U_t = \begin{bmatrix} u_{t|t}^T & \varepsilon_{t+1|t}^T & u_{t+1|t}^T & \varepsilon_{t+2|t}^T & \cdots & u_{t+N-1|t}^T & \varepsilon_{t+N|t}^T \end{bmatrix}^T$ with $\varepsilon = \begin{bmatrix} \varepsilon_1 & \varepsilon_2 \end{bmatrix}^T$ denoting the vector of two slack variables. Slack variable ε_1 relaxes the upper bounds ($\bar{x} = \begin{bmatrix} \bar{T}_{S_1} & \bar{T}_{S_2} & \bar{T}_B \end{bmatrix}^T$) on the state constraints while ε_2 relaxes the lower bounds ($\underline{x} = \begin{bmatrix} \underline{T}_{S_1} & \underline{T}_{S_2} & \underline{T}_B \end{bmatrix}^T$) as indicated in (3-36b) where $x = \begin{bmatrix} T_{S_1} & T_{S_2} & T_B \end{bmatrix}^T$. The constraint violations are penalized by using the sum of a linear cost with penalty ρ_1 and a quadratic cost with penalty ρ_2. In order to ensure that the slack variables are non-zero only at time instants when the original hard-constrained problem is infeasible (exactness), the weights ρ_1 and ρ_2 must be such that we have 'exact soft constraints' as defined and described in detail in [22]. To have exact soft constraints, the weight ρ_1 must be greater than the infinity norm of the vector of Lagrange multipliers of the original problem as derived in [23]. The weight ρ_2 is an extra (quadratic cost) penalty which can be zero as it is not necessary for ensuring exactness and moreover, only using a quadratic weight does not satisfy conditions for exactness [16], [23] but it can be used with the exact (linear) penalty for smoothness of the problem (except for linear programming formulation) [16]. Hence, ρ_1 (constant) was tuned to be sufficiently high such that exactness is guaranteed and that it does not cause numerical issues due to poor scaling. This approach guaranteed feasibility of the optimization problem while satisfying conditions for 'exactness' of the soft-constrained problem's solution.

3-3-5 Dead-zone treatment

As explained earlier in Section 2-1, the heat pump has a dead-band, the range of which roughly corresponds to around 15% of maximum capacity. Neglecting this characteristic while designing a control strategy leads to constraint violations when the desired control input corresponds to the dead-band range. Notably, the constraint violations caused by neglecting it would be different for different control strategies which does not provide a fair comparison. A possible solution is to raise the lower bounds to be maintained but this option does not lead to best solution as it increases costs and heat losses. Hence, to guarantee constraint satisfaction while considering this dead-zone characteristic for a fair comparison of different formulations, a post-processing step was used as proposed in [4] such that the solution of the optimal control problem is not modified. This is possible by following the post-processing step described below:

- When the control input is such that (referring (3-31)):

$$\dot{Q}_{HP} < \underline{\dot{Q}}_{HP},$$

- The heat pump is operated by the lower level controllers at the minimum capacity $\underline{\dot{Q}}_{HP}$ for a duration such that the same amount of absolute heat Q_{HP} is delivered during the sampling period of h units.

- The duration of this operation is the product of sampling time for the control input and, the ratio of $\underline{\dot{Q}}_{HP}$ to $\dot{Q}_{HP}$. After this the heat pump is switched off as the required amount of heat to be transferred is delivered as indicated by the supervisory controller.

Usually, the thermal load is such that the heat pump does not need to operate much at the minimum capacity in this manner. However, since the dead-zone is not treated directly by the optimal control problem, the results include the number of times this switching process occurs (KPI); so that if it is too frequent it can be concluded that additional considerations need to be made in the controller design for implicit treatment. This would also indicate whether the heat pump is over-sized considering the thermal load (assuming the load profile to be appropriate). It is important to note that switching to operate at a more efficient frequency would seem to be an obviously better solution but it has not been done considering that it decreases the run-time for the heat pump between two 'on' phases. It was confirmed from the heat pump manufacturer (Stiebel Eltron) that 10 minutes or higher is the target minimal run-time for maintaining compressor durability.

3-3-6 Linear programming formulation

The cost function (J in (3-1a)) to be optimized can be derived as a function of the exogenous signals as follows by using the COP model (2-8) and substitution in (3-19):

$$\text{COP} = (a_0 + a_1 T_{\text{sup}} + a_2 T_{\text{amb}}) \left(1 + a_3 \frac{\dot{Q}_{HP}}{\underline{\dot{Q}}_{HP}}\right)$$

Based on the explanation of heat pump operation in two modes (Section 3-3-2),

$$\mathrm{COP}_i = (a_0 + a_1 T_{\mathrm{sup}i} + a_2 T_{\mathrm{amb}}) \left(1 + a_3 \frac{\dot{Q}_{HP}}{\bar{\dot{Q}}_{HP}}\right), \; i \in \{1, 2\}$$

Substituting the supply temperature to be 2 degrees higher than the storage temperature, we get,

$$\mathrm{COP}_i = (a_0' + a_1 T_{S_i} + a_2 T_{\mathrm{amb}}) \left(1 + a_3 \frac{\dot{Q}_{HP}}{\bar{\dot{Q}}_{HP}}\right), \; i \in \{1, 2\} \tag{3-37}$$

where, $a_0' = a_0 + 2a_1$ (Table 2-2). Equation (3-37) describes the COP as a nonlinear function of state variables and inputs. Substituting it in (3-19) leads to a nonlinear non-convex optimization problem. In order to obtain a convex optimal control problem, simplifications are required. Linearizing the COP with respect to T_S and $\dot{Q}_{HP}$ also leads to a nonlinear non-convex formulation because the linearized result is multiplied with decision variables as indicated in (3-19). Hence, the influence of part load operation and storage temperatures must be neglected. It is important to note that in this way, the problem formulation essentially becomes independent of the detailed heat pump model as the variation of COP w.r.t. ambient temperature can be explicitly defined without the model. This also means that the COP becomes a function (g) of ambient temperature only and does not vary with respect to the state and input variables. The relation is shown below where the storage temperatures were replaced by their lower bounds (function of T_{amb}) and the rate of heat transfer was replaced by the estimated value at optimal efficiency which varies with respect to ambient temperature (Section 3-3-3).

$$\mathrm{COP}_i = (a_0' + a_1 \underline{T}_{S_i} + a_2 T_{\mathrm{amb}}) \left(1 + a_3 \frac{\dot{Q}_{opt}}{\bar{\dot{Q}}_{HP}}\right) = g(T_{\mathrm{amb}}) \tag{3-38}$$

$$\text{Let, } C_i = \frac{1}{\mathrm{COP}_i}, i \in \{1, 2\} \tag{3-39}$$

Using the above relations in (3-19), the heating bill can be expressed as follows:

$$\mathrm{Bill} = \mathrm{ecost} \times \left(C_1 \cdot \dot{Q}_{HP_1} + C_2 \cdot \dot{Q}_{HP_2} + \dot{Q}_{BH_1} + \dot{Q}_{BH_2}\right) + \mathrm{PVcost} \times \left(C_1 \cdot \dot{Q}_{HP_{1_{PV}}} + C_2 \cdot \dot{Q}_{HP_{2_{PV}}}\right) \tag{3-40}$$

Equation (3-40) can be written in matrix form as a linear function of the control input vector ($u \in \mathbb{R}^8$) as follows:

$$\mathrm{Bill} = l \cdot u \tag{3-41}$$

$$\text{where, } l = \begin{bmatrix} \mathrm{ecost} \cdot C_1 \\ \mathrm{ecost} \cdot C_2 \\ 0 \\ \mathrm{ecost} \\ \mathrm{ecost} \\ \mathrm{PVcost} \cdot C_1 \\ \mathrm{PVcost} \cdot C_2 \\ 0 \end{bmatrix}^T \text{ and } u = \begin{bmatrix} \dot{Q}_{HP_1} \\ \dot{Q}_{HP_2} \\ \dot{Q}_{Htg} \\ \dot{Q}_{BH_1} \\ \dot{Q}_{BH_2} \\ \dot{Q}_{HP_{1_{PV}}} \\ \dot{Q}_{HP_{2_{PV}}} \\ \dot{Q}_{STC} \end{bmatrix} \tag{3-42}$$

The time-varying values in matrix l are defined by the electricity price and ambient temperature data (forecast). Substituting the above expression in (3-36a), the following constrained optimal control problem can be defined:

$$\min_{U_t} \sum_{k=0}^{N-1} l_{t+k} \cdot u_{t+k|t} + \sum_{k=1}^{N} \rho_1 \mathbf{1}_{(1\times 2)} \varepsilon_{t+k|t} \tag{3-43a}$$

$$\text{s.t. } x_{t+k+1|t} = A_d x_{t+k|t} + B_d u_{t+k|t} + E_d z_{t+k}, \forall k = 0, 1, ..., N-1 \tag{3-43b}$$

$$M u_{t+k|t} \leq m_{t+k} \text{ and } -I_8 u_{t+k|t} \leq \mathbf{0}_{(8\times 1)}, \forall k = 0, 1, ..., N-1 \tag{3-43c}$$

$$x_{t+k|t} \leq \bar{x}_{t+k|t} + \mathbf{1}_{(3\times 1)} \varepsilon_{1_{t+k|t}}, \forall k = 1, 2, ..., N \tag{3-43d}$$

$$-x_{t+k|t} \leq \mathbf{1}_{(3\times 1)} \varepsilon_{2_{t+k|t}} - \underline{x}_{t+k|t}, \forall k = 1, 2, ..., N \tag{3-43e}$$

$$\begin{bmatrix} -1 & 1 & 0 \end{bmatrix} x_{t+k|t} \leq 0, \forall k = 0, 1, ..., N \tag{3-43f}$$

$$x_{t|t} = x(t) \tag{3-43g}$$

$$-I_2 \varepsilon_{t+k|t} \leq \mathbf{0}_{(2\times 1)} \tag{3-43h}$$

Equation (3-43a) represents the cost function for optimal control as a linear function of the decision variables. The matrix notation I_a denotes an identity matrix of size a whereas $\mathbf{1}$ and $\mathbf{0}$ denote matrices with ones and zeros as all entries respectively with their dimensions indicated in the subscript. Equations (3-43b) to (3-43h) mathematically represent the linear constraints explained in Section 3-3-3 where the matrices $M \in \mathbb{R}^{6\times 8}$ and $m \in \mathbb{R}^6$ which define the upper bound on inputs (Referring eqs. (3-30) and (3-32) to (3-35)) are:

$$M = \begin{bmatrix} 1 & 1 & 0 & 0 & 0 & 1 & 1 & 0 \\ 0 & 0 & 1 & 0 & 0 & 0 & 0 & 0 \\ 0 & 0 & 0 & 1 & 0 & 0 & 0 & 0 \\ 0 & 0 & 0 & 0 & 1 & 0 & 0 & 0 \\ 0 & 0 & 0 & 0 & 0 & 1 & 1 & 0 \\ 0 & 0 & 0 & 0 & 0 & 0 & 0 & 1 \end{bmatrix} \text{ and } m = \begin{bmatrix} \bar{\dot{Q}}_{HP} \\ 40 \\ 5 \\ 5 \\ \bar{\dot{Q}}_{HP_{PV}} \\ \bar{\dot{Q}}_{STC} \end{bmatrix}$$

The optimal control problem (3-43) is convex as it has a linear cost function subject to linear constraints. It can be compactly written by describing (3-43a) and constraints over the prediction horizon as a function of the vector of decision variables U_t (defined in Section 3-3-4), by substituting the state-space equations (3-43b) using the initial condition (3-43g), in eqs. (3-43d) to (3-43f):

$$\min_{U_t} L_t \cdot U_t \tag{3-44a}$$

$$\text{s.t. } G \cdot U_t \leq H_t \tag{3-44b}$$

Where,

$$L_t = \begin{bmatrix} l_t & \rho_1 \mathbf{1}_{(1\times 2)} & l_{t+1} & \rho_1 \mathbf{1}_{(1\times 2)} & \cdots & l_{t+N-1} & \rho_1 \mathbf{1}_{(1\times 2)} \end{bmatrix} \tag{3-45}$$

$$U_t = \begin{bmatrix} u_{t|t}^T & \varepsilon_{t+1|t}^T & u_{t+1|t}^T & \varepsilon_{t+2|t}^T & \cdots & u_{t+N-1|t}^T & \varepsilon_{t+N|t}^T \end{bmatrix}^T \in \mathbb{R}^{10N} \tag{3-46}$$

G and H_t are obtained by stacking block diagonal matrices and vectors respectively which is explained as follows in detail.

Constraint matrices over the prediction horizon

Let, $M' = \begin{bmatrix} M & \mathbf{0}_{(6\times 2)} \end{bmatrix}$, $M_1 = \begin{bmatrix} -I_8 & \mathbf{0}_{8\times 2} \\ \mathbf{0}_{2\times 8} & -I_2 \end{bmatrix} = -I_{10}$, then the upper and lower bounds on the control inputs and slack variables can be written as:

$$\begin{bmatrix} G_{\bar{U}} \\ G_{\underline{U}} \end{bmatrix} \cdot U_t \leq \begin{bmatrix} H_{\bar{U}} \\ H_{\underline{U}} \end{bmatrix} \tag{3-47}$$

where, $G_{\bar{U}} \in \mathbb{R}^{6N\times 10N}$ and $G_{\underline{U}} \in \mathbb{R}^{10N\times 10N}$ are block diagonal matrices whereas $H_{\bar{U}} \in \mathbb{R}^{6N}$ and $H_{\underline{U}} \in \mathbb{R}^{10N}$ are vectors:

$$G_{\bar{U}} = \begin{bmatrix} M' & \mathbf{0} & \cdots & \mathbf{0} \\ \mathbf{0} & M' & & \mathbf{0} \\ \vdots & & \ddots & \vdots \\ \mathbf{0} & \mathbf{0} & \cdots & M' \end{bmatrix}, \quad G_{\underline{U}} = \begin{bmatrix} -I_{10} & \mathbf{0} & \cdots & \mathbf{0} \\ \mathbf{0} & -I_{10} & & \mathbf{0} \\ \vdots & & \ddots & \vdots \\ \mathbf{0} & \mathbf{0} & \cdots & -I_{10} \end{bmatrix} = -I_{(10N\times 10N)} \tag{3-48a}$$

$$H_{\bar{U}} = \begin{bmatrix} m_t \\ m_{t+1} \\ \vdots \\ m_{t+N-1} \end{bmatrix}, \quad H_{\underline{U}} = \begin{bmatrix} \mathbf{0}_{(10\times 1)} \\ \mathbf{0}_{(10\times 1)} \\ \vdots \\ \mathbf{0}_{(10\times 1)} \end{bmatrix} = \mathbf{0}_{(10N\times 1)} \tag{3-48b}$$

Using (3-43b) and (3-43g), by recursive substitution the following vector ($X_t \in \mathbb{R}^{3N}$) of predicted states at time t is obtained:

$$X_t = \begin{bmatrix} x_{t+1} & x_{t+2} & \cdots & x_{t+N} \end{bmatrix}^T = \mathbf{A}x_t + \mathbf{B}U_t + \mathbf{E}Z_t \tag{3-49}$$

Where,

$$\mathbf{A} = \begin{bmatrix} A_d \\ A_d^2 \\ \vdots \\ A_d^N \end{bmatrix} \in \mathbb{R}^{3N\times 3}, \quad \mathbf{B} = \begin{bmatrix} B'_d & \mathbf{0} & \mathbf{0} & \cdots & \mathbf{0} \\ A_dB'_d & B'_d & \mathbf{0} & \cdots & \mathbf{0} \\ A_d^2B'_d & A_dB'_d & \ddots & \ddots & \vdots \\ \vdots & \vdots & \ddots & \ddots & \mathbf{0} \\ A_d^{N-1}B'_d & A_d^{N-2}B'_d & \cdots & \cdots & B'_d \end{bmatrix} \in \mathbb{R}^{3N\times 10N} \quad \text{with,}$$

$$B'_d = \begin{bmatrix} B_d^T \\ \mathbf{0}_{(2\times 3)} \end{bmatrix}^T \in \mathbb{R}^{3\times 10}, \quad \mathbf{E} = \begin{bmatrix} E_d & \mathbf{0} & \mathbf{0} & \cdots & \mathbf{0} \\ A_dE_d & E_d & \mathbf{0} & \cdots & \mathbf{0} \\ A_d^2E_d & A_dE_d & \ddots & \ddots & \vdots \\ \vdots & \vdots & \ddots & \ddots & \mathbf{0} \\ A_d^{N-1}E_d & A_d^{N-2}E_d & \cdots & \cdots & E_d \end{bmatrix} \in \mathbb{R}^{3N\times 4N}, \quad \text{and}$$

$$Z_t = \begin{bmatrix} z_t & z_{t+1} & \cdots & z_{t+N-1} \end{bmatrix}^T \in \mathbb{R}^{4N}$$

The state (upper bound) constraint over the prediction horizon, represented by (3-43d) can be written as:

$$X_t \leq \underbrace{\begin{bmatrix} \bar{x}_t \\ \bar{x}_{t+1} \\ \vdots \\ \bar{x}_{t+N} \end{bmatrix}}_{\bar{X} \in \mathbb{R}^{3N}} + \underbrace{\begin{bmatrix} F & F & \cdots & F \\ F & F & \cdots & F \\ \vdots & \vdots & \ddots & \vdots \\ F & F & \cdots & F \end{bmatrix}}_{\mathbf{B}' \in \mathbb{R}^{3N \times 10N}} U_t \quad \text{where,} \quad F = \begin{bmatrix} \mathbf{0}_{(3\times 8)} & \mathbf{1}_{(3\times 1)} & \mathbf{0}_{(3\times 1)} \end{bmatrix} \tag{3-50}$$

Similarly, for the lower bounds (3-43e):

$$X_t \leq \underbrace{\begin{bmatrix} F' & F' & \cdots & F' \\ F' & F' & \cdots & F' \\ \vdots & \vdots & \ddots & \vdots \\ F' & F' & \cdots & F' \end{bmatrix}}_{\mathbf{B}'' \in \mathbb{R}^{3N \times 10N}} U_t - \underbrace{\begin{bmatrix} \bar{x}_t \\ \bar{x}_{t+1} \\ \vdots \\ \bar{x}_{t+N} \end{bmatrix}}_{\underline{X} \in \mathbb{R}^{3N}} \quad \text{where,} \quad F' = \begin{bmatrix} \mathbf{0}_{(3\times 9)} & \mathbf{1}_{(3\times 1)} \end{bmatrix} \tag{3-51}$$

And the remaining state constraints (3-43f):

$$\underbrace{\begin{bmatrix} s & \mathbf{0} & \cdots & \mathbf{0} \\ \mathbf{0} & s & \cdots & \mathbf{0} \\ \vdots & \vdots & \ddots & \vdots \\ \mathbf{0} & \mathbf{0} & \cdots & s \end{bmatrix}}_{S \in \mathbb{R}^{N \times 3N}} X_t \leq \underbrace{\begin{bmatrix} 0 \\ 0 \\ \vdots \\ 0 \end{bmatrix}}_{\mathbf{0}_{(N\times 1)}} \quad \text{where,} \quad s = \begin{bmatrix} -1 & 1 & 0 \end{bmatrix} \tag{3-52}$$

Substituting (3-49) in eqs. (3-50) to (3-52) the state constraints can finally be written as a linear function of decision variables as follows:

$$\begin{bmatrix} G_{\bar{X}} \\ G_{\underline{X}} \\ G_X \end{bmatrix} U_t \leq \begin{bmatrix} H_{\bar{X}} \\ H_{\underline{X}} \\ H_X \end{bmatrix} \tag{3-53}$$

Where,

$$\begin{aligned} G_{\bar{X}} &= \mathbf{B} - \mathbf{B}' \\ G_{\underline{X}} &= -\mathbf{B} - \mathbf{B}'' \\ G_X &= S\mathbf{B} \in \mathbb{R}^{N \times 10N} \\ H_{\bar{X}} &= \bar{X} - \mathbf{A}x_t - \mathbf{E}Z_t \in \mathbb{R}^{3N} \\ H_{\underline{X}} &= -\underline{X} + \mathbf{A}x_t + \mathbf{E}Z_t \in \mathbb{R}^{3N} \\ H_X &= -S \cdot (\mathbf{A}x_t - \mathbf{E}Z_t) \in \mathbb{R}^{N} \end{aligned}$$

Combining (3-47) and (3-53), the constraint matrices $G \in \mathbb{R}^{23N \times 10N}$ and $H_t \in \mathbb{R}^{23N}$ are expressed as:

$$G = \begin{bmatrix} G_{\bar{U}} \\ G_{\underline{U}} \\ G_{\bar{X}} \\ G_{\underline{X}} \\ G_X \end{bmatrix} \quad \text{and} \quad H_t = \begin{bmatrix} H_{\bar{U}} \\ H_{\underline{U}} \\ H_{\bar{X}} \\ H_{\underline{X}} \\ H_X \end{bmatrix} = v(x_t) \tag{3-54}$$

This completes the definition of the (convex) optimal control problem formulation (OCPF) (3-44) with a linear cost function and linear constraints, the solution of which is obtained using a linear programming algorithm. The problem (3-44) was solved using the `conelp` function of Python software for convex optimization (CVXOPT [24]) which uses an interior point algorithm for linear programming (LP). The first input sequence of the optimal solution $U_t^\star$ was then applied to the system (LTI state-space model (2-5)) to obtain the state update which also defines the constraint matrix $H_{t+1} = v(x_{t+1})$ for the next time step. The information from external signals define the time-varying cost function and constraints. The optimal control problem is similarly solved recursively until the end of simulation following the receding horizon principle.

Performance

The performance of this control strategy was studied in simulations based on 12 days data representing typical days of the year. Figure 3-2 shows the controller performance when the electricity prices are time-varying (the price signal is obtained from the EEX - European energy exchange price data for German market in 2012). The plot shows that the controller is successful in load shifting w.r.t. electricity price. It maximizes the heating operation when the electricity prices are low. The heating depends on the thermal load as well, which needs to be compensated while satisfying constraints. Even though it is not completely clear from this figure, it can be observed that the heating operation is lower during the night times when the ambient temperatures are lower. This is because the COP is relatively higher during the day times when ambient temperature is higher which leads to more efficient performance.

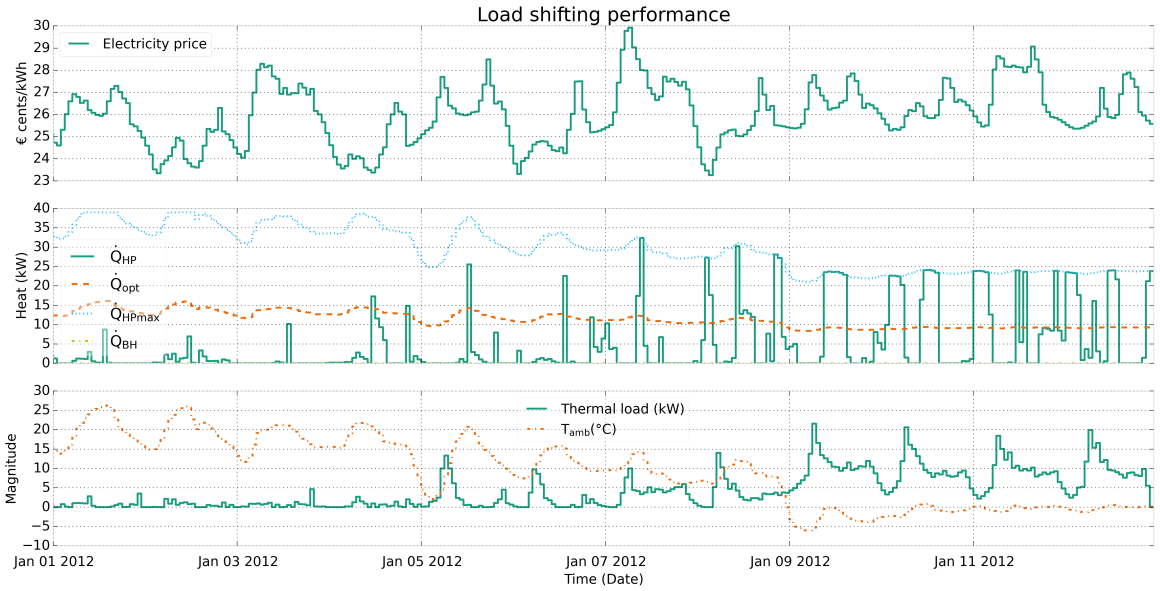

Figure 3-2: Load shifting performance of LP OCPF based MPC in dynamic tariff scenario

This characteristic is clearly observed in Figure 3-3 when the electricity prices are fixed. However, in the fixed price case, since the bill only varies with the heating power consumed, the main purpose of the controller is to minimize the energy consumption. In order to do that

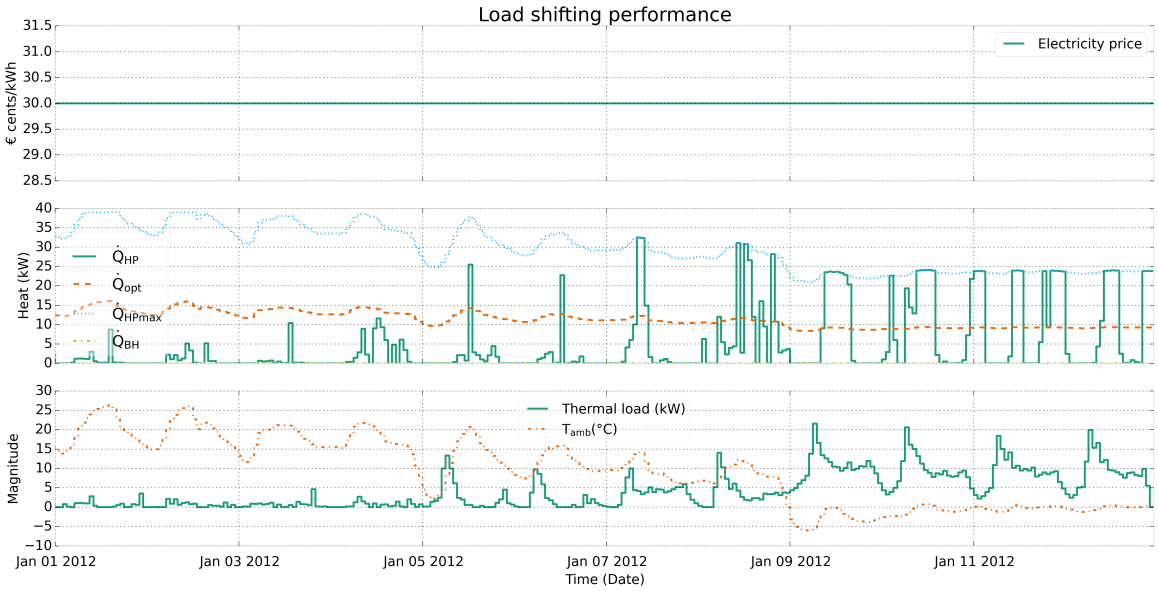

Figure 3-3: Performance of LP OCPF based MPC in a fixed price case

the controller not only needs to shift heat production during day time but also operate at part load condition corresponding to better efficiency depending on the thermal load condition. Figure 3-4 shows the storage temperatures in the same simulation. The heat pump overheats the storage as observed in the warmer days (first 6 days in the timeseries) when the thermal load is low. The building's thermal inertia was exploited for space heating load shifting by the controller as observed in Figure 3-5. The zone temperature, storage temperatures and heating input plots show that the controller perfectly satisfies the bounds. The following statements

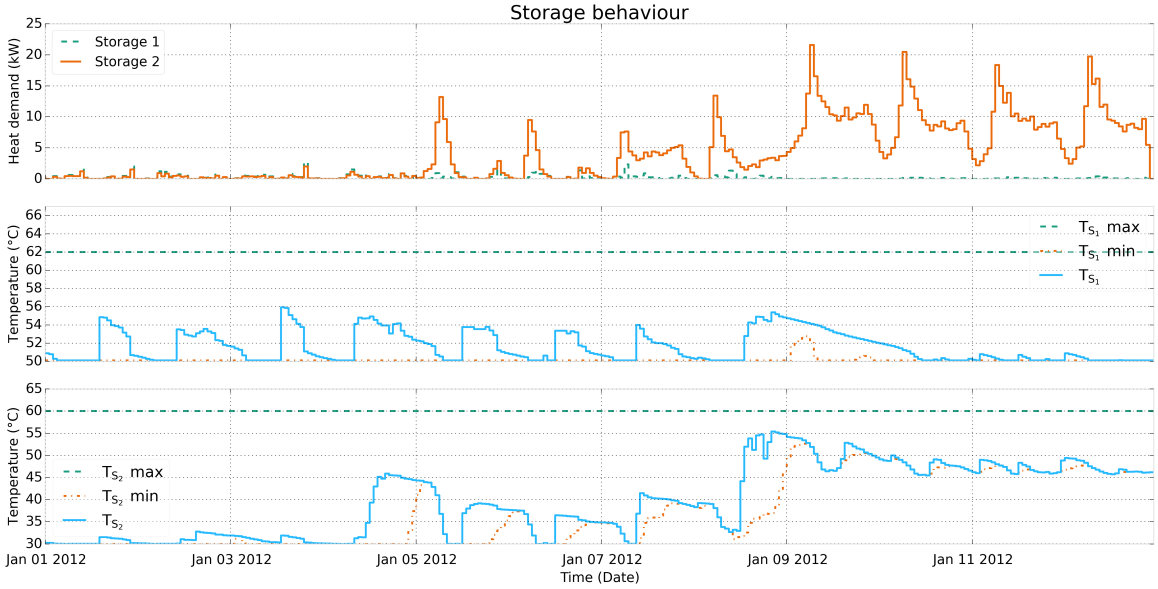

Figure 3-4: Storage behaviour in a fixed price case with LP OCPF based MPC

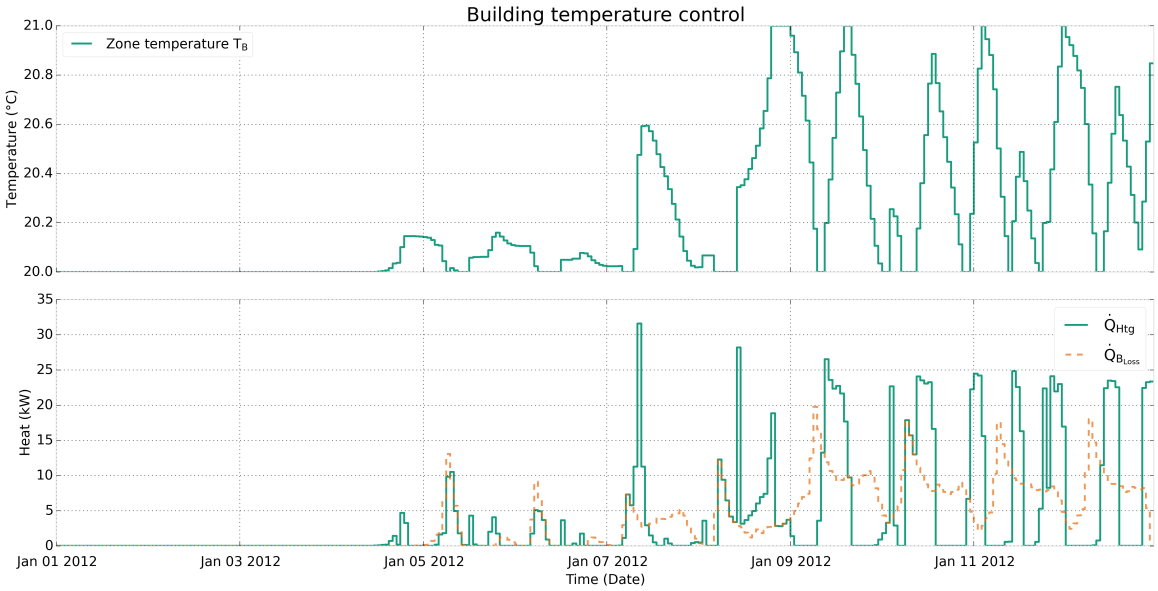

Figure 3-5: Zone temperature behaviour in a fixed price case with LP OCPF based MPC

can be inferred from the simulations performed with LP OCPF based MPC strategy:

- The controller solves the trade-off of minimizing energy consumption while satisfying constraints and maximizing cost savings but only partially.
- The load shifting performance shows that MPC is a promising control strategy for grid balancing.
- The heating input ($\dot{Q}_{HP}$) was observed to be fluctuating near extreme values (Figure 3-2) which might not be undesirable in the EEX price scenario. However, the fixed price case performance (Figure 3-3) was similar which proved that the controller does not optimize the part load operation.
- The storage was unnecessarily overheated as observed during the warmer days as a result of the extreme input values. This again means that the controller does not consider the part load factor and storage losses.

The limitations can be attributed to the fact that the influence of part load operation and storage (supply water) temperatures were neglected from the control problem formulation. Clearly, the performance suggests that a smoother operation is required such that the trade-off between electricity consumption and cost savings is optimal. This motivates that the squares of heating inputs need to be penalized instead of linear penalties for a smoother operation. This idea is similar to the one proposed in recent literature [4] where the limitations of a linear formulation which showed fluctuating input behaviour were compensated by squaring the cost function which had a single heating input. The formulation is explained in the following section.

3-3-7 Quadratic convex programming formulations

In order to penalize the power peaks, square of the heating inputs must be penalized which results in a smoother operation. In [4], the best performing formulation had a quadratic cost function which also used ambient temperature variation to penalize the heating inputs. The idea was motivated by observing results of different formulations in [4] concluding that the performance of proposed quadratic cost was close to the one corresponding to a detailed heat pump model due to flat nature of the cost function near optimum in spite of a variable part load operation and influence of supply temperatures. This statement about the nature of cost function cannot be directly generalized to this case. However, the detailed analysis of heat pump performance through the simplified heat pump model (2-9) suggests that the behaviour of the cost with part load factor is nearly quadratic in nature if the variation with other factors is neglected. Hence, a similar approach was tested for the system considered in this thesis in order to determine the influence on the controller performance considering the nature of heat pump part load operation. The corresponding OCPF (3-55) is stated as follows (cf. (3-38), (3-39), (3-44)):

$$\min_{U_t} \quad U_t^T \underbrace{\begin{bmatrix} r_t & \mathbf{0} & \cdots & \mathbf{0} \\ \mathbf{0} & r_{t+1} & \cdots & \mathbf{0} \\ \vdots & \vdots & \ddots & \vdots \\ \mathbf{0} & \mathbf{0} & \cdots & r_{t+N-1} \end{bmatrix}}_{R_t} U_t + L_t' \cdot U_t \tag{3-55a}$$

$$\text{s.t. } G \cdot U_t \leq H_t \tag{3-55b}$$

Where,

$$r = \left[\begin{array}{cccccccc|c} \text{ecost} \cdot C_1^2 & 0 & 0 & 0 & 0 & 0 & 0 & 0 & \mathbf{0} \\ 0 & \text{ecost} \cdot C_2^2 & 0 & 0 & 0 & 0 & 0 & 0 & \mathbf{0} \\ 0 & 0 & 0 & 0 & 0 & 0 & 0 & 0 & \mathbf{0} \\ 0 & 0 & 0 & \text{ecost} & 0 & 0 & 0 & 0 & \mathbf{0} \\ 0 & 0 & 0 & 0 & \text{ecost} & 0 & 0 & 0 & \mathbf{0} \\ 0 & 0 & 0 & 0 & 0 & \text{PVcost} \cdot C_1^2 & 0 & 0 & \mathbf{0} \\ 0 & 0 & 0 & 0 & 0 & 0 & \text{PVcost} \cdot C_2^2 & 0 & \mathbf{0} \\ 0 & 0 & 0 & 0 & 0 & 0 & 0 & 0 & \mathbf{0} \\ \hline \mathbf{0} & \mathbf{0} & \mathbf{0} & \mathbf{0} & \mathbf{0} & \mathbf{0} & \mathbf{0} & \mathbf{0} & \mathbf{0}_{(2\times 2)} \end{array}\right] \tag{3-56a}$$

$$L_t' = \begin{bmatrix} \mathbf{0}_{(1\times 8)} & \rho_1 \mathbf{1}_{(1\times 2)} & \mathbf{0}_{(1\times 8)} & \rho_1 \mathbf{1}_{(1\times 2)} & \cdots & \mathbf{0}_{(1\times 8)} & \rho_1 \mathbf{1}_{(1\times 2)} \end{bmatrix} \in \mathbb{R}^{10N} \tag{3-56b}$$

The diagonal elements of the quadratic penalty matrix r_t represent the penalty on the control inputs. The approach is same as in the linear formulation but here the square of the product of heating input and its corresponding COP inverse is penalized. This ensures that part load characteristics are considered in the formulation such that peak shaving of the power consumption can be achieved. There is no penalty on the variables which do not add to the electricity bill i.e. $\dot{Q}_{STC}$. A linear cost with weight expressed in (3-56b) is included in order to penalize the slack variables which contain the constraint violations. The matrix R_t can be guaranteed to be positive semi-definite by adding an offset to the electricity price such that

it makes the minimum value to be greater than or equal to zero. This does not change the nature of its variation over time and prevents excessive penalties on the inputs which would be caused by squaring it for instance. For the simulations presented, this was not required as the prices were always non-negative. The positive semi-definite R_t matrix which represents the Hessian matrix of the quadratic objective function guarantees that the resulting optimization problem is convex. Hence, the OCPF (3-55) can be solved using a quadratic programming algorithm. The `conelq` function of the convex optimization solver CVXOPT was used to obtain the solution.

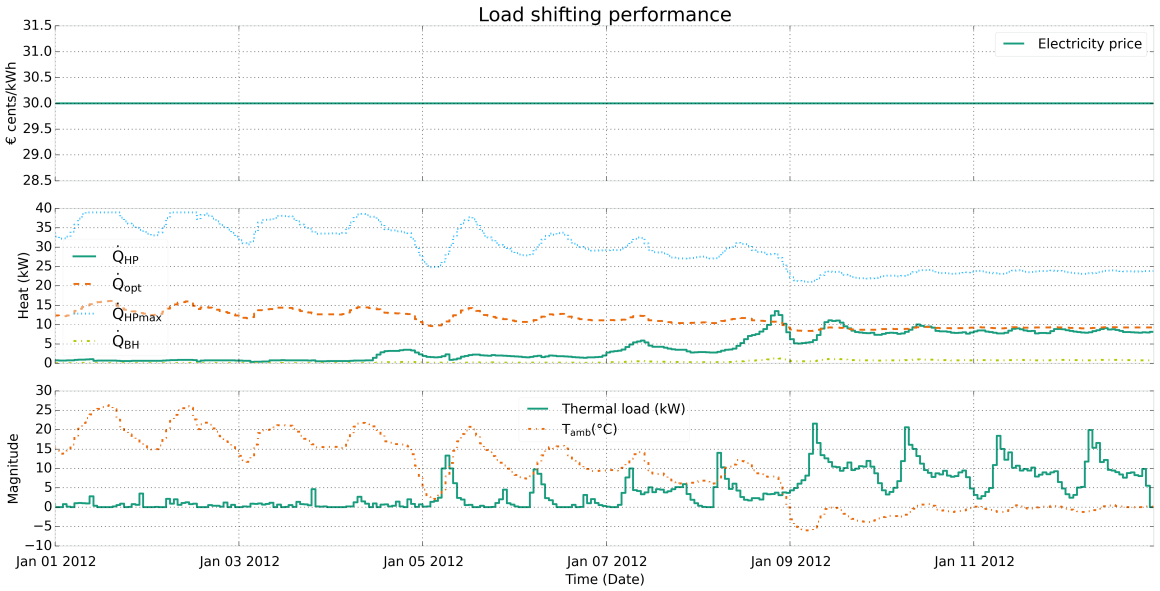

Figure 3-6: Performance of QP OCPF in constant tariff case

Performance of the QP OCPF based MPC

Figure 3-6 shows that the controller minimizes the peak of the power consumed for heating as expected. However, while doing so the heating load is not shifted to off-peak hours as desired. This results in less efficient operation as the heat pump operates during the night hours as well. This is in contrast to the results observed in [4] because on a closer observation it was noticed that in [4], the ambient temperature variation itself was assumed to be the variation in thermal load. However, that does not exactly comply with the data considered here as it is not only depends on ambient temperature but also other factors such as influence of occupancy and ventilation. Due to penalties on the squared input variables, the load shifting incentive becomes negligible in comparison with peak shaving incentive for the cost minimization of the OCPF. This is evident from the load shifting performance plot (Figure 3-7). Furthermore, Figure 3-8 shows that the controller keeps the lower storage temperature at its lower bound which makes the storage redundant as no load shifting is observed. However, it also indicates that the quadratic input costs also penalize the storage losses which helps to minimize energy consumption. Another disadvantage of this formulation was that the heat pump operation was forced in or around the dead-zone region during warm days at very low input values which are either infeasible to achieve or correspond to poor efficiency values.

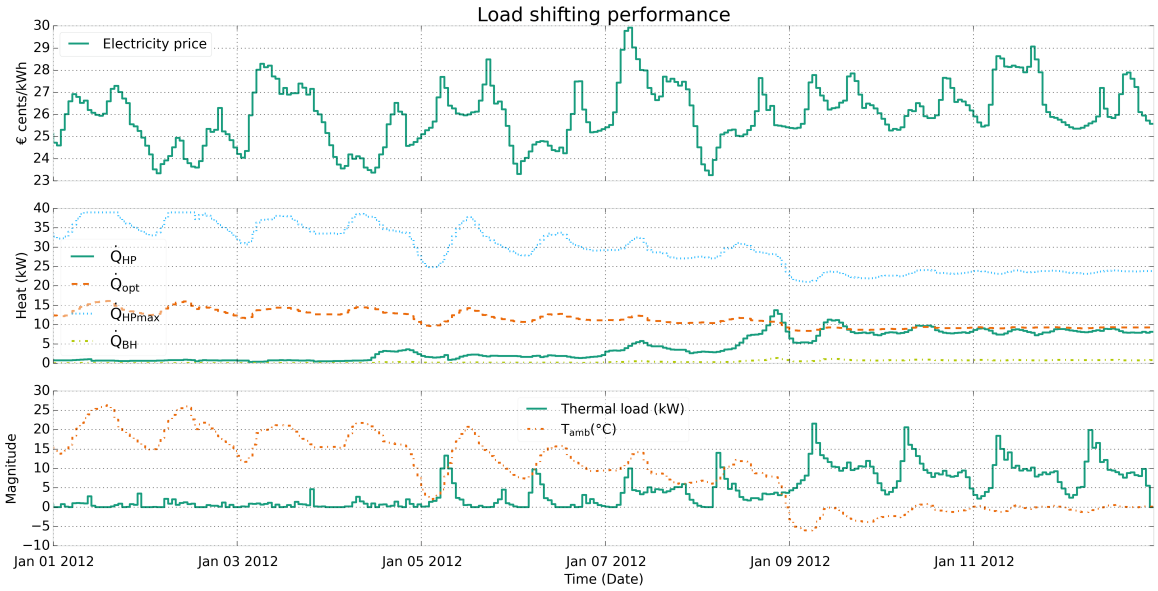

Figure 3-7: Performance of QP OCPF in dynamic price case

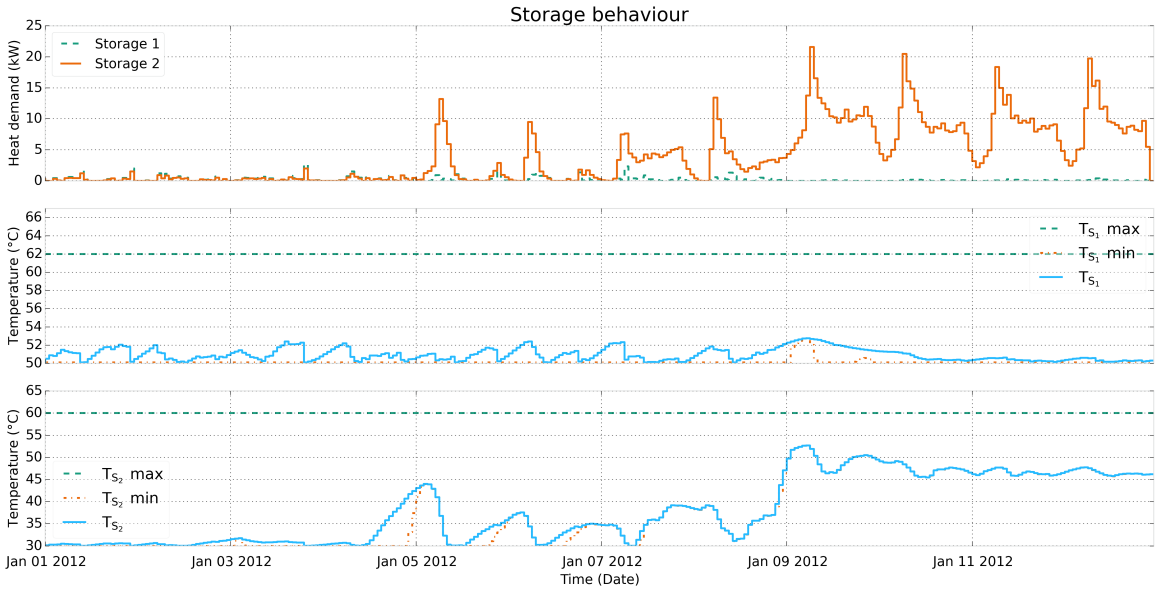

Figure 3-8: Storage behaviour in the EEX price case with QP OCPF based MPC

From the simulation results it is clear that the simplifications made to have a convex OCPF lead to inaccurate representation of the control objectives in the formulation. However, each formulation resulted in contrasting behaviour i.e. the limitations of the LP OCPF were compensated by the QP OCPF at the cost of losing essential performance characteristics of the former approach. The contrast in heat pump performance is clear from the histograms (EEX

price case[6]) in Figures 3-9a and 3-9b. The quadratic cost function effectively minimizes the part load ratio but this is conflicting with the objective of load shifting which was observed in the performance with linear case.

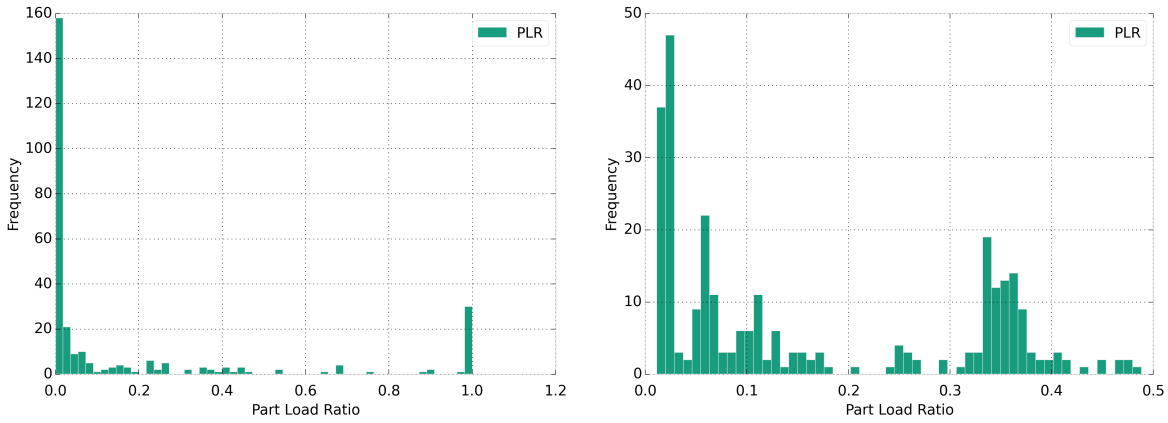

(a) LP OCPF **(b)** QP OCPF

Figure 3-9: Part load ratio of the heat pump

This proves that load shifting for minimum costs and peak minimizing for minimum consumption or better efficiency are conflicting objectives which cannot be included in a single convex objective function. Hence, a formulation with a linear combination (positive-weighted sum) of the previous two objective functions was considered for the reasons summarized below. The objective of minimizing electricity bill can be split into the following conflicting objectives:

- Heat during off-peak hours when the electricity prices are low or the ambient temperature is higher.
- Minimize the power consumption by controlling the part load behaviour and reduce peaks.

The first objective was achieved with the linear formulation and the second with the quadratic formulation which justifies the use of a combination of these two cost functions as it serves the purpose of incorporating key characteristics of the electricity bill variation while still having a convex optimization problem formulation.

Multiobjective approach

As stated earlier, a positive-weighted sum of the LP and QP OCPFs is considered for the multiobjective approach which can be mathematically expressed as (cf. (3-44), (3-55)):

$$\min_{U_t} \quad U_t^T \cdot R_t \cdot U_t + \kappa \cdot L_t \cdot U_t \tag{3-57a}$$

$$\text{s.t. } G \cdot U_t \leq H_t \tag{3-57b}$$

[6]The same was observed for the fixed price case

The constant term $\kappa\,(>0)$ introduced above in (3-57a) is a positive scalar parameter which determines the relative weight between the two objectives. Since the objective function is a positive-weighted sum of a (quadratic) convex and a linear function with the same linear constraints, the resulting optimization problem is also quadratic convex and the solution is obtained using the same algorithm with which the previous QP problem was solved.

Performance of the modified convex QP (mQP) OCPF based MPC

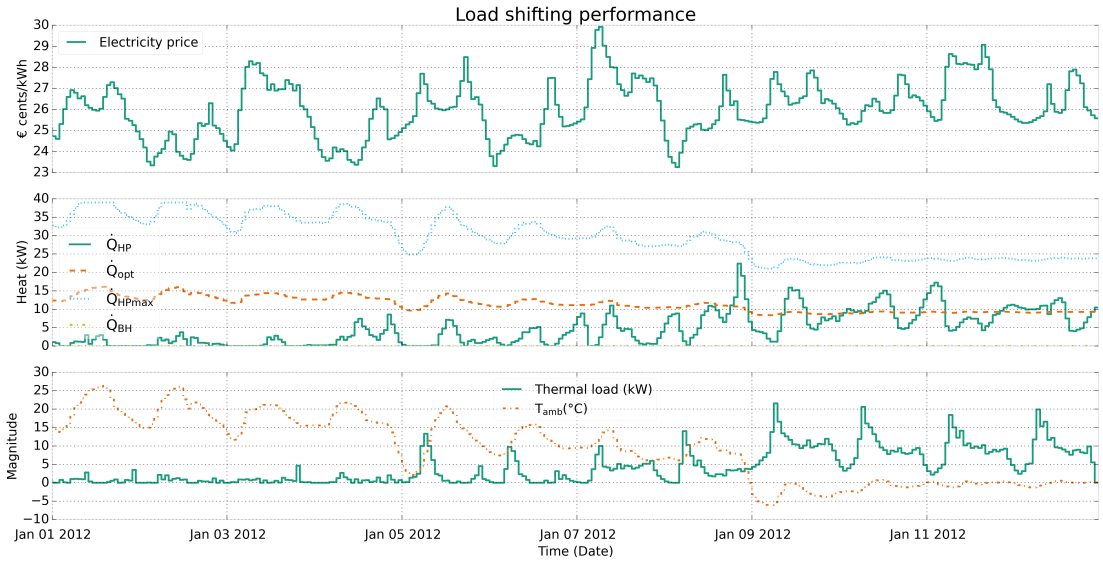

Figure 3-10: Controller performance in a dynamic tariff scenario with the multiobjective approach

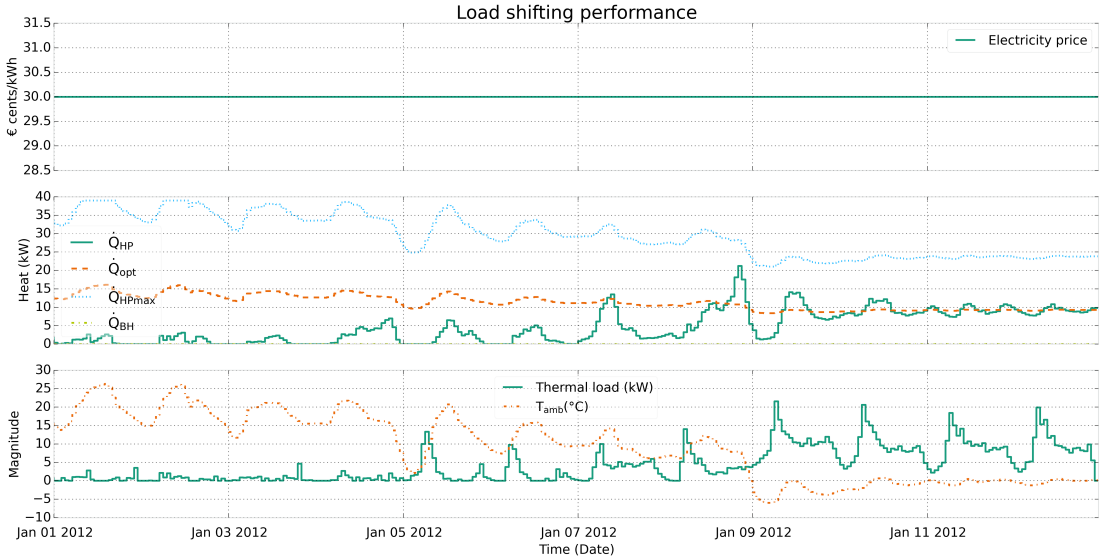

Figure 3-11: Controller performance in a constant tariff scenario with the multiobjective approach

The performance plots (Figures 3-10 and 3-11) prove that the heat pump now has a balanced part load behaviour and is capable of load shifting as well, which is essential for optimizing the heating bill. A quantitative comparison with previous formulations and further explanation is given in the next chapter (Section 4-2-1). The main drawback of this approach lies in the tuning of parameter κ which determines the trade-off to be optimized between the two conflicting objectives. However, the tuning is intuitive if some heat pump characteristics are known. For example, smaller capacity heat pumps have negligible change in efficiency at part load operation which means that a high value of κ is suitable. The value of κ was set to 14.0 and was tuned iteratively through a few simulations by noting the KPIs.

The performance of this convex formulation must be compared to the nonlinear non-convex formulation based MPC which has the complete COP model in the cost function to estimate electricity bill, in order to know that how much the performance is compromised by not using a detailed heat pump (COP) model. Finally, the performance of the MPC approaches need to be compared against the baseline control method for quantification of benefits. The two control methods are described in the following sections before a detailed comparison in the next chapter.

3-3-8 Nonlinear (non-convex) programming (NLP) formulation

This formulation represents the control objectives such that no key characteristic of the economics of the system is neglected. The electricity bill itself is used as the economic objective function. As explained earlier the electricity bill (3-19) is expressed as:

$$\text{Bill} = \text{ecost} \times \left(\frac{\dot{Q}_{HP_1}}{\text{COP}_1} + \frac{\dot{Q}_{HP_2}}{\text{COP}_2} + \dot{Q}_{BH_1} + \dot{Q}_{BH_2} \right) + \text{PVcost} \times \left(\frac{\dot{Q}_{HP_{1_{PV}}}}{\text{COP}_1} + \frac{\dot{Q}_{HP_{2_{PV}}}}{\text{COP}_2} \right)$$

Using the heat pump performance model (2-9) (cf. Table 2-3), we have:

$$\frac{1}{\text{COP}_1} = a_0 + a_1 \cdot T_{\text{sup}_1} + a_2 \cdot T_{\text{amb}} + a_3 \cdot \dot{Q}_{HP} + a_4 \cdot (\dot{Q}_{HP} - a_5)^{a_6} \tag{3-58a}$$

$$\frac{1}{\text{COP}_2} = a_0 + a_1 \cdot T_{\text{sup}_2} + a_2 \cdot T_{\text{amb}} + a_3 \cdot \dot{Q}_{HP} + a_4 \cdot (\dot{Q}_{HP} - a_5)^{a_6} \tag{3-58b}$$

Where,

$$T_{\text{sup}_i} = T_{S_i} + 2, \quad i \in \{1, 2\} \tag{3-58c}$$

$$\dot{Q}_{HP} = \dot{Q}_{HP_1} + \dot{Q}_{HP_2} + \dot{Q}_{HP_{1_{PV}}} + \dot{Q}_{HP_{2_{PV}}} \tag{3-58d}$$

Substituting the above equations in (3-19) defines the electricity bill which is used for the objective function evaluation in the following nonlinear non-convex optimal control problem:

$$\begin{aligned} \min_{U_t} \quad & \sum_{k=0}^{N-1} \text{Bill}_{t+k|t}(x_{t+k|t}, u_{t+k|t}, z_{t+k}, d_{t+k}) + \sum_{k=1}^{N} \sum_{i=1}^{2} (\rho_1 \varepsilon_{i_{t+k|t}} + \rho_2 \varepsilon^2_{i_{t+k|t}}) \\ \text{s.t.} \quad & x_{t+k+1|t} = A_d x_{t+k|t} + B_d u_{t+k|t} + E_d z_{t+k}, \forall k = 0, 1, ..., N-1 \\ & x_{t|t} = x(t) \\ & G \cdot U_t \leq H_t \end{aligned} \tag{3-59}$$

The constraints in the formulation (3-59) are same as defined in the previous OCPFs. As explained earlier, since the COP is not defined in the dead-zone region, the models (3-58) hold only when $\dot{Q}_{HP} \geq \underline{\dot{Q}}_{HP}$. Since the COP must be defined even in the dead-zone region for this formulation, the value of COP inverse substituted for objective function evaluation corresponding to input values such that $\dot{Q}_{HP} \leq \underline{\dot{Q}}_{HP}$, was set to 1. This corresponds to the maximum value of COP inverse. The value was chosen as 1 because operation in dead-zone is not desired as justified earlier (Section 3-1). This indeed creates a discontinuity in between the values of COP inverse predicted from the model and otherwise. However, since analytic gradients were not required, this definition was feasible to implement. The solution of the OCPF (3-59) was obtained by using the sequential least squares programming (SLSQP) solver of the `scipy` library in Python through the OpenOpt optimization framework. The gradient evaluations were automatically calculated by the framework using numerical methods [10]. The accuracy of gradient evaluations of this framework was tested while solving the mQP OCPF and it was found that the numerical gradient calculation results were very precise in approximating the gradients and the solution for the mQP problem was also the same using this solver without providing gradient evaluation functions.

A major limitation of this solver was that it required an initial guess value which was feasible i.e., an initial guess which satisfies all the constraints without which the solver algorithm terminates. To tackle this problem, a solution calculated from one of the previously explained (LP, QP or mQP) OCPFs could be used at each time step at the cost of small computation time which was negligible in comparison to the mean time taken by the NLP solver. This guaranteed a feasible initial guess for any time step as the constraints were same for the previous formulations.

Even though this formulation represents the system economics most accurately, it does not necessarily mean that the best results will be obtained through this formulation. This is because the solution of the NLP problem could be a *local minimum* which satisfies optimality and feasibility conditions. This is the main drawback of this method. A multi-start approach was not used because of the solver limitations with the initial guess requirements which are hard to satisfy as explained in previous paragraph. The performance of this control strategy is presented in the next chapter while comparing with other methods.

3-4 Baseline control strategy

For quantifying the benefits and drawbacks of using MPC strategy, the current state-of-the-art method for intelligent heat pump control was used which is termed as baseline control strategy here. This pre-programmed control method is based on a set of rules such that the heat pump can operate efficiently. The main advantage of this method is that it does not need a model of the system dynamics. It however needs feedback measurements to determine the set-points to be followed in order to satisfy constraints. A notable drawback is that it does not make use of forecasts for optimizing system operation i.e., it is not a predictive strategy. Since the controller does not make use of forecasts, it cannot perform load shifting which means the only objective of this controller is to optimize the energy consumption and satisfy the constraints as precisely as possible while maximizing self consumption of solar heat and power. Based on this objective, the control algorithm is explained briefly by the following set

of *if-then-else* rules which are based on the calculated heat demand (for each storage and the building) and temperature measurements at each time step:

1. If the total heat demand which is calculated based on the heating curve dependent lower bounds, is low (below 20% of heating capacity), switch off the heat pump.
2. If the heat demand is higher than the threshold or if storage or zone temperature is below setpoint, check for availability of solar inputs and consume its maximum possible power such that constraints are satisfied.
3. If solar power is not available, check whether the heat demand corresponds to 20% higher or lower than the optimal operating point of the heat pump. If that is true, then operate the heat pump at optimal compressor frequency (rpm), otherwise proceed to the next step.
4. In this step the heat demand must be greater than supply corresponding to optimal rpm. If that is true, then the heat pump is operated at capacity equivalent to the heat demand. If the heat demand is beyond the maximum capacity then the algorithm proceeds to the next step.
5. When the demand is above the heat pump capacity, use the backup heaters (at full load) corresponding to the storage layer where additional heat supply is required.

Since this controller needs frequent action for constraint satisfaction, a holding time period of 30 minutes was used for each control action (also used as the minimal runtime for the heat pump in this case). The reason is that this controller does not allow the heat pump to operate in the dead-zone as a result of the rules defined above.

Summary In this chapter, the objectives of the control strategy were defined. The main idea of this chapter was to explain the working of control algorithms which were designed to achieve the control objectives. The predictive control strategies differed in formulation of the cost function. A convex formulation which can achieve all the goals was derived as a combination of two cost functions independent of a detailed heat pump model. This was followed by a predictive control method which uses a perfect heat pump model to have the ideal representation of control objectives, and a rule based method which represents the performance benchmark. The performance of these control methods is presented in the next chapter along with the comparison of results which are evaluated on the basis of KPI values.

Chapter 4

Performance comparison and results

The previous chapter explained the different control strategies. In this chapter, the simulation results of the control strategies applied to the building heating system are discussed. The different test cases for comparison are briefly described in Section 4-1. The comparison results are presented in detail in Section 4-2. This chapter is concluded by summarizing the findings from the simulations in Section 4-3.

4-1 Comparison scenarios

Three different scenarios were considered for assessing the performance of the control strategies based on comparison and evaluation of the key performance indicators (Section 3-1). The scenarios are briefly described below:

1. Fixed price scenario (Scenario 1): In this test case the electricity price is assumed to be constant, that means the only objective of the control strategy is to minimize electricity consumption (cf. Equation 3-2). The comparison in this scenario (Section 4-2-1) is done to test how effectively each control strategy optimizes the heating efficiency which results in minimum energy consumption. For this scenario, the solar inputs were not included in order to ensure fair comparison as they are not utilized in same quantities.

2. Variable price scenario (Scenario 2): The comparisons in this test case indicate the load shifting performance of control strategies with respect to the electricity price. In this case as well, the inputs from solar energy devices are excluded. The results (Section 4-2-2) obtained in this case are then compared with the next scenario, to quantify the influence of local renewable energy production and potential cost savings.

3. Smart grid scenario with renewable energy (Scenario 3): This simulation scenario includes all smart grid characteristics such as dynamic electricity tariff (EEX price) and local renewable energy production. This is the main comparison scenario in order to quantify the potential benefits of model predictive control and to determine the best

OCPF. The comparisons (Section 4-2-3) also indicate how effectively each control strategy utilizes domestic or local renewable energy produced.

For fair comparisons in each scenario, simulation settings were fixed. For example, the settings: length of prediction horizon, prediction data, constraints and the initial condition of the system remained same. A twelve hour prediction horizon was considered which equals 12 time steps. The simulations were initialized with the building zone temperature at 20° C, the upper storage at 50°C and lower storage at 30°C. The prediction data[1] (Section 3-3-3) available contained information viz. ambient temperature, heat load profiles, electricity price signals, solar radiation data and residual PV electricity available for the year 2012 with 15 minutes time steps. This one year data was resampled to one hour time steps for MPC based controllers and to half hour time steps for the baseline controller based on statistical mean. For better visualization, the derived 12 test days dataset [21] which represented typical days of all seasons was used to compare performance of the control strategies. For exact comparison and quantification of benefits, simulation results using the whole year's data have been included in Section 4-2-4. For calculation of the bill (3-19), the COP inverse model (3-58) was used for all simulations, representing the true heat pump. This also means that the NLP formulation has no heat pump model mismatch and thus, has perfect representation of control objectives.

4-2 Results

In this section, results of all test cases mentioned earlier are presented. In the first scenario (Section 4-2-1), the performance of baseline controller is compared with all MPC strategies derived in the previous chapter. In the remaining scenarios (Sections 4-2-2 and 4-2-3), only the main control strategies are compared, which include the rule based baseline strategy (Section 3-4), the modified convex quadratic programming (mQP) formulation (multiobjective approach in Section 3-3-7) and the nonlinear non-convex programming (NLP) formulation (Section 3-3-8) based MPC strategies. In the end, simulation results with 1 year test data have been included for further comparison and conclusions (Section 4-2-4).

4-2-1 Fixed price scenario

In this case, the objective was to determine the most energy efficient control strategy. In order to achieve that objective, the heat pump must be operated to optimize the COP. Table 4-1 shows how each control strategy performed and the comparison was done using five KPIs as shown. The NLP OCPF based MPC had the best cost and energy efficient performance. This was clear as the reference controller consumed 13.73% more energy and since the tariff was constant for all test days, it also led to 13.73% higher costs. The seasonal performance factor was the highest (best) with the NLP based strategy which explains why it performed better.

Figure 4-1 shows that the baseline controller supplied the heat as per demand (thermal load) while trying to operate the heat pump at its most efficient rpm (or part load) disregarding the

[1]The experimental data obtained from Fraunhofer ISE [21] corresponds to a German multifamily house with 6 dwellings in Potsdam

Table 4-1: Comparison of control strategies in fixed price scenario

Scenario 1: Fixed tariff		MPC problem formulation type			
Performance indicator	Baseline	LP	QP	mQP	NLP
Money spent (€)	94.60	90.19	118.16	84.92	83.18
Electricity consumed (kWh)	315.31	300.62	393.89	283.08	277.25
SPF	4.37	4.63	3.4	4.73	4.91
Storage heat loss (%)	12.6	13.8	9.31	9.58	11.42
Average computation time per step (seconds)	0.001	0.069	0.082	0.092	3.99

influence of ambient temperature. The NLP based strategy exploited the ambient temperature information to operate at the best COP by optimally solving the trade-off with overheating and part load efficiency. This is evident from Figure 4-2.

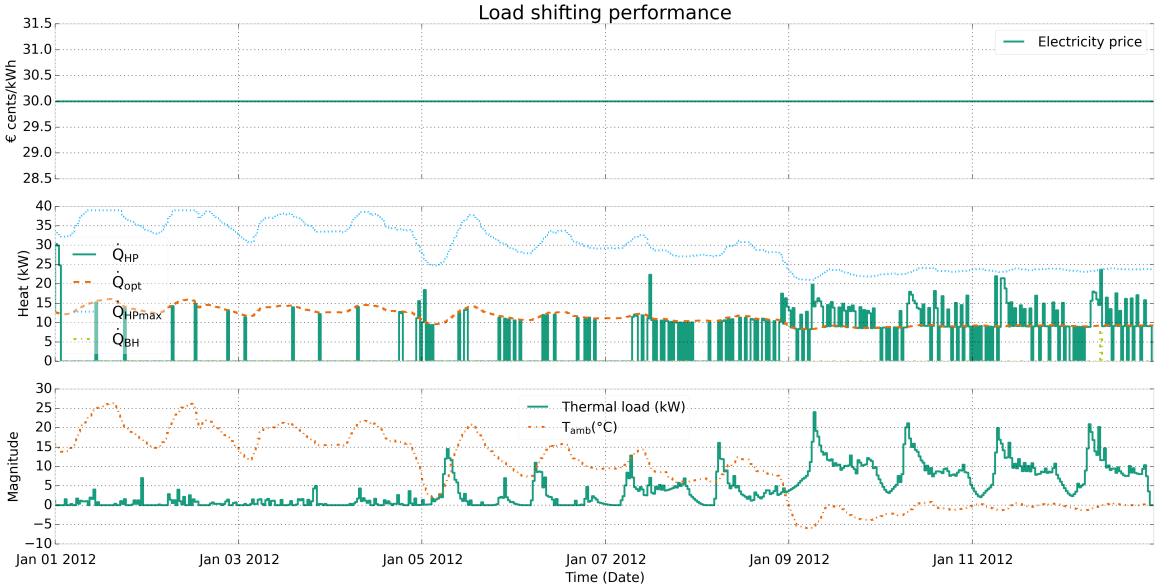

Figure 4-1: Baseline controller performance in a constant tariff scenario

The performance of remaining three formulations was already presented in the previous chapter (Figures 3-3, 3-6, 3-11). From Table 4-1 it is clear that the linear formulation LP was more efficient (higher SPF) than the QP formulation as it performed load shifting with respect to the ambient temperature (Figure 3-3). However, the overheating was excessive (higher storage losses) when compared to results with NLP because the LP formulation did not include the influence of part load and supply temperatures. The QP formulation performed the worst of all because it not only failed to operate more during off-peak hours (no load shifting as in Figure 3-6) but also excessively penalized the part load factor. However, it minimized the storage losses which meant that the quadratic costs incorporated the influence of supply temperature and, though not in the desired way, also the influence of part load behaviour. The mQP formulation successfully overcame the limitations posed by the LP and QP formulations as indicated by the values in Table 4-1. Its performance was not far from the solution of the

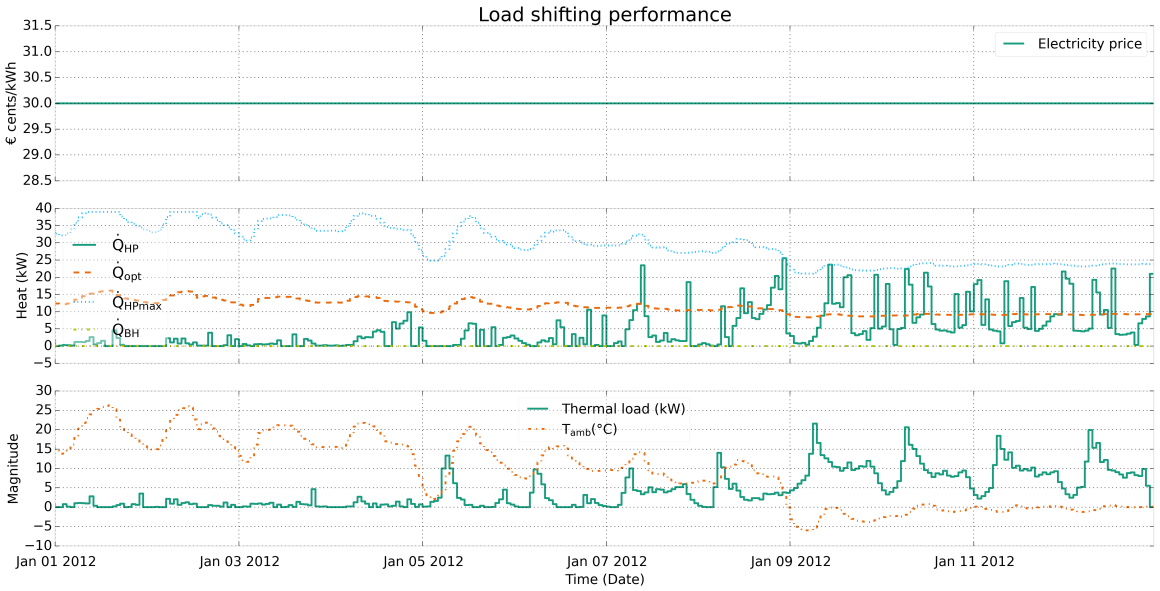

Figure 4-2: Predictive controller performance in a constant tariff scenario with the NLP OCPF

NLP case as it could save 11.4% costs and energy over the baseline control strategy.

The computation time performance indicator shows that for simulations with a 12 step prediction horizon, the time consumed by NLP was at an average almost 4000 times higher than the baseline controller at every step for calculation of control action. The convex formulations were much better in comparison as observed and consumed 40 (LP) to 60 (mQP) times lesser time as compared to the NLP algorithm. During the simulations it was also observed that the time taken for convergence of the NLP algorithm was highly uncertain and took longer duration for some iterations. One reason for this uncertainty is the initial guess solution. The convergence time of NLP cannot be predicted to be in a small range. For all other control strategies, the computation time per step did not vary appreciably.

From Table 4-1 it can be concluded that the mQP formulation is the best convex formulation and that MPC is more energy efficient than baseline strategy even though it does not maximize operation at the most efficient compressor frequency. Since the performance of LP and QP based control did not change appreciably in scenario 2 (Figures 3-2, 3-7) and considering the aforementioned limitations, the results with these OCPFs are not compared further for brevity.

4-2-2 EEX price scenario

In this scenario, for best performance, the control strategies must adapt to the predicted behaviour of the electricity pricing. The baseline controller performs exactly in the same manner as in the fixed price scenario as it cannot make decisions such as when to overheat and when to underheat w.r.t. the electricity price and ambient temperature which are essential for optimal load shifting. In this scenario, the most important performance indicator is the money spent on heating and not the efficiency. However, the control strategy needs to make optimal trade-off between the conflicting objectives of overheating during times with lower tariffs and

efficiency of heating. The performance comparison is shown in Table 4-2 by evaluation of relevant KPIs. The results do not comply with conclusions of scenario 1 because the NLP based MPC did not give the best performance. However, the baseline controller resulted in 13.34% higher costs than the best MPC strategy. This means that MPC saves higher in a dynamic tariff scenario through load shifting abilities, as compared to the fixed tariff scenario.

Table 4-2: Comparison of control strategies in dynamic price scenario

Scenario 2: EEX tariff	Control Strategy		
Performance indicator	Baseline	mQP	NLP
Money spent (€)	83.6	73.76	74.57
Electricity consumed (kWh)	315.31	283.03	288.06
SPF	4.37	4.75	4.72
Storage heat loss (%)	12.6	9.95	11.16
Dead-zone operation of HP (No. of switchings per hour)	-	0.55	0.45

The results in this case clearly indicate that the solution of the NLP formulation did not converge to the global optimum. Otherwise, it would certainly have the best performance. Even though the NLP formulation best represents the economics of the heating system, the solution is suboptimal (local optimum) because a globally optimal solution cannot always be found in a single start with limited maximum number of iterations (= 150). It is also impossible to verify with deductive reasoning whether the obtained solution is the global optimum. In other words, the solution of non-convex formulation does not exactly reflect the ideal performance but rather a realistic one which is suboptimal. On the contrary, the solution of convex formulation is unique and represents the best solution which is the global optimum of the formulated problem. This supports the use of convex formulation to represent the control objectives provided they are accurately represented directly or indirectly. Since the solution of NLP is not the theoretically best possible performance due to the above mentioned limitations, it cannot be verified without uncertainty that the convex formulation accurately represents the control objectives. Moreover, this means that even though perfect predictions and models have been used, the results do not indicate the theoretical performance bound which can only be determined by computing the global solution for the non-convex formulation. This highlights the main limitation of the simulation results in achieving the research goals.

The load shifting results did not indicate where the NLP OCPF performance differed from mQP as the results were very close considering the KPI values in Table 4-2. In order to have better insights, the performance of mQP and NLP solutions was compared through respective storage behaviour. The storage was excessively heated in the NLP case as compared to the mQP case. This behaviour can be observed in Figures 4-3 and 4-4 around Jan 9. On account of this, the supply temperatures were higher which also result in lower heating efficiency.

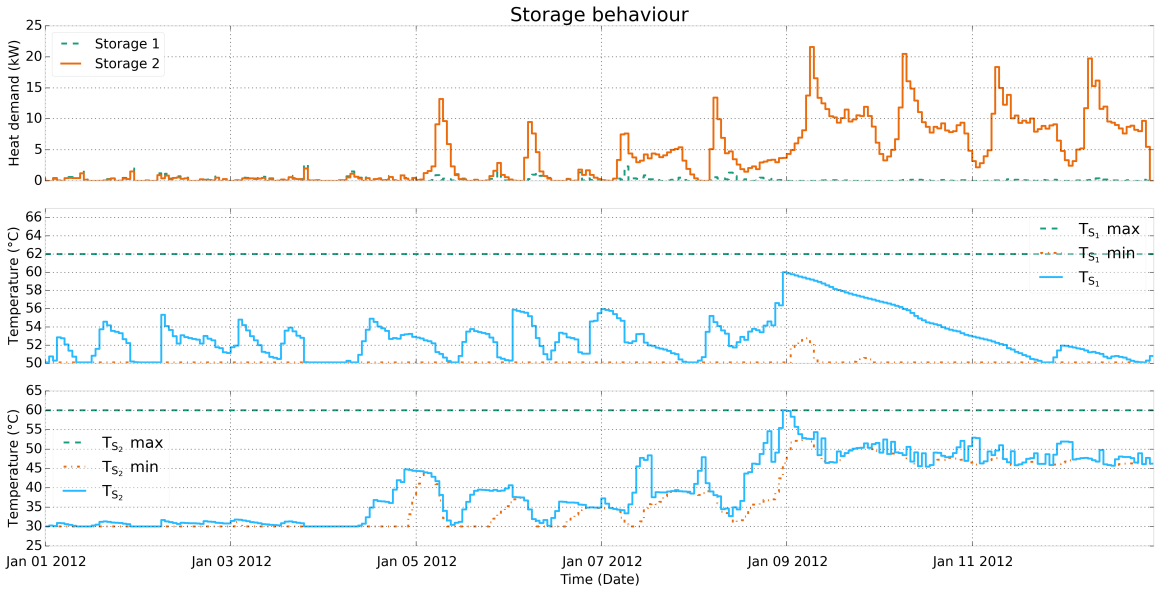

Figure 4-3: Storage behaviour in a variable tariff scenario with the non-convex OCPF based MPC

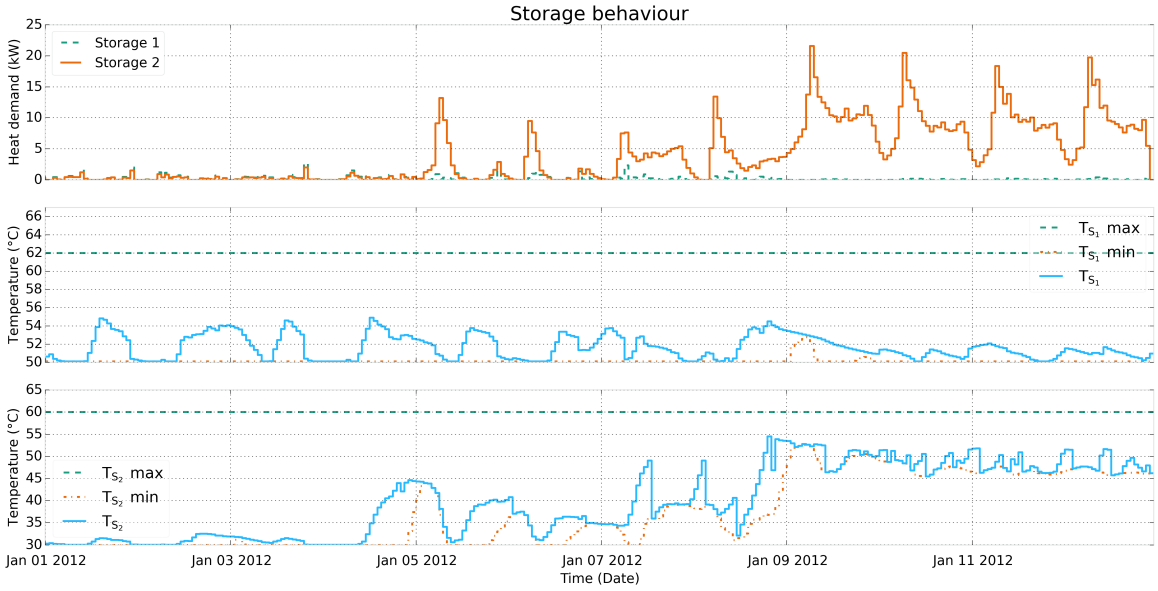

Figure 4-4: Storage behaviour in a variable tariff scenario with the modified convex quadratic OCPF based MPC

The last performance indicator in Table 4-2 shows that since higher penalties on inputs were placed in the dead-zone region in the NLP formulation, the HP operates less frequently in that region as compared to the mQP case. The baseline controller does not operate in that region. This means that to avoid the dead-zone region, slightly higher supply temperatures and part load ratio are maintained as higher costs and lower efficiency values were observed.

This cannot be concluded from 12 test days simulations and better insights are obtained in the one year simulation results as the strategies are tested for whole range of data in the latter case. However, this rationale might also contribute to the slightly inferior overall performance of the NLP based strategy in this case besides the uncertainty of proximity of its suboptimal solution to the global one.

4-2-3 Smart grid scenario

The results (Table 4-3) in this scenario show how effectively solar power was utilized by each control strategy and also indicate the contribution of solar energy in cost savings when compared to the previous scenario. The expenditure on heating is reduced for all controllers and the MPC strategies perform better in self-consumption of the residual PV power which is indicated by the second KPI in Table 4-3. The baseline control strategy feeds in more power to the grid which is not desirable when the incentive (feed-in tariff) is reduced. This concludes that MPC makes better use of solar energy by use of forecasts. The predictions enable the MPC strategies to decide whether to wait for cheaper electricity or overheat with it in order to save costs. Such decisions cannot be made by the baseline control strategy.

Table 4-3: Comparison of control strategies in dynamic price scenario including solar energy

Scenario 3: Smart Grid	Control Strategy		
Performance indicator	Baseline	mQP	NLP
Money spent (€)	78.82	69.2	67.98
Money saved by PV (€)	0.91	2.46	2.52
Money earned from feed-in (€)	20.98	18.76	18.7
Electricity consumed (kWh)	297.65	273.9	270.64
SPF	4.33	4.6	4.70
Storage heat loss (%)	13.35	10.55	11.33
STC Heat utilization (%)	26.07	24.6	24.59

When comparing the overall performance in this case, the NLP based MPC had better results even though the storage losses were higher as compared to the convex formulation. This contradicts the results in previous scenario as the use of solar energy is also almost the same in case of both MPC strategies. However, the performance of the mQP formulation based MPC was still comparable to the NLP one and it saved 12.2% costs against the baseline controller. The slight reduction in savings as compared to previous scenario and slightly lower utilization of heat available from STC as compared to the baseline controller can be attributed to the undesirable but unavoidable constraint violations (Figure 4-5) by the baseline control strategy. The baseline control strategy was programmed to utilize maximum possible free heat from the STC which influences the upper storage temperature. However, in this case the utilization was not always permitted by the constraints which resulted in 'unfair' use of free heat from STC. This explains that the predictive control strategies lost some savings in order to respect the upper storage temperature limit.

The baseline controller cannot react to sharp changes in the bounds as it does not predict the system state (storage temperatures) and does not possess the knowledge of future bounds which are calculated using ambient temperature forecasts. This can be observed in Figure

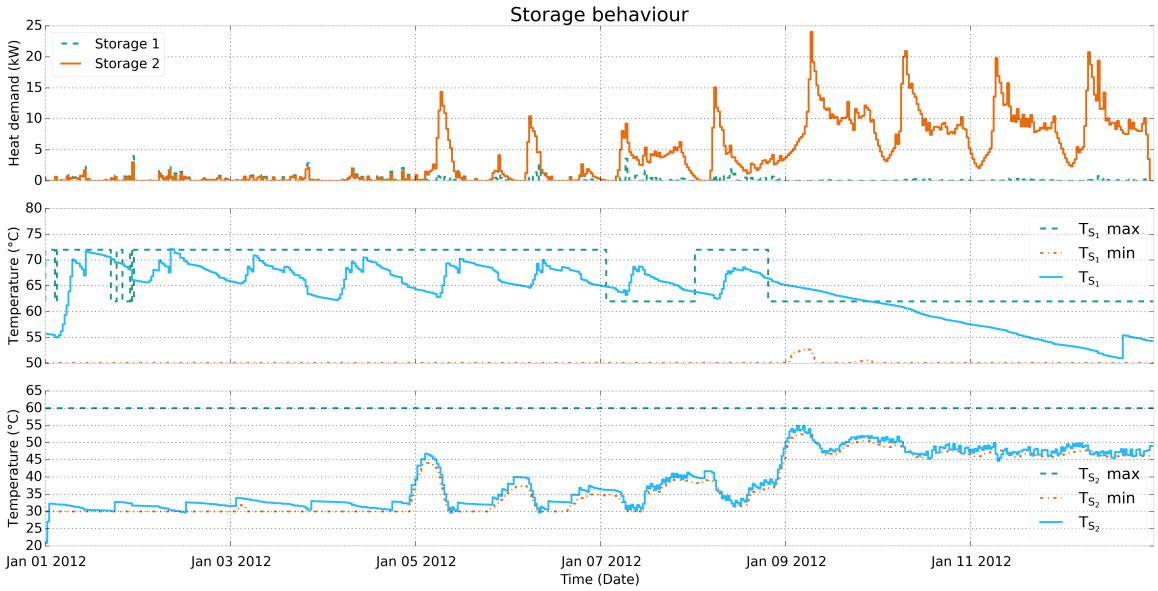

Figure 4-5: Storage behaviour in a smart grid scenario with baseline control strategy

4-5 where the upper bound ($\bar{T}_{S_1}$) on upper storage temperature (T_{S_1}) is violated during the days Jan 1, 7 and 9. On the contrary, the MPC strategy avoids these constraint violations as observed in Figure 4-6. This shows the superior performance of predictive control in constraint satisfaction. In Figure 4-7 it could be seen that in the early hours of Jan 7, the temperature of the upper storage was marginally higher than the upper limit. As explained in Section 3-3-4, such a situation makes the optimization problem infeasible as the heat pump

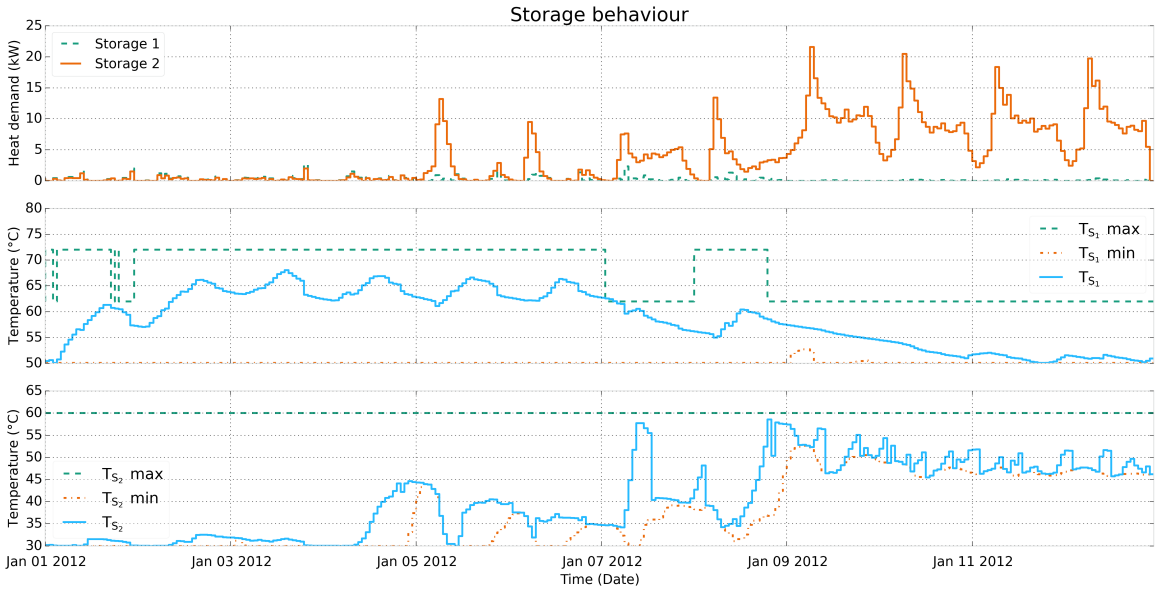

Figure 4-6: Storage behaviour in a smart grid scenario with predictive control strategy (mQP OCPF)

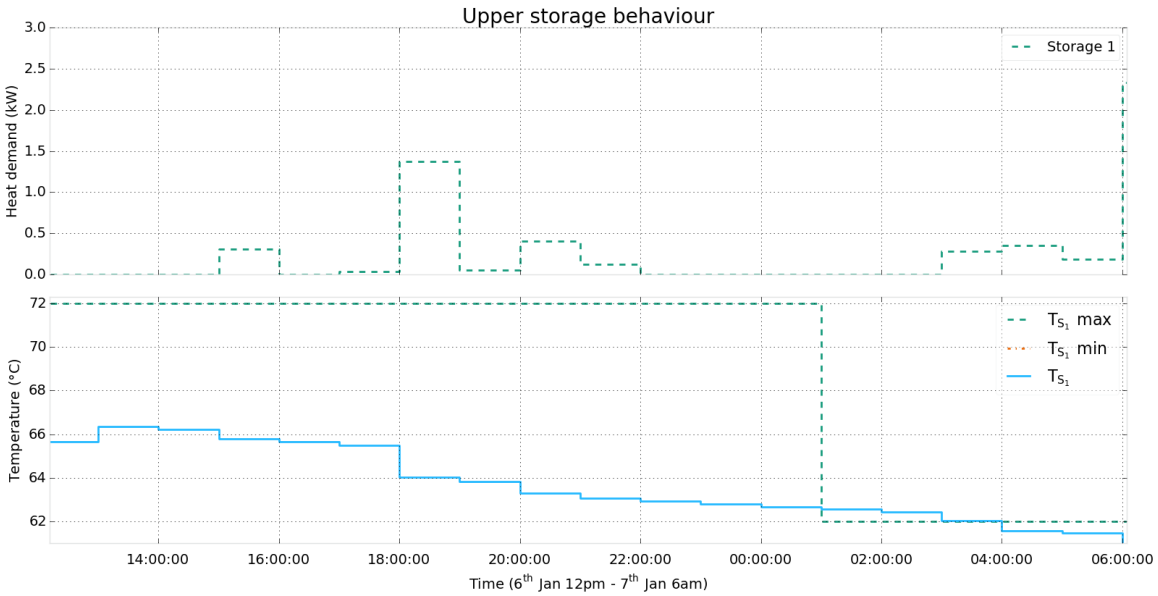

Figure 4-7: Storage temperature control with MPC showing the marginal constraint violation. This figure is a zoomed in version of the plot in Figure 4-6

considered in our system cannot cool. The controller stops heating the upper storage when the predictions indicate 12 hours in advance that the upper bound will be lower than current temperature. However, since the requirement to have the temperature lower than the desired upper limit was impossible to satisfy in the available time, the hard constrained optimization problem becomes infeasible in this situation. This is exactly when the upper bounds need to

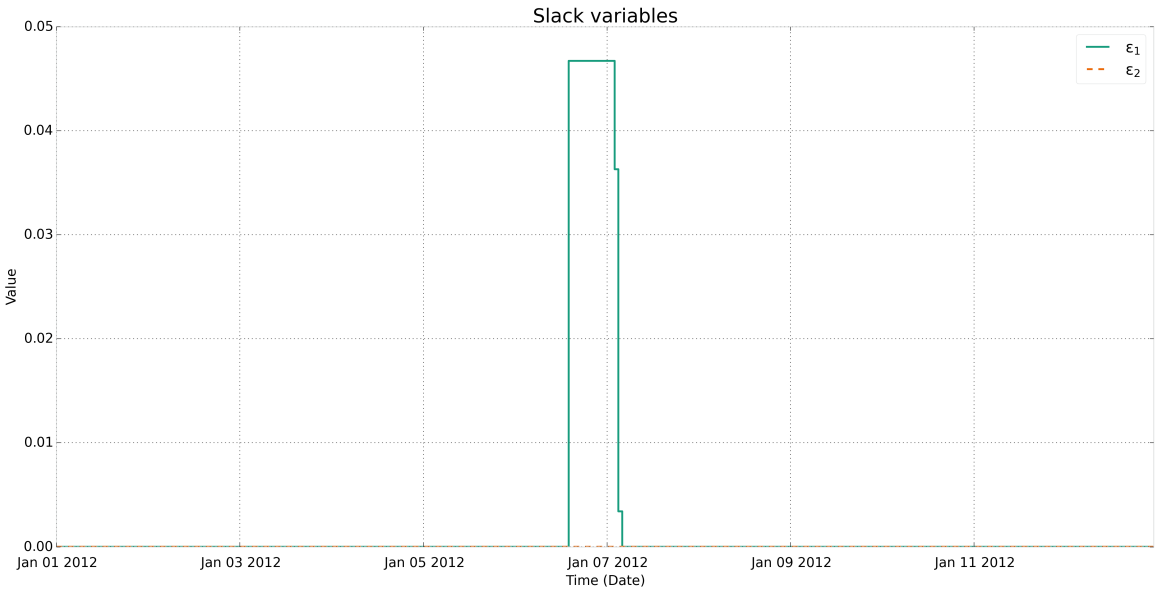

Figure 4-8: Slack variable values during the MPC simulation

be relaxed i.e. the slack variable ε_1 should be active. The timeseries plot of the slack variables (Figure 4-8) shows that this variable was only non-zero during the period of infeasibility of the hard-constrained problem and not for any other time instant which satisfies the exactness property explained in Section 3-3-4.

4-2-4 Simulation results with one year data

The simulation results obtained in the previous three test cases already prove that the predictive control strategies perform reasonably better than the baseline controller in all aspects except for the computational complexity. The results also showed that in general the performance quality of the mQP formulation based MPC is fairly comparable to the non-convex case. However, the 12 test days dataset was used to have a performance comparison which can be visualized. In order to have more realistic values for the KPIs, simulations using the whole avaiable dataset for the year 2012 were performed. The resulting values can obviously not be generalized for any other dataset but they give a general perception regarding how much savings (minimum potential) can be expected from the different control strategies against the baseline strategy. Since the 12 test days data includes typical days of a year, the results already give a fair and general idea about the quantification of potential benefits that can be expected by using predictive control. However, the 365 days dataset tests the performance of control strategies for all types of days including extreme weather conditions during summer and winter seasons. The plots for this case only give an overall idea of how the system behaves in different seasons rather than detailed visualization of the performance but the insights obtained from these simulations also help in making conclusive comments concerning the sizing of the system components. Table 4-4 shows the resulting comparison of control strategies in a smart grid scenario.

Table 4-4: 365 days simulation results for the year 2012

Scenario: Smart Grid	Control Strategy		
Performance indicator	Baseline	mQP	NLP
Money spent (€)	2041.00	1904.07	1850.46
Money saved by PV (€)	40.18	76.13	75.77
Money earned from feed-in (€)	636.57	578.7	579.18
Electricity consumed (kWh)	7671.02	7457.59	7320.46
SPF	4.33	4.44	4.52
Storage heat loss (%)	6.89	6.36	6.39
STC Heat utilization (%)	26.4	25.34	25.40
Dead-zone operation of HP (No. of switchings per hour)	-	0.39	0.38

It is clear from Table 4-4 that the non-convex formulation based MPC is the most energy and cost efficient strategy (cf. KPIs money spent, SPF and electricity consumed). The cost by using baseline control strategy was 10.3% higher than the NLP OCPF based MPC and 7.2% higher than the mQP OCPF based MPC. The resulting comparison of KPI values reasonably comply with the 12 test days results for the smart grid scenario. Hence, for the

reasons explained earlier, the baseline controller contributes to higher earnings from feed-in compensation. If the feed-in tariff policy is eradicated as expected in future, then self-consumption becomes essential which supports the use of predictive control strategies.

The storage heat losses are considerably lesser for all the control strategies when compared to previous results. This is because of the extreme weather conditions included in the data during which the heating system has no option but to operate at full capacity and the rate at which heat is extracted from the storage tank is as fast as the rate at which heat is stored (Figure 4-10). Due to this, the storage temperatures are very close to their lower bounds which further reduces the losses. Such an operation also explains why the savings from predictive control strategies were found to be lower in comparison with the 12 test days simulations. When the heating system has no option but to operate at its full capacity, the control strategy does not have a decision to make for load shifting with respect to price or sometimes even w.r.t. the ambient temperature. This means that the heating system behaviour is same for the baseline and predictive control strategies during those situations. Moreover, during the summer season, when there is no heat demand (from HP) for certain periods, the system simply needs to switch off and again the control strategy does not have to make any trade-offs, which renders the performance of predictive control strategy similar to the baseline controller. In summary, the lesser savings indicated by the one year simulations are simply because of the durations when heating system was either redundant (hot days) or there was no scope of manipulating control actions (winter days when the heating system must operate at maximum capacity).

The STC heat utilization remains same as the heat available was always more than the demand for upper storage (Figures 4-12 and 4-10). As mentioned earlier, this makes the baseline control utilize the heat from STC in an unfair manner (constraint violation) which contributes in lowering the difference in costs. Since the occurence of this behaviour was more frequent, the percentage difference in costs was lower as compared to 12 test days simulations (scenario 3). The last KPI's values in Table 4-4 indicate that the dead-zone operation controlled by post-processing step (Section 3-3-5) is acceptable considering minimal runtime of the heat pump (10 to 15 minutes). The values indicate that the switching instants occur at an average once in every two and a half hours which means that the durability of the equipment is not harmfully affected by the dead-zone treatment procedure considered.

Performance plots

The performance of predictive controller (mQP OCPF) is shown in the following plots in order to show the controlled system behaviour over all seasons of the year and also to draw conclusions on the sizing of the system components. Figure 4-9 shows the range of data for which the controller was tested for its performance in achieving the control objectives. It shows the heating trend in different seasons. In summer, the heat load for space heating is zero or negative (cooling load) but for the simulations cooling loads are not considered.

A special case of electricity price is observed during the Christmas period when the electricity was free (in reality in the year 2012) and the predictive controller successfully exploited the chance to store it by operating the heating system at maximum capacity. This case notably highlights the potential of predicitive control in grid balancing, because on 25^{th} of December 2012 in Germany, due to sudden input from solar energy production (cf. first subplot of Figure

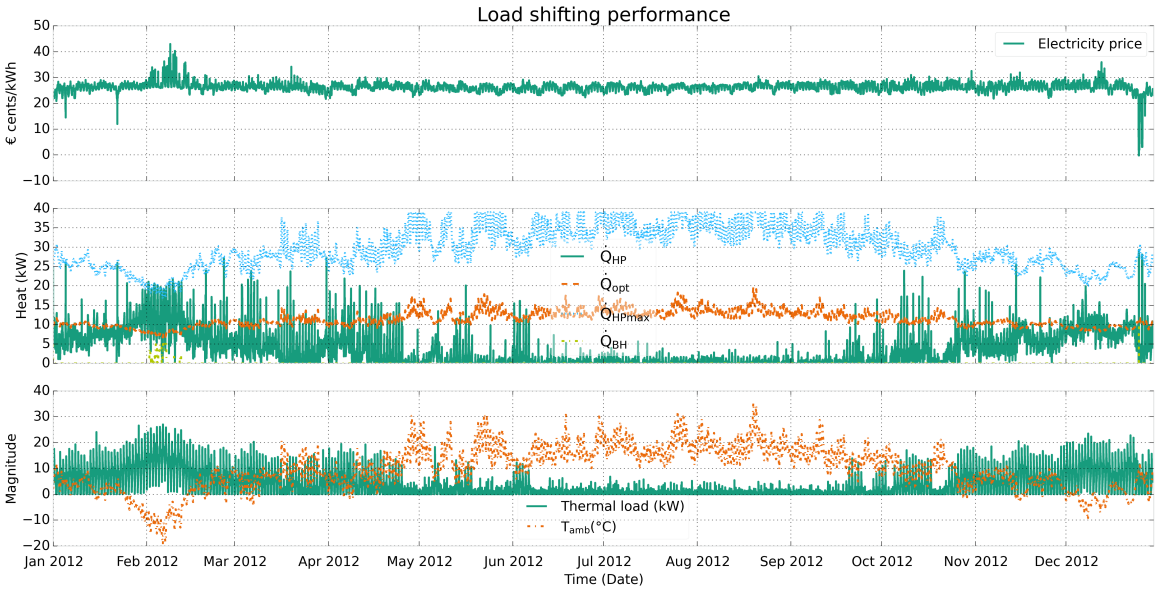

Figure 4-9: Heating system performance with predictive control strategy. The figure shows that the backup heaters were only used as the last resource in February (second subplot). The data covered whole range of temperatures in all seasons of the year.

4-12) on account of unexpected sunshine, the electricity had to be made so cheap (free or negative prices) such that it is utilized even though there is no sufficient demand in order to maintain grid balance.

Figure 4-10: Storage behaviour over the year which shows that the controller successfully satisfied the bounds imposed. The frequent fluctuation in temperatures shows that the storage was utilized for load shifting.

Figures 4-9, 4-10 and 4-11 confirm that the heat pump and storage sizing was appropriate considering the guaranteed thermal comfort even during extreme weather conditions.

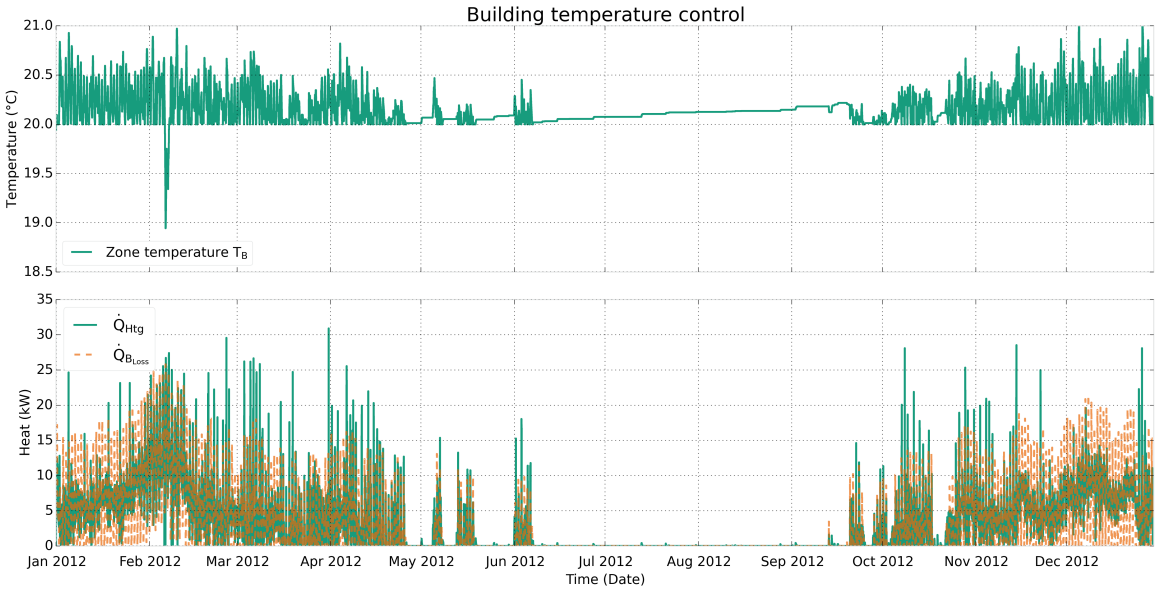

Figure 4-11: Zone temperature control throughout the year. Except for the sharp drop on the coldest day of the year, the temperature was maintained within desired range by the heating system.

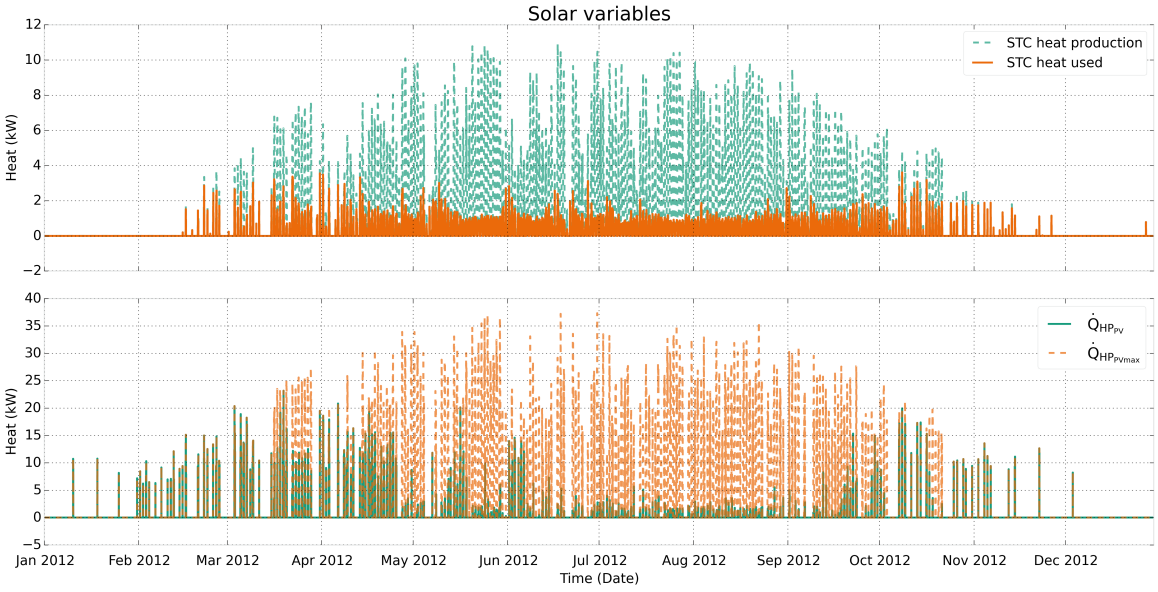

Figure 4-12: Heat input from solar devices

Figure 4-12 (second subplot) shows that the solar PV power unused by the house was mostly utilized for heating during the cold days (roughly September to April) and the surplus which

was fed to the electricity grid, was mostly during the spring and summer seasons. The first subplot of Figure 4-12 shows that the heat available from STC was unused whenever the production was over 2 kW in the warm days. This proves that the STC was oversized. The solar PV sizing would need alteration depending on the change in feed-in tariff policies because self-consumption for heating in the warm season is unlikely as observed in second subplot of Figure 4-12.

4-3 Findings

The simulation results presented in the previous section helped to answer the research questions (Section 1-2). The results with 12 test days data indicated that directly neglecting all the non-linearities (LP formulation) of the system results in performance which is far from the true cost and energy saving potential of predictive control strategy (4-2-1). However, the multiobjective approach (mQP formulation) which was also convex, incorporated essential characteristics of the electricity bill variation w.r.t. ambient temperature, system state and control inputs which was clear from the results with 12 test days data as the performance was comparable to the NLP control strategy whereas over 10% savings were achieved against the baseline control strategy in each scenario. The argument mentioned in the previous statement was weakened by the more realistic one year simulation results as the NLP control strategy had the best performance which was not comparable to other controllers. However, the mQP formulation based MPC strategy still saved substantially against the baseline one. The NLP formulation needs a perfect heat pump model which is hard to obtain and also limits widespread use of the same control strategy because a different heat pump would need a different model. The computational complexity was higher for solving the NLP formulation but it was not prohibitive considering the slow dynamics of the system. The speed of solving the NLP problem however depends on the computational power of the device used, solver (algorithm) and also the size of the problem. Hence, if the computational aspect and obtaining a detailed heat pump model are not a concern, then the NLP based MPC strategy is the recommended solution. Otherwise, considering a large scale application and also substantial benefits, the convex (mQP OCPF) optimization based MPC strategy is the most suitable one as it does not rely on a detailed heat pump model.

It was clear from the results in different scenarios that the exact quantification of benefits of using predictive control depends on a variety of factors. For example, electricity pricing policy, climate of the location, sizing of the heating system etc. Hence, it is difficult to state the exact quantity of savings that may be expected from use of predicitve control over the baseline control strategy. However, considering the 12 typical test days simulation results to be more general, it can be stated that around 10% savings can be expected. While, this only indicates the potential cost savings at the users' end, the advantage of using predictive control for grid balancing through its load shifting ability is promising and could have a positive monetary impact even higher than the demand side. The quantification of costs and energy saving potential on electricity source side (grid) was not in the scope of this thesis but is a research problem which needs attention and investigation.

Additional findings include the comments on sizing of the heating system components. It was found that the STC was amply oversized as around 74% of the heat produced was not utilized and the underutilization was quite uniform throughout the year (Figure 4-12). The

heating system seemed to be oversized by observing the 12 test days simulation results but the one year data based simulations proved that the sizing was appropriate.

Summary In this chapter, the performance of different control strategies was compared in detail. The advantages and disadvantages of each control methodology were apparent from the simulation results (Section 4-2). The potential of predictive control approach for residential heating system in smart grid scenario was quantified through the simulations performed with real test data (Section 4-2-4). In summary, the results obtained accomplished the research goals. The next chapter includes a summary of this thesis and recommendations for future work.

Chapter 5

Conclusions

This thesis focussed on finding answers to the following research questions regarding predictive control for residential capacity controlled heat pumps in a smart grid scenario:

- Which is the best optimization problem formulation to achieve the control objectives?
- How is the controller performance influenced by using simplified convex formulations, instead of the nonlinear non-convex one defined using an accurate heat pump model?
- What are the benefits of using a model predictive control strategy as compared to current state-of-the-art rule based approach? How much is the cost saving and energy reduction potential?

In order to find the answers to the above mentioned questions, different control algorithms were tested in this thesis. The control methodologies were described in detail in Chapter 3 which include the baseline controller (rule based approach), nonlinear non-convex, and convex optimization based predictive control approaches. The nonlinear non-convex OCPF was based on a heat pump model. The heat pump model with suitable inputs and outputs for the formulation was derived from a high fidelity model as described in Chapter 2. The influence of using simplified formulations which did not rely on an accurate heat pump model were described by testing different problem formulations (Section 3-3). Simulations in multiple scenarios were performed in order to compare the control strategies while determining and quantifying the benefits of predictive control method in Chapter 4.

The results obtained through this thesis work which answered the research questions are summarized in Section 5-1. Due to limited time, some work that could have contributed to more results in the scope of this thesis was excluded and is mentioned in Section 5-2. In future, the control algorithm developed in this preliminary work needs to be tested on detailed simulation software (*ColSim*) followed by tests on a real setup in the *Smart energy lab* at Fraunhofer ISE. The future work for the same concerning the control design is described in Section 5-3.

5-1 Summary of results

Based on a detailed study of the nonlinear heat pump characteristics in Chapter 2, a new approach to model the heat pump performance was proposed (Section 2-3-2). The resulting model was simple yet accurate because a simpler model structure could be derived for the inverse of COP to estimate the heat pump performance as compared to the traditional method of fitting a COP model which has a more complicated structure for achieving the same accuracy.

Formulations which neglected all nonlinearities of the system (LP in Section 3-3-6, QP in Section 3-3-7) were not suitable as the performance loss due to simplifications was considerable which could be concluded through a comparison in Section 4-2-1 with the best formulation (NLP in Section 3-3-8). A control strategy that does not rely on a detailed heat pump model and is based on a faster optimization (convex) method was described in Section 3-3-7 i.e. the mQP OCPF based MPC. It was found through the 12 test days simulations that the performance of this control strategy was comparable to the one based on NLP method and it saved more than 10% costs and energy over the baseline controller in all tariff scenarios. The results with simulations using the same 12 typical days data also showed how predictive control exploited the forecasts of weather and electricity prices to perform load shifting, save energy and costs by operating the heat pump at a suitable part load which was not feasible with the rule based control method.

The simulations carried out using the one year (2012) data gave realistic quantification of potential benefits of using MPC and also the savings through renewable energy devices. It was found that the NLP OCPF approach was the most suitable method for achieving the control objectives as it resulted in minimum costs, energy consumption and higher efficiency as compared to other methods. However, this was based on the assumption that a perfect heat pump model is available and that the implementation is feasible considering the computation time. Hence, it was concluded that since the convex formulation (mQP) based MPC approach also saved substantially as compared to the reference control strategy, it is the most suitable method considering that it does not rely on accurate heat pump models which supports wide-spread use. Taking into account the results using 12 test day data and the advantage of faster performance w.r.t. NLP reinforces this conclusion. The main disadvantages of this method were that it needs tuning of one parameter and that the solution is suboptimal w.r.t. the theoretical performance bound.

5-2 Scope of improvement

The nonlinear non-convex optimization problem was solved using the solver `scipy`-SLSQP. By solving the problem with other NLP solvers, it can be verified whether it is possible to have a faster or a better performance. The attempts to do this in the last phase of this thesis work using relevant open source tools failed due to installation issues, lack of developer support and in other cases the effort involved in switching to a completely new framework for optimization. However, using a faster and perhaps a better solver is recommended considering future research on the topic during software-in-the-loop (SiL) and hardware-in-the-loop tests.

If feasible, the immediate next step in this thesis work would be to perform and present a sensitivity analysis of all tuning parameters involved and prediction data errors. This would

contribute to more results and also help to determine all the conditions of validity of the results.

5-3 Future work

The following tasks are suggested for future work:

- **Model validation** The performance of the predictive control strategy strongly relies on the accuracy of the system model. The LTI system model presented in Section 2-2-2 needs to be validated which can be done by testing it for modeling errors on the *ColSim* framework used for SiL simulations.
- **Online parameter estimation** For having a plug and play approach, parameter estimation techniques are suggested to be used for identifying the system's unknown model parameters online. The literature review [8] preceding this thesis work suggested that a recursive least squares algorithm would be suitable for parameter estimation with the current modeling approach.
- **Electricity source side benefits of MPC** While quantifying the benefits of MPC in demand side management, it was realized that the monetary savings by grid balancing through load shifting were not accounted for. The research question that how much costs and energy does predictive control potentially save by contributing to grid stability, needs investigation.
- **Increasing storage divisions** The stratified thermal storage tank was modeled as two ordinary tanks (two layers with a specific temperature). For better accuracy while modeling the dynamic behaviour of the stratified storage, the number of layers must be increased which would result in more number of system state variables (temperatures at different points of storage). This is essential considering that a stratified storage has multiple layers and approximating it to two layers would decrease the accuracy of the model. The number of divisions to be made depends on the validation results with current modeling approach.
- **Influence of prediction uncertainties** The model and prediction data profiles were all assumed to be perfect. However, considering a realistic scenario, the forecast for electricity price, weather, thermal loads etc., will not be deterministic. A sensitivity analysis is needed to determine how robust is the controller performance to such uncertainties. Based on this analysis, it can be concluded whether explicit robustness considerations are required in the predictive controller.

Appendix A

Miscellaneous

A-1 Air source heat pump system

The air source heat pump (using a vapor compression cycle) has four main components namely the compressor, expansion valve (or metering device) and two heat exchangers on the source and the sink side which are evaporator and condenser respectively (Figure A-1). For residential applications, air to water heat pumps can be used for heating space and also hot water supply. In that case, the fluid heated in the condenser is water which can be supplied for the two purposes mentioned. Alternatively, instead of direct supply, the hot water can be stored in a thermal storage to decouple the heat demand and supply.

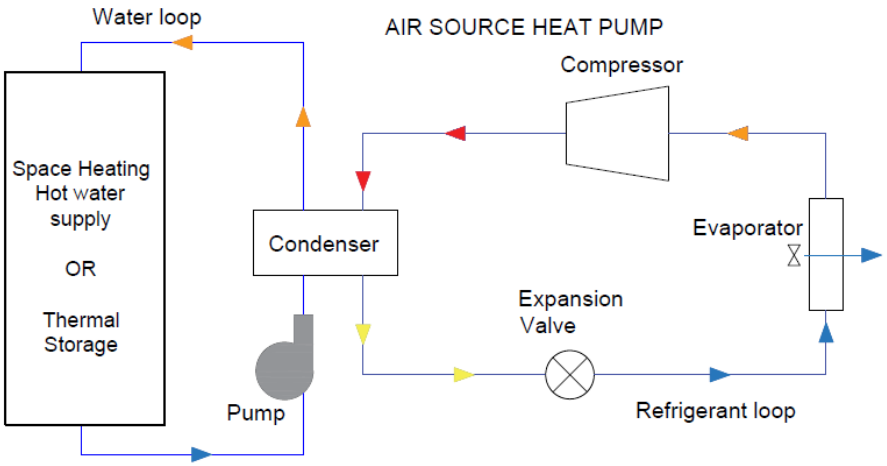

Figure A-1: Block diagram of the heat pump system

The above figure shows a block diagram of the system with the air source heat pump (refrigerant loop) and the load side which is the water loop. As seen in the figure, heat is exchanged to the water loop through the condenser. The rate at which heat is gained in the condenser

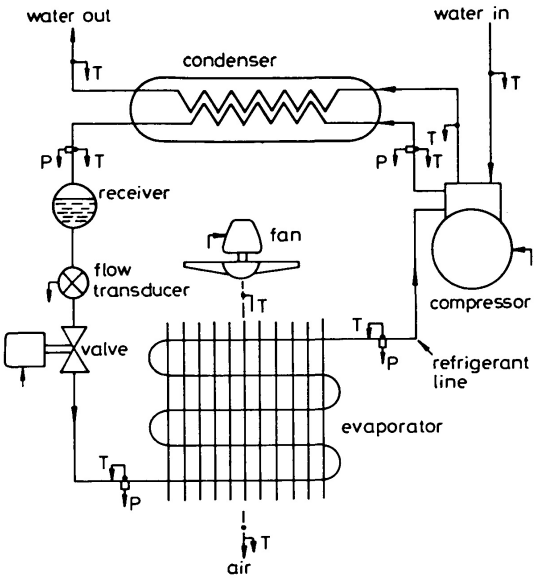

Figure A-2: Configuration of the heat pump system [25]

depends on the mass flow rate of the water in the load side loop. This flow rate is controlled by an ordinary variable capacity pump shown in the water loop. The control of this flow is necessary to control the temperature of water (supply and return) at the inlet and outlet of the condenser to meet the temperature requirements of supply. This is because the heat supplied from the condenser (heat pump) has a certain maximum capacity limit. This allows to have a supply temperature higher or lower than what can be delivered through a fixed flow rate when operating at maximum capacity of the heat pump.

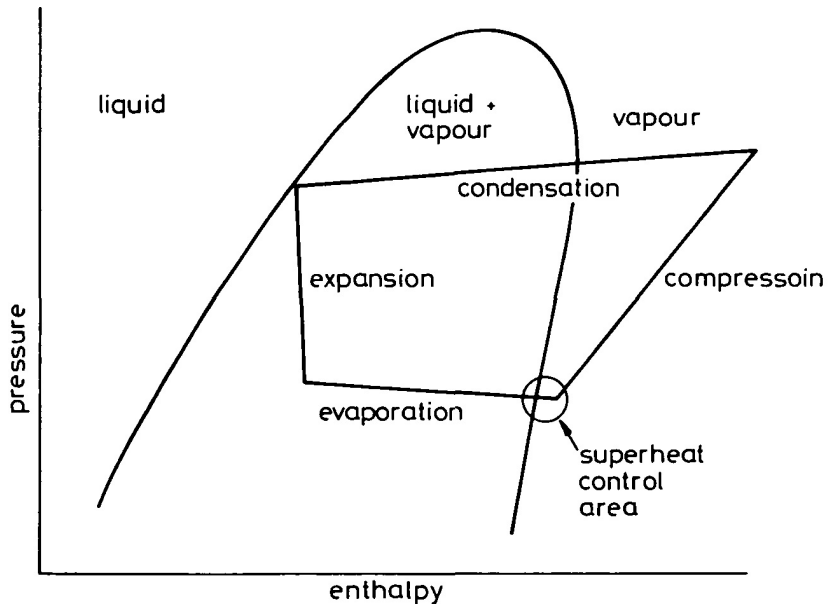

Figure A-3: Vapor Compression Cycle [25]

A detailed description for the control of each component is given in [25]. Figure A-2 describes the system considered in [25]. The following paragraph explains the thermodynamic cycle of this system.

The Cycle `Compressor` isentropically increases the pressure and temperature of the working fluid (refrigerant). It consumes most of the energy supplied to the heat pump system [25]. The refrigerant then heats the water in the `condenser`. In the `expansion` valve (throttle) the refrigerant pressure and temperature drop through an isenthalpic expansion. The low temperature refrigerant then gains heat from the heat source (ambient air) in the `evaporator` before entering the compressor which completes the thermodynamic cycle shown in Figure A-3.

A-2 Heat extraction for domestic hot water from each storage part

This section includes the details on how the domestic hot water (DHW) load profile ($\dot{Q}_{DHW}$) was distributed for heat extraction ($\dot{Q}_{DHW_1}$, $\dot{Q}_{DHW_2}$) from the two storage layers. The DHW is supplied from the upper layer at temperature T_{S_1} whereas the cold water return is in the lower layer of the storage at temperature $T_{\text{cw}} = 15°\text{C}$. The following equation describes the rate of heat extracted from the storage where $\dot{m}$ is the mass flow rate of DHW supply and c_p is the specific heat capacity of water:

$$\dot{Q}_{DHW} = \dot{m} \cdot c_p \cdot (T_{\text{cw}} - T_{S_1}) \tag{A-1}$$

Balancing the mass flow rate through each layer gives the following equations:

$$\dot{Q}_{DHW_1} = \dot{Q}_{DHW} \cdot \frac{(T_{S_2} - T_{S_1})}{(T_{\text{cw}} - T_{S_1})} \tag{A-2}$$

$$\dot{Q}_{DHW_2} = \dot{Q}_{DHW} \cdot \frac{(T_{\text{cw}} - T_{S_2})}{(T_{\text{cw}} - T_{S_1})} \tag{A-3}$$

The last two equations explain how the share of DHW load for each storage layer was calculated. During winters the lower storage needs to be maintained at higher temperatures which reduces the temperature difference between the two storage layers. Considering this, the last two equations also explain why the upper storage layer has a lower DHW share during winters. Since supplying DHW is the only function of the upper storage layer, it has much lower heat load as compared to the lower storage layer and, its load share becomes almost negligible in winters.

A-3 Discretization details

The `cont2discrete` function from `scipy` library was used for zero order hold discretization. Since the model has a disturbance matrix E and the function accepts only the matrices A, B, C and D (Defined in (2-2)), the disturbance vector was stacked vertically with the state

vector to have a new A matrix (A_1). The normal state space description after this procedure can be described as:

$$\left[\begin{array}{c|c} A_1 & B_1 \\ \hline C_1 & D_1 \end{array}\right] = \left[\begin{array}{cc|c} A & E & B \\ 0 & 0 & 0 \\ \hline C & 0 & D \end{array}\right]$$

The discrete-time matrices A_d, B_d, C_d and D_d were extracted from the discretized version of A_1, B_1, C_1 and D_1:

$$\left[\begin{array}{cc|c} A_d & E_d & B_d \\ 0 & I & 0 \\ \hline C_d & 0 & D_d \end{array}\right] = \left[\begin{array}{c|c} A_{d_1} & B_{d_1} \\ \hline Cd_1 & D_{d_1} \end{array}\right] = \texttt{cont2discrete}\left(\left[\begin{array}{c|c} A_1 & B_1 \\ \hline C_1 & D_1 \end{array}\right]\right)$$

The resulting values of matrices A_d, B_d, C_d, D_d and E_d:

$$A_d = \begin{bmatrix} 0.9970611 & 0 & 0 \\ 0 & 0.9970611 & 0 \\ 0 & 0 & 1 \end{bmatrix} \tag{A-4a}$$

$$B_d = \begin{bmatrix} 0.97186 & 0 & 0 & 0.97186 & 0 & 0.97186 & 0 & 0.97186 \\ 0 & 0.41651 & -0.41651 & 0 & 0.41651 & 0 & 0.41651 & 0 \\ 0 & 0 & 0.0136 & 0 & 0 & 0 & 0 & 0 \end{bmatrix} \tag{A-4b}$$

$$E_d = \begin{bmatrix} -0.97186 & 0.00294 & 0 & 0 \\ 0 & 0.00294 & 0 & -0.41651 \\ 0 & 0 & -0.0136 & 0 \end{bmatrix} \tag{A-4c}$$

C_d is an identity matrix of size 3 and D_d is a null matrix of dimension 3×8. Same (upto 4 decimal places) resulting discrete-time matrices were manually calculated by using the forward Euler method for discretization. This verification was done in order to check if there were any numerical issues because of the low values in continuous-time matrices.

A-4 Calculation of key performance indicators

This section includes the formulae used to calculate the KPIs.

- Money spent on heating: This is calculated from eqs. 3-19 and 3-58. The value of 'bill' so obtained from these equations is multiplied by the sampling time in hours to get the resulting units in euro cents.
- Money saved by local consumption of PV electricity is calculated as:

  $$\text{Money saved by PV} = (\text{ecost} - \text{PVcost}) \times P_{el_{PV}} \times \text{Sampling time in hours}$$

  Where, 'ecost' and 'PVcost' are grid and feed-in electricity tariffs with units euro cents per kWh and $P_{el_{PV}}$ is the PV electricity consumed (in kW) as defined in (3-17).
- Money earned by feed-in of surplus PV electricity = $P_{el_{PV}} \times$ Sampling time in hours

- Electricity consumed for heating (in kW) (P_{el}) = $P_{el_{HP}} + P_{el_{PV}} + P_{el_{BH}}$
  (terms as defined in eqs. (3-16) to (3-18))
- Seasonal performance factor (SPF): Using its definition, it is calculated as the ratio of total rate of heat transfer values to the total power consumed.

$$\text{SPF} = \frac{\sum (\dot{Q}_{HP} + \dot{Q}_{BH})}{P_{el}}$$

The remaining KPI calculations are obvious from their definition.

Bibliography

[1] D. Sturzenegger and D. Gyalistras, "Model Predictive Control of a Swiss office building," *11th REHVA World Congress*, 2013.

[2] D. Neves and C. A. Silva, "Modeling the impact of integrating solar thermal systems and heat pumps for domestic hot water in electric systems – The case study of Corvo Island," *Renewable Energy*, vol. 72, pp. 113–124, Dec. 2014.

[3] S. Mueller, R. Tuth, D. Fischer, B. Wille-Haussmann, and C. Wittwer, "Balancing Fluctuating Renewable Energy Generation Using Cogeneration and Heat Pump Systems," *Energy Technology*, vol. 2, pp. 83–89, Jan. 2014.

[4] C. Verhelst, F. Logist, J. Van Impe, and L. Helsen, "Study of the optimal control problem formulation for modulating air-to-water heat pumps connected to a residential floor heating system," *Energy and Buildings*, vol. 45, pp. 43–53, Feb. 2012.

[5] F. Oldewurtel, A. Parisio, C. N. Jones, D. Gyalistras, M. Gwerder, V. Stauch, B. Lehmann, and M. Morari, "Use of model predictive control and weather forecasts for energy efficient building climate control," *Energy and Buildings*, vol. 45, pp. 15–27, Feb. 2012.

[6] "Heat pumps in smart grids and smart cities." Newsletter, IEA Heat Pump Centre, vol. 30, Feb. 2012. http://web.ornl.gov/sci/ees/etsd/btric/usnt/HPCNewsltr22012.pdf.

[7] "Heat pumps in domestic housing and demand side management." Positioning paper, Dutch Heat Pump Association, Apr. 2015. http://www.dhpa-online.nl/wp-content/uploads/2011/03/DHPA-32-pag.ENG_.LR_.pdf.

[8] N. Saraf, "Adaptive predictive control for capacity controlled heat pumps." Literature review, Nov. 2014. https://www.dropbox.com/s/d74rr2ts89ar580/mscLiterature.pdf?dl=0.

[9] G. Rossum, "Python reference manual," tech. rep., CWI (Centre for Mathematics and Computer Science), Amsterdam, The Netherlands, 1995.

[10] D. Kroshko, "OpenOpt: Free scientific-engineering software for mathematical modeling and optimization." http://www.openopt.org/, 2007.

[11] A. A. Safa, "Performance analysis of a two-stage variable capacity air source heat pump and a horizontal loop coupled ground source heat pump system," Master's thesis, Ryerson University, Toronto, 2012.

[12] D. Fischer, S. Braungarth, H. Madani, D. Reisener, T. Toral, and Z. Andreas, "Next generation heat pump for retrofitting buildings." Fraunhofer ISE, 2012.

[13] K. J. Åström and B. Wittenmark, *Computer-Controlled Systems*. Prentice Hall, 1997.

[14] S. Li, J. Joe, J. Hu, and P. Karava, "System identification and model-predictive control of office buildings with integrated photovoltaic-thermal collectors, radiant floor heating and active thermal storage," *Solar Energy*, vol. 113, pp. 139–157, Jan. 2015.

[15] S. Klein, J. Duffie, and W. Beckman, "TRNSYS - A Transient Simulation Program," *ASHRAE Transactions*, vol. 82, pp. 623–633, 1976.

[16] F. Borrelli, A. Bemporad, and M. Morari, *Predictive Control for linear and hybrid systems*. 2011. http://www.mpc.berkeley.edu/mpc-course-material/MPC_Book.pdf?attredirects=0&d=1.

[17] Y. Ma, *Model Predictive Control for Energy Efficient Buildings*. PhD thesis, University of California, Berkeley, USA, 2013.

[18] D. Angeli, "Economic model predictive control," in *Encyclopedia of Systems and Control*, pp. 1–9, Springer London, 2014.

[19] J. Rawlings, D. Angeli, and C. Bates, "Fundamentals of economic model predictive control," in *Decision and Control (CDC), 2012 IEEE 51st Annual Conference on*, pp. 3851–3861, Dec 2012.

[20] M. Ellis, H. Durand, and P. D. Christofides, "A tutorial review of economic model predictive control methods," *Journal of Process Control*, vol. 24, no. 8, pp. 1156 – 1178, 2014.

[21] D. Fischer, T. Wirtz, K. Dallmer Zerbe, B. Wille-Haussmann, and H. Madani, "Test cases for hardware in the loop testing of air to water heat pump systems in a smart grid context." Fraunhofer ISE, 2015.

[22] P. O. M. Scokaert and J. B. Rawlings, "Feasibility issues in linear model predictive control," *AIChE Journal*, vol. 45, no. 8, pp. 1649–1659, 1999.

[23] E. C. Kerrigan and J. M. Maciejowski, "Soft constraints and exact penalty functions in model predictive control," in *Proc. UKACC International Conference (Control)*, 2000.

[24] "CVXOPT home page." http://abel.ee.ucla.edu/cvxopt.

[25] Y. Wang, D. Wilson, and D. Neale, "Heat-pump control," *IEE Proceedings D Control Theory and Applications*, vol. 130, no. 6, p. 328, 1983.

Glossary

List of Acronyms

DCSC	Delft Center for Systems and Control
ISE	Institute for Solar Energy Systems
COP	Coefficient of Performance
MPC	Model Predictive Control
TES	Thermal energy storage
LTI	Linear time-invariant
PV	solar Photovoltaic panels
STC	Solar thermal collector
HP	Heat pump
DHW	Domestic hot water
rpm	Revolutions per minute
RMSE	Root mean square error
KPI	Key performance indicator
SPF	Seasonal performance factor
OCPF	Optimal control problem formulation
LP	Linear programming
QP	Quadratic programming
NLP	Nonlinear (non-convex) programming
mQP	modified convex quadratic programming
EEX	European Energy eXchange

List of Symbols

Q	Absolute heat transferred
$\dot{Q}$	Rate of heat transfer
P_{el}	Electrical power
T	Temperature
K	Kelvin (a Kelvin = a + 273 °C)
°C	degree Celcius
kW	kilo Watt
kWp	kilo Watt peak
kWh	kilo Watt hour
x	State vector
u	Vector of control inputs
z	Vector of known disturbances
N	Prediction horizon
t	Time
U	Vector of decision variables
$\mathcal{U}$	Feasible set of inputs
$\mathcal{X}$	Permissible set of state variables
$\mathbb{R}$	Set of real numbers
h	Sampling period
T_{sup}	Supply water temperature
T_{amb}	Ambient air temperature
ρ_i	Penalty on slack variable number i
ε	Vector of slack variables
€	Euro
$\dot{m}$	mass flow rate
c_p	Specific heat capacity of water